KINETICS OF SOME ION-MOLECULE REACTIONS ASSOCIATED WITH CHEMICAL-IONIZATION MASS SPECTROMETRY.

by

R. WALDER

A thesis submitted in partial fulfilment of the requirements of the Degree of Doctor of Philosophy in the University of London.

February 1979

The Bourne Laboratory,
Royal Holloway College,
Englefield Green,
Surrey.

To Janet -

for her support, encouragement, and assistance.

Acknowledgements

My thanks are due to my supervisor, Dr. H. Weigel, for his assistance, and, in particular, for his help in securing for me a Jubilee Research Studentship without which the completion of this research would not have been possible.

I am deeply indebted to Dr. Richard Hancock for his continued support, unflagging interest, and for several thousand stimulating and thought-provoking discussions. It is to his eternal credit that he laboured and sought no reward apart from the satisfaction gained from solving complicated problems. Words cannot express my gratitude to him.

I would like to thank Messrs. Brian Smethurst, Ray Lane, and Les Burgess for technical assistance, Professor K. Singer and Dr. David Fincham for help with the mathematics and computing, and Dr. Arthur Finch for the loan of the Texas gauge.

Finally, I am indebted to Mrs. Anita Smith for the cheerful typing of an unending manuscript and to the workers at the 'factory' for all their assistance in the preparation of diagrams.

KINETICS OF SOME ION-MOLECULE REACTIONS ASSOCIATED WITH CHEMICAL-IONIZATION MASS SPECTROMETRY.

by R. Walder.

ABSTRACT

Studies of the kinetics of ion-molecule reactions associated with isobutane chemical-ionization mass spectrometry have shown that many of these reactions proceed via the formation of a collision complex which undergoes either unimolecular decomposition to reactants, or collision-induced decomposition to products. Rate constants for the formation of collision complexes between isobutane reactant ions and various ketones, nitriles, alcohols, and anisoles were obtained. Comparisons between these rate constants and collision frequencies calculated from the Average-Dipole-Orientation theory showed that, in general, the reactions proceeded with efficiencies less than unity. The lifetimes of most of the collision complexes were found to lie in the range 1 - 10 μsec. The relative efficiencies with which several compounds effected the collision-induced decomposition of the complex suggested that the third-body efficiencies were determined by the collision duration. Charge - transfer reactions between the isobutane reactant ions and anisoles occur by a direct mechanism.

The magnitude of the rate constants for the formation of collision complexes were related to the structures of the compounds under study. For the reactions of certain reactant ions with the anisoles and halohydrins the rate constants were correlated with the appropriate substituent constants.

It was suggested that differences between the mechanism proposed herein and that proposed by Field for the reaction between $C_4H_9^+$ and benzyl acetate were due to differences in sample-pressure ranges.

Kinetic studies of the ion-molecule reactions consequent upon electron-impact ionization of methane and of isobutane, have suggested a novel method of estimation of reagent-gas pressures.

CONTENTS

CHAPTER 1

INTRODUCTION

1.1 General aspects of ion-molecule reactions.

A. The production of ions, and the analysis and detection of ion-beams.

Ionization of a chemical substance may be effected in a variety of ways. Three of the more common methods involve passing beams of electrons, or α-particles, or photons through the vaporized substance. A fourth method relies upon subjecting the sample to a high-strength electric field. Ions produced by any of these methods will, in general, also effect ionization of a substance, since a collision between an ion and a molecule often results in an ion-molecule reaction:

$$A^+ + B \longrightarrow C^+ + D \qquad (1.1\text{-}1)$$

When an organic compound is ionized by any of the above methods, so-called 'molecular' ions produced are, in general, unstable and fragment to form smaller ions (hereinafter referred to as 'primary' ions).

A mass spectrometer is an instrument which utilizes ionization and subsequent fragmentation processes for chemical analysis. A schematic diagram of this type of instrument is given in figure (1-1). The ion-source and flight tube are evacuated to low pressure ($<10^{-6}$ torr). A sample is introduced into the inlet system where it is vaporized. The vapour flows into the ion-

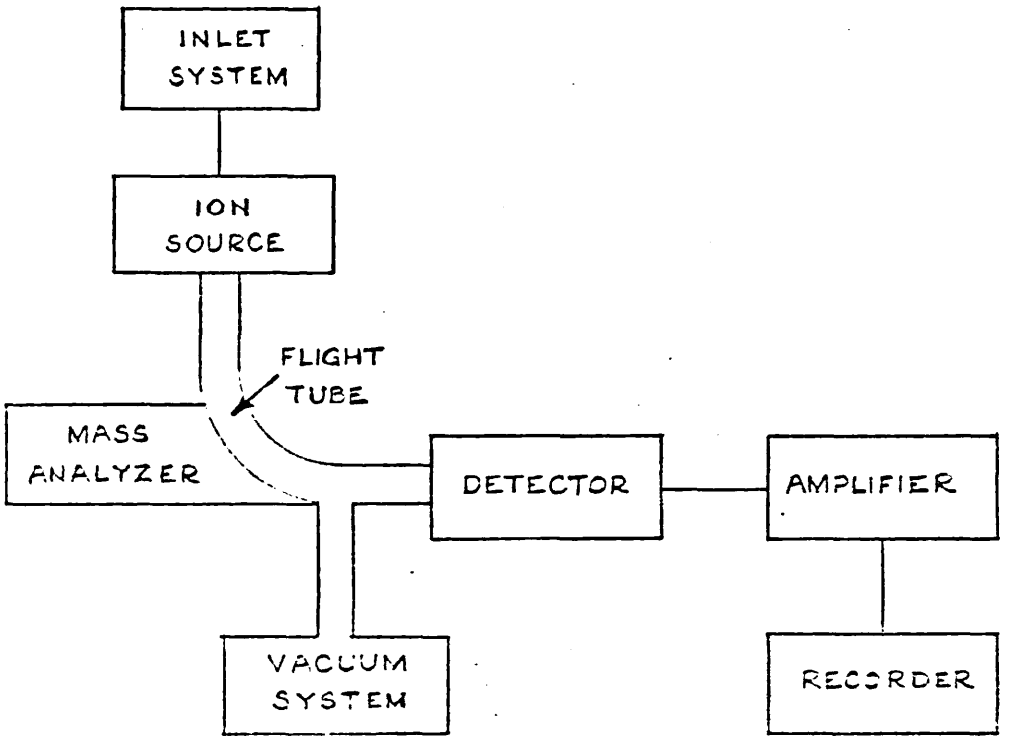

FIGURE (1-1). Schematic diagram of a mass spectrometer.

source where it is ionized, and where the resulting ions may undergo fragmentation*. The assembly of ions will not undergo reactions with the neutral molecules present, but merely pass through a slit (the 'ion-exit'slit) out of the ion-source†. Thereafter the ions are accelerated by an electric field applied between the ion-exit slit and a slit some 2-3mm removed from it. The latter slit is also used to focus the ion-beam; the sign of the potential applied to this slit determines whether it is positive or negative ions that are extracted from the ion-source. The ion-beam now passes through an analyzer (vide infra) where it is resolved into its component ion-beams according to the mass-to-charge ratios (m/z) of the ions. After analysis, the mass-resolved ion-beam passes through another slit (the 'collector' slit) and impinges upon a detector (vide infra). Signals from the detector are amplified and recorded. In the present work the initial ionization of compounds was effected by means of electron impact. This method of ionization will be described in some detail in Chapter 2.

A number of different types of mass analyzers and detector systems are employed in mass spectrometry. Details of these may be found in the books by Beynon [1], Kiser [2], and McFadden [3]. The following discussion will be concerned only with the analyzer and detector systems employed for this work: a magnetic-sector analyzer and electron-multiplier tube respectively.

---

* A detailed account of an ion-source will be given in section 2.2.

† At 10^{-6} torr the mean free path of an ion is several metres.

When the ions produced in the ion-source are accelerated by falling through a potential difference of V volts, the work done on an ion is zeV, where z is the number of charges on the ion, and e is the electronic charge. This work is equal to the kinetic energy gained by the ions. Thus

$$mv^2/2 = zeV \qquad (1.1\text{-}2)$$

where m and v are respectively the mass and velocity of the ion. The application of a magnetic field of strength B, applied perpendicular to the direction of motion of the ion-beam, causes each ion to experience a force, F_B, orthogonal to both its direction of motion and the field direction. The magnitude of the force is given by

$$F_B = Bzev$$

If the trajectory of the ion-beam is an arc of radius-of-curvature r, then the centripetal force experienced by the ion is given by

$$F_c = mv^2/r$$

Now since for a stable trajectory $F_B = F_c$, it can be seen that

$$v = Bzer/m$$

and hence (from equation 1.1-2)) that

$$m/z = eB^2r^2/2V \qquad (1.1\text{-}3)$$

Mass spectrometers employing magnetic-sector analyzers are generally constructed with a fixed radius-of-curvature so that for given values of B and V the ion-beams with m/z given by equation (1.1-3) pass through the collector slit and are detected. Thus systematic variation (scanning) of either the magnetic field, or the accelerating voltage, results in systematic variation of the

mass-to-charge ratio of ions passing through the collector slit.

The electron-multiplier tube consists of a series of plates ('dynodes') electrically connected by a network of resistors. The ion-beam passing through the collector slit impinges upon the first dynode (the so-called conversion dynode) and causes a shower of electrons to be emitted. These electrons are accelerated toward the second dynode where their impact causes additional electron emission. This process is repeated down each stage of the multiplier, and the final dynode (the 'collector') is connected to an electrometer for amplification and recording. Most multiplier tubes in common use contain between 12 and 20 dynodes.

The number of electrons emitted from the conversion dynode per incident ion, and for each subsequent electron impact at the other dynodes, is a complicated function of the mass, kinetic energy, and atomic composition of the impinging ion, and also of the accelerating voltage between each dynode and of the nature of the dynode material[4] . A typical 17-stage multiplier tube with a potential difference of 200 volts between each dynode, and with the dynodes constructed from a mixture of beryllium (2%) and copper, has a gain of approximately 10^7.

It was stated above that the initial ionization of the sample and subsequent fragmentation of the ions occurs in the ion-source before the ions are accelerated into the analyzer. Some of the ions formed are, however, metastable: they are withdrawn from the ion-source while remaining intact, but undergo fragmentation during

acceleration. When this happens a somewhat diffuse peak appears in the spectrum at a position often corresponding to a non-integral mass. The presence of such peaks can be understood by considering what happens when an ion of mass m_1 falls through a potential difference V_1 before decomposing to give an ion of mass m_2. The following assumptions are made about the behaviour. The original ion is assumed to be formed with zero kinetic energy, and the fragmentation occurs with a very small release of internal energy. In addition, if the ion and the neutral fragment formed in the dissociation, traverse the remainder of the accelerating field together, then the ion of mass m will enter the analyzer region with velocity, v, given by equation (1.1-4) (cf., equation (1.1-2),

$$m_2v^2/2 = (m_2/m_1)zeV_1+ze(V-V_1) \qquad (1.1\text{-}4)$$

This ion will now traverse the magnetic field with a radius of curvature given by

$$r = \frac{m_2v}{Bze} = \left(\frac{2V}{B^2ze}\right)^{\frac{1}{2}}\left[\frac{m_2^2}{m_1}\left(1+\frac{(m_1-m_2)(V-V_1)}{m_1V}\right)\right]^{\frac{1}{2}} \qquad (1.1\text{-}5)$$

Furthermore the radius of curvature of an ion m^* in the magnetic field is given by

$$r = \left(\frac{2V}{B^2ze}\right)^{\frac{1}{2}}(m^*)^{\frac{1}{2}} \qquad (1.1\text{-}6)$$

so that comparison of equations (1.1-5) and (1.1-6) shows that a metastable transition gives rise to a peak in the spectrum at a position corresponding to m^* on the mass scale, where

$$m^* = \frac{m_2^2}{m_1}\left(1+\frac{(m_1-m_2)(V-V_1)}{mV}\right)$$

If the dissociation occurs after essentially full acceleration, but

prior to the entrance of the ion into the analyzer region, then $V \sim V_1$, and

$$m^* = m_2^2/m_1 \qquad (1.1\text{-}7)$$

In spectra obtained using mass spectrometers with magnetic-sector analyzers the positions of peaks arising from fragmentation of metastable ions are given by equation (1.1-7). Such peaks are generally referred to as 'metastable peaks', despite the fact that this term could be misleading. Examples of metastable peaks will be found in the spectra described herein.

B. Reactions between ions and molecules in the gas phase.

In 1912 Thomson [5], in his study of the parabolas formed by ions in his equipment, observed a particle having a mass of 3 a.m.u. He speculated that this particle might be triatomic hydrogen. In 1916 Dempster [6] observed an ion having a mass-to-charge ratio (m/z) of 3 in the mass spectrograph of hydrogen and suggested that this might be H_3^+. Nine years later the ionization of hydrogen was studied by Hogness and Lunn [7], who also observed an ion having m/z = 3. Furthermore, they observed that the intensity of the ion-beam corresponding to m/z = 3 increased as the pressure of hydrogen increased. Similar observations were also made in 1925 by Smyth [8] who later stated [9] that the evidence suggested that H_3^+ was formed by the ion-molecule reaction

$$H_2^{+\cdot} + H_2 \longrightarrow H_3^+ + H^\cdot \qquad (1.1\text{-}8)$$

Probably the first definitive study of ion-molecule reactions was carried out by Hogness and Harkness [10] in 1928. These workers studied both the positive and negative ions formed from iodine vapour and showed that I_2^+ was formed both by electron-impact ionization and by charge transfer from I^+

$$I^+ + I_2 \longrightarrow I + I_2^+ \qquad (1.1\text{-}9)$$

and that I_3^+ was produced in the reaction

$$I_2^+ + I_2 \longrightarrow I_3^+ + I \qquad (1.1\text{-}10)$$

The only primary negative ion observed was I^-, which underwent a charge-transfer reaction with I_2 so that I_2^- was formed by the reaction

$$I^- + I_2 \longrightarrow I + I_2^- \qquad (1.1\text{-}11)$$

Furthermore, I_3^- was formed by the reaction

$$I_2^- + I_2 \longrightarrow I_3^- + I \qquad (1.1\text{-}12)$$

In 1936 Eyring, Hirschfelder, and Taylor obtained the collision frequency of reaction (1.1-8) from a theoretical treatment based upon absolute rate theory [11]. The result obtained was in excellent agreement with the experimental result measured subsequently [12].

Modern studies of ion-molecule reactions were begun in the mid - 1950's when Stevenson and Schissler [13], and Field, Franklin, and Lampe [14], in the United States, and Tal'roze and Lyubimova [15], in the U.S.S.R., all observed the formation of the CH_5^+ ion from methane (reaction 1.1-13)

$$CH_4^{+\cdot} + CH_4 \longrightarrow CH_5^+ + CH_3^{\cdot} \qquad (1.1\text{-}13)$$

Since the discovery of this reaction, interest in ion-molecule

reactions has grown at such a rate that, in recent years, the number of articles published per year on this subject alone is greater than the total number of articles on all aspects of mass spectrometry published prior to the discovery of reaction (1.1-13).

The principal types of reaction now known to occur between ions and molecules in the gas phase are charge-transfer reactions, transfers of protons, hydride ions, or atoms, and clustering processes. Examples of proton-transfer, atom-transfer, and charge-transfer reactions were given in equations (1.1-8) to (1.1-13). Examples of hydride-ion transfer are found in the reactions of carbenium ions with alkanes,

$$C_nH_{2n+1}^+ + C_mH_{2m+2} \longrightarrow C_nH_{2n+2} + C_mH_{2m+1}^+ \qquad (1.1\text{-}14)$$

These were first observed by Field and Lampe[16]. Clustering processes have been extensively studied by Kebarle[17]. Examples of such reactions are given by

$$H_3O^+ + nH_2O \longrightarrow (H_2O)_{n+1}H^+ \qquad (1.1\text{-}15)$$

An example of a two-atom-transfer reaction is the H_2^- transfer reaction [18]

$$C_3D_6^{+\cdot} + C_4H_{10} \longrightarrow C_3D_6H_2 + C_4H_8^{+\cdot} \qquad (1.1\text{-}16)$$

in which C_4H_{10} is isobutane. Other types of reaction which may occur between an ion and a molecule are energy-transfer processes, in which no chemical change is observed.

An important result obtained from early kinetic studies of ion-molecule reactions was that the rate constants of many such reactions were much larger than the collision frequencies predicted from calculations based on the assumption that the interaction

between an ion and a molecule was dominated by Van der Waals forces. Such large rate constants have recently been rationalized by the Average-Dipole-Orientation theory [19] in which ion-dipole forces are included in the ion-molecule interaction potential. Although early results suggested that many ion-molecule reactions proceeded without energy of activation, it is now realized that, while there is often no activation barrier in exothermic ion-molecule reactions, the energy of activation can be significant in endothermic reactions (vide infra).

C. Reasons for the study of ion-molecule reactions.

Ion-molecule reactions play an important role in the chemistry of flames [20], in the study of radiation chemistry [21], and the chemistry of the ionosphere [22]. Furthermore, the growing use of chemical-ionization mass spectrometry means that ion-molecule reactions are steadily becoming more important in general analytical chemistry.

An understanding of combustion processes, and in particular combustion of hydrocarbons with metal additives, is vital to any society that relies extensively upon the internal-combustion engine. Firstly, with the forseeable diminishing availability of hydrocarbon fuels, it is of paramount importance that, when they are burnt, the maximum amount of useful energy is obtained. Secondly, it is of obvious environmental importance that the concentrations of toxic metals (eg., lead) in the atmosphere should be kept as small as possible. A knowledge of the kinetics and thermodynamics of ion-molecule reactions may be of assistance

in attaining both these goals.

There are also ecological reasons for understanding the ionosphere, since it is this region which prevents dangerous high-energy solar radiation from reaching the earth's surface. The evolution of the ionosphere is largely determined by the occurrence of ion-molecule reactions. A knowledge of the ion-molecule reactions, together with other information, eg., densities of neutral gases in the ionosphere, will ultimately, it is hoped, enable the time-development of the region to be predicted. With this knowledge it would be possible to foresee, for example, changes in climatic conditions.

Very recent work has suggested that certain physiological disorders, for example, headaches and migraine, may result from the removal of negative ions from the atmosphere[23] . (Negative ions are removed from the atmosphere by central-heating systems.) It is possible then that the study of atmospheric ion-molecule reactions resulting from the use of central-heating systems may come to be of medical interest.

For the chemist, an important aspect of the study of ion-molecule reactions in the gas phase is that kinetic and thermodynamic parameters are measured in the absence of solvent. Furthermore, gas-phase studies of reactions like (1.1-15) actually give information on the solvations of ions. For example, results [24] have shown that there is no preferred value of n in the clusters $(H_2O)_nH^+$ for n = 1 to 9. As the size of such clusters is increased their behaviour approaches that of the solvated ion in the liquid phase.

Hence, in principle, information upon the behaviour of ions in liquids could be obtained by extrapolation of data obtained from the study of ion-molecule reactions in the gas phase. The significance of this work lies in the fact that, up to now, the "microscopic" details of ionic reactions in solution are little understood.

The particular reasons for the present study of ion-molecule reactions are connected with the analytical applications of such reactions, chemical-ionization mass spectrometry. These reasons are discussed in section 1.2.B.

D. Use of the relative intensities of ion-beams for the determination of the rates of ion-molecule reactions.

A mass spectrometer permits rapid and accurate measurement of the intensities of ion-beams corresponding to reactant and product ions in reaction (1.1-1), and is therefore a convenient piece of apparatus for studying the rates of ion-molecule reactions. The concentrations of ions in the ion-source are much lower than that of neutral molecules [25]. Consequently the probability of reaction between an ion and a neutral stable molecule is much larger than that of reaction between the ion and neutral fragments formed in the course of either the primary fragmentation process or the collision reactions. Furthermore, the ion-molecule reactions can be considered as pseudo-first-order processes.

The rate equation for the disappearance of reactant ions in reaction (1.1-1) is

$$-\frac{d[A^+]}{dt} = k[A^+][B] \qquad (1.1\text{-}17)$$

where k is the rate constant of the reaction. Integration of this equation gives

$$\log [A^+]/[A^+]_o = -k[B]\tau \qquad (1.1\text{-}18)$$

in which τ is the residence time of A^+ in the ion-source, $[A^+]$ is the instantaneous concentration of A^+, and $[A^+]_o$ is the concentration of the reactant ion in the absence of reaction (1.1-1). It is immediately apparent that the determination of the rate constant requires a knowledge of the ion-source pressure of the neutral species (B), the ion residence time, τ, and the concentration of the ion A^+ in the ion-source. The measurement of pressures of gases in the ion-source will be discussed in section 2.3, and the estimation of ion residence times in section 3.1.

If the appropriate scan mode is used (see section 2.2) the time spent in collecting ions of a given mass is the same for all masses, making it possible to estimate the relative concentrations of ions in the ion-source. Furthermore, the variation in width of the bases of spectral peaks is sufficiently small that the heights of the peaks are directly proportional to the areas under them. Thus, the heights of the peaks relative to one another should, in principle, directly reflect the relative concentrations of the ions in the ion-source. If this is true, then the relative concentration of an ion having m/z = n is given by $I_n/\sum I$ where I_n is the height of the relevant peak and $\sum I$ is the sum of the heights of all peaks in the spectrum (ie., the total ion current). The expression $I_n/\sum I$ will be referred to as the

relative abundance of the ion having m/z = n throughout this thesis. Equation (1.1-18) now becomes

$$\log (I_n/I_n^{\circ}) = -k[B]\tau \qquad (1.1\text{-}19)$$

provided it is appreciated here that I_n refers to the relative abundance of the corresponding ion.

For the heights of spectral peaks to reflect accurately the abundances of ions in the ion-source, the following conditions must also be valid: the efficiency with which ions are extracted from the ion-source must be the same for all ions whatever their mass and kinetic energy; the losses of ions during their passage through the various slits must be independent of the mass of the ions; and the gain of the multiplier must be independent of the nature of the ions impinging on the first dynode. None of these conditions are, however, strictly valid, and it will be seen in section 2.2 that, for the purposes of the present work some attempt has been made to minimize mass-discrimination effects arising from the ion-source and collector slit. It is unfortunate that so little data on the variation of electron-multiplier gain with the mass, kinetic energy, and atomic composition, of ions is available [4].

It is apparent from equation (1.1-19) that the rate constant, k, of a simple bimolecular reaction can be obtained by observing the variation of the relative abundance of the reactant ion, A^+, as either the concentration of neutral molecules, B, or the reaction time, τ, is varied. Kinetic data for more complicated reactions can similarly be obtained by such methods. This will be discussed in Chapter 4.

1.2 Chemical-ionization mass spectrometry.

It was stated in section 1.1.A that ions produced from bombardment of a gas by electrons, α-particles, or photons, may themselves be used to effect ionization of molecules via ion-molecule reactions. This is the principle of chemical-ionization mass spectrometry: the utilization of a specific set of ions to effect a few specific types of ion-molecule reactions with a wide variety of different compounds.

In chemical-ionization mass spectrometry[26] a gas (the so-called reagent gas) is introduced into the ion-source at a pressure generally in the range 0.1 - 2.0 torr. This gas is ionized by one of the above-mentioned methods, usually electron impact. As the gas pressure is comparatively high (cf. section 1.1.A) the resulting primary ions are able to undergo reactions with molecules of the reagent gas. The ions produced from these reactions may now react with a second substance (referred to herein as the 'sample') introduced into the ion-source. In general the pressure of the sample is kept much smaller than the reagent-gas pressure so that the extent of ionization of sample molecules directly, by the electron beam, is negligible.

The chemical-ionization technique may be illustrated by reference to isobutane, the reagent gas of choice in the present work. Ionization of isobutane by an electron beam results in the formation of the molecular ion-radical:

$$C_4H_{10} + e \longrightarrow C_4H_{10}^{\cdot +} + 2e \qquad (1.2\text{-}1)$$

This ion-radical then fragments to give the primary ions- the ions observed in the electron-impact mass spectrum of isobutane. An example of a fragmentation reaction is the reaction which results in the formation of the $C_3H_7^+$ ion*,

$$C_4H_{10}^{\dagger} \longrightarrow C_3H_7^+ + CH_3^{\cdot} \qquad (1.2\text{-}2)$$

which undergoes a hydride-transfer reaction with isobutane:

$$C_3H_7^+ + C_4H_{10} \longrightarrow C_3H_8 + C_4H_9^+ \qquad (1.2\text{-}3)$$

Similar reactions are undergone by the other primary ions with the result that at moderately high pressures (>0.15 torr) the spectrum of isobutane consists almost entirely of $C_4H_9^+$ ions. These ions are used to effect the ionization of the sample molecule †, AH. The reactant ion $C_4H_9^+$ has been found to react predominantly as a Brønsted acid, transferring a proton to the sample molecule (reaction (1.2-4)), although it may also act as a Lewis acid and either accept a hydride ion from the sample molecule (reaction 1.2-5)) or form an association complex with it (reaction (1.2-6)):

$$C_4H_9^+ + AH \longrightarrow C_4H_8 + AH_2^+ \qquad (1.2\text{-}4)$$

$$C_4H_9^+ + AH \longrightarrow C_4H_{10} + A^+ \qquad (1.2\text{-}5)$$

$$C_4H_9^+ + AH \longrightarrow C_4H_9.AH^+ \qquad (1.2\text{-}6)$$

---

* Other fragmentation reactions of $C_4H_{10}^{\dagger}$ are discussed in section 3.2.

† It is necessary here to represent sample molecules by AH, but in subsequent chapters the letter M will represent a sample molecule as this notation is more convenient there.

The ionic products of any of these reactions may decompose before leaving the ion-source. When the sample is, for example, an alcohol, ROH, reactions (1.2-4) and (1.2-5) may both occur, but the extent to which each of the reactions proceeds depends on the nature of R:

$$C_4H_9^+ + ROH \longrightarrow C_4H_8 + ROH_2^+ \qquad (1.2\text{-}7)$$

$$C_4H_9^+ + ROH \longrightarrow C_4H_{10} + RO^+ \qquad (1.2\text{-}8)$$

Furthermore, some of the ROH_2^+ ions may undergo decomposition reactions

$$ROH_2^+ \longrightarrow R^+ + H_2O \qquad (1.2\text{-}9)$$

Hence the principal ions in the chemical-ionization mass spectrum of an alcohol are likely to be R^+, RO^+, and ROH_2^+.

A wide variety of reagent gases can be used in chemical-ionization mass spectrometry, although by far the most common are isobutane, methane [27], and ammonia [28]. The principal reactant ions produced from methane are CH_5^+ and $C_2H_5^+$, while those produced from ammonia are NH_4^+ and the $(NH_3)_nH^+$ ions. Other reagent gases can be hydrogen, the inert gases, nitrogen, water, methanol, and tetramethylsilane. Review articles in which the uses of these gases are discussed have been published [29], [30], [31], [32]. Recently the use of chemical-ionization mass spectrometry involving negative ions has been realized [33].

In general, chemical-ionization spectra are far simpler than the corresponding electron-impact spectra. Furthermore, the chemical-ionization techniques often afford ions having masses near the molecular weight of the sample (eg., AH_2^+ or A^+) which are comparatively stable. Whereas an electron-impact mass

spectrum of a sample may often not show the presence of molecular ions, the corresponding chemical-ionization mass spectrum will most likely indicate ions from which a molecular weight may be deduced. In addition, ions produced by chemical-ionization processes undergo decomposition reactions (eg. reaction (1.2-9)) which are more easily rationalized than are many of the fragmentation processes associated with electron-impact ionization.

A great deal of current research into chemical-ionization mass spectrometry is being directed towards finding reactant ions (both positive and negative) which react with specific types of compounds. An example of such an ion is NH_4^+ which will protonate $\alpha\beta$-unsaturated ketones, but undergoes only addition reactions with saturated ketones [34].

Chemical-ionization mass spectrometry is an important analytical method in all those areas of research in which electron-impact mass spectrometry has previously been a principal method of analysis. It is finding a particular importance in the analysis of natural products [35] and in applications in forensic science [36]. From these fields, the data obtained from chemical ionization is very often complementary to that obtained from electron-impact ionization. Taken together the two techniques provide an extremely powerful analytical method.

1.3 Methods available for the study of the kinetics of ion-molecule reactions in the gas phase.

A. Introduction.

Some of the more common methods for the study of the kinetics of ion-molecule reactions are described in this section. Only a brief outline of each of the techniques will be given, together with some indication of possible sources of error and of the information available from each method. Although the description of each technique is brief, the references given will provide details of the construction and usefulness of the instruments. Recent reviews of the methods include those by Wilson[31], Franklin [37], and Jennings [33].

It was shown in section 1.1.D that the kinetics of ion-molecule reactions may be studied by observing the variation of the relative abundances of ions as either the concentration of the neutral species, or the reaction time, is varied. These two procedures form the basis of all the techniques described below.

B. Continuous Ion-Extraction Mass Spectrometry.

All mass-spectrometric techniques in which ions are formed continuously in the ion-source, and are continuously extracted from the ion-source by an accelerating field, are referred to generally as continuous ion-extraction techniques. Electron-impact mass spectrometry, chemical-ionization mass spectromoetry and high-pressure mass spectrometry are examples of such techniques. The term 'high-pressure mass spectrometry' is used when pressures

in the ion-source are greater than ca. 10^{-3}torr.

As electron-impact mass spectrometry has been discussed in section 1.1.A, and chemical-ionization mass spectrometry in section 1.2.A, no further description of the methods need be given here. This section will be used, however, for a discussion of the possible sources of error inherent in the determination of rate constants by continuous ion-extraction methods. This is important as the method was used for the determination of rate constants in the present work.

At best, continuous ion-extraction methods yield experimental rate constants, k_{exp}, which are time-averaged rate constants:

$$k_{exp} = \frac{1}{\tau} \int_0^{\tau} k(t)dt \qquad (1.3\text{-}1)$$

where k(t) is the rate constant which would be obtained if all the reactant ions remained in the ion-source for exactly the same length of time, t, and τ is the ion residence time. For this condition to hold, all the reactant ions should be formed with no excess energy at the same distance from the ion-exit slit, and should drift from their point of formation under the influence of a constant electric field to the exit slit. Thus, for electron-impact ionization, the nature of the time-average is not defined unless the following assumptions are valid :-

(1) the electron beam is infinitely narrow;

(2) the ion initially has zero energy;

(3) the electric field in the ion-source is constant.

If these assumptions are valid, then

$$t = v\tau/v_e \qquad (1.3\text{-}2)$$

where v is the instantaneous velocity of the ion, and v_e is the exit velocity of the ion. Under these conditions, the measured rate constant is characteristic of the reaction and independent of the particular conditions of the measurement. In this case k_{exp} is identified with $k(v_e)$, a rate constant which is a velocity-average of a rate constant, k(v), and which depends on the ion velocity, v. Thus

$$k_{exp} = \frac{1}{v_e} \int_o^{v_e} k(v)dv \qquad (1.3\text{-}3)$$

The rate constants obtained from continuous-extraction mass spectrometry may be compared with rate constants obtained from other methods only if the three assumptions stated above are valid, and then only if the exit velocity of the ion is the same in both cases. If the assumptions are not valid then the experimental rate constant may show a dependence upon the conditions of the measurement, and may be in error by as much as a factor of two [38]. Details of experiments which test the validity of assumptions (1) -(3) are given by Henchman[38].

A major obstacle to the determination of accurate rate constants from high-pressure mass spectrometry is a consequence of the occurrence of reactions throughout an energy range $0 \leq E \leq E_e$, where E_e is the exit energy of the ions. Furthermore, the energy distribution is pressure-dependent owing to the attenuation of the reactant-ion beam along the reaction path.

Rate constants determined from chemical-ionization mass spectrometry are likely to be somewhat more accurate than those determined from high-pressure mass spectrometry. Since,owing to

the sample pressure being much smaller than the total ion-source pressure, the distribution of energies in a given type of reactant ion will be essentially independent of the nature of the sample. The energy distribution will be the same for given conditions of temperature, reagent-gas pressure, electric-field strength, and electron energy, so that rates of reaction of samples with a given reactant ion should be correct relative to each other. Furthermore, if a rate constant is obtained from an experiment in which the sample pressure is varied over a comparatively small range while the reagent-gas pressure is held constant, then the effects of the pressure-dependence of the reactant-ion energy distribution will be negligible.

Despite this, the measured rate constant may still be in error by as much as a factor of two as a consequence of the lack of validity of assumptions (1) -(3). Such an error is not, perhaps, too serious for the purposes of the present work, provided relative rates are accurate. These problems are discussed further in section 1.4.

C. Pulsed-ion-source mass spectrometry.

Probably the earliest technique developed for the specific purpose of evaluating rate constants was pulsed-ion-source mass spectrometry [39]. In this technique an electron beam is passed through a gas in the ion-source for a brief period (ca.0.1 μsec). During this time ions are formed from the gas. After the electron-beam has been switched off, ions may be retained in the ion-source for a measurable 'delay' period, before being extracted and

analyzed. This delay period may be varied from zero to a few microseconds. Ions are extracted by application of a voltage pulse of the appropriate sign either to a repeller plate, or to an ion-withdrawal plate, or to both simultaneously. In this method reaction rates are determined by observing the variation of ion-abundances as the delay time is varied.

One of the problems associated with the method is that the extraction pulse can exert mass-discrimination effects, and the magnitudes of such effects increase as the delay time is increased. The effects are due, at least in part, to the fact that rates of diffusion away from the sampling region are different for different ions. They can, however, be minimized by working with delay times for which loss of ions by diffusion is small (ca.0-2μsec).

It is also difficult to employ this method with high ion-source pressures since reactant and product ions are scattered differently when the ejection pulse is applied. Despite such problems, thermal rate constants with an error as small as 10 to 20% can be obtained from the method.

An elegant variation of the pulsing technique is the so-called trapped-ion method which was originally suggested by Baker and Hasted [40] and developed by Harrison [41]. In this method ions are produced by an electron-beam pulse of ca.1 μsec. These ions are then held for a variable delay time in the space-charge well generated by the passage of a low-energy (ω4 eV) beam of electrons through the ion-source. During this storage period reactive collisions may occur between the trapped ions

and neutral molecules flowing through the ion-source. The trap is then destroyed by applying a voltage pulse to the repeller plate, thus ejecting ions from the ion-source. Delay times as long as 0.01 seconds are readily achieved.

An important feature of the technique is that rate constants may be measured under conditions for which the translational energy of reactant ions is significantly less than 0.1 eV. Furthermore, the technique may be incorporated at low cost into any conventional ion-source to give it chemical-ionization capabilities at low pressure.

D. Drift-tube mass spectrometry.

In a drift-tube ion-source[42], ions are formed by electron-impact ionization of a gas at one end of a tube several centimetres in length. The tube is constructed with a series of metal rings electrically insulated from one another. After formation in the ionization region, the ions drift down the tube under the influence of an electric field produced by applying steadily decreasing voltages to the metal rings. At the end of the drift tube the ions pass through an exit slit into the mass spectrometer analyzer region. If the pressure in the drift tube is sufficiently large, and the field strength sufficiently small, then the mean energy of collisions of ions with neutral molecules is low, and hence rate constants are determined at near-thermal conditions.

An important feature of this method is that a characteristic drift velocity is established in the drift tube, and hence the

spatial and velocity distributions of the ions are well defined. The reaction region is well separated from the ion-source region and is sufficiently large that, either the reaction path length may be altered by using a movable ion-source [43], or the reaction time may be varied by reversal of the field [44]. By altering these two parameters the individual contributions of drift, diffusion, and reaction, to the experimental data may be obtained.

The advantage of being able to carry out experiments over a wide range of pressure is that it aids identification of kinetic orders of reaction. Furthermore, the rates of slow reactions can be obtained from work conducted at high pressures.

E. Ion-Cyclotron-Resonance Spectrometry.

An ion-cyclotron-resonance spectrometer [45] consists of a cell (typical dimensions 1 x 1 x 5 inches) which is placed in a magnetic field. Ions are generated by electron-impact ionization of a gas at one end of the cell and drift through it under the influence of crossed electric and magnetic fields into the so-called resonance region. In this region the ions are irradiated by an alternating electric field.

The motion of a free charged particle in a uniform magnetic field B is constrained to a circular orbit of angular frequency ω_c in a plane normal to B, and is unrestricted parallel to B. The cyclotron frequency, ω_c, is given by

$$\omega_c = \frac{zB}{mc} \qquad (1.3\text{-}4)$$

where z is the charge of the particle, B is the magnetic field strength, m is the mass of the particle, and c is the velocity of light. If an alternating electric field with frequency ω_1 is applied normal to the magnetic field and the latter is scanned an ion will absorb energy when ω_c becomes equal to ω_1. Thus a spectrum linear in mass can be obtained by scanning the magnetic field while irradiating with an alternating electric field of constant frequency.

If, in an ionized gas, a reaction of the type

$$A^+ + B \longrightarrow C^+ + D \qquad (1.3\text{-}5)$$

occurs, then both C^+ and A^+ can be detected by the method given above. Furthermore, if a second alternating electric field of frequency ω_2 is applied such that ω_2 is the cyclotron frequency of A^+, then a significant change in the absorption of energy by C^+ will occur as the reactant ion, A^+, is energized. This double-resonance technique thus provides a simple means of identifying reactant ions in a reaction mixture, even in the presence of competing processes.

The unique feature of ion-cyclotron-resonance spectrometry is its mode of ion detection and measurement. Since the ions are detected <u>in situ</u> in the reaction cell problems of mass discrimination, which arise during extraction and analysis in other mass spectrometric methods, are eliminated.

F. Flowing-afterglow mass spectrometry.

Flowing-afterglow mass spectrometry was devised by Ferguson and his associates [46] in 1969 for the purpose of studying ion-molecule reactions at thermal energies. In this technique ions are formed, either by passage of an electron beam, or by an electric discharge, through one of the inert gases. These ions then flow down a tube (the 'flight tube') through which a stream of the gas is passing. The time of flight of the ions is determined by the rate of flow of the gas. Now suppose it is required to study the ion-molecule reaction

$$A^+ + B \longrightarrow \text{products} \qquad (1.3\text{-}6)$$

in which A^+ is an ion which can be formed by charge-transfer reactions of the above inert-gas ions with a gas C. Then molecules of the gas C are injected into the 'flight-tube' such that they undergo just this reaction with the inert-gas ions. The A^+ ions so produced are allowed to come to thermal equilibrium with the main body of gas by flowing a few centimetres downstream, at which point molecules of the gas B are introduced into the stream of gas. Reaction (1.3-6) proceeds during the remaining time in the flight tube and the ions are sampled at the end of the tube into a quadrupole mass filter. Obviously it is a simple procedure to vary the temperature of the system, and thus to study the influence of temperature on reaction rate.

Not only is the technique particularly useful for the

study of ion-molecule reactions at thermal energies, but it is possible to introduce neutral species such as atoms or free radicals into the flowing afterglow, and to study their reactions with various ions in the system. Indeed, this is the only technique that has been successful in studying ion-molecule reactions involving unstable neutral species.

1.4 Reasons for the study of the kinetics of ion-molecule reactions in chemical-ionization mass spectrometry.

It was shown in the section 1.3.B that chemical-ionization mass spectrometry is not a good method for the study of the kinetics of ion-molecule reactions. Rate constants obtained from the method are time-averaged rate constants, and the details of the averaging process are ill-defined. Furthermore, reactions occur throughout a range of energies as a result of the energy distribution of the reactant ions.

Nevertheless there is a growing, general need for quantative data on the processes which occur in the chemical-ionization ion-source. This data is best obtained from chemical-ionization studies per se, since data obtained from another, albeit a "better", method is liable to be inapplicable. (For example, thermal-energy rate constants of reactions whose rates depend on reactant-ion energy cannot be applied to the chemical-ionization process for which reactant-ion energies are considerably larger than thermal.) It should be added, therefore, that because the data is critically dependent upon the conditions of measurement, these conditions must be known accurately. The important parameters are electron energy, repeller voltage and electric field strength, reagent-gas pressure, sample pressure, and ion-source-block temperature. The accelerating voltage may also be important as there is often penetration of the accelerating field through the ion-exit slit into the ion-source.

Although rate constants obtained from chemical-ionization

mass spectrometry may not be correct in an absolute sense, they are likely to be of more use to practitioners of the technique than rate constants obtained from the other techniques described in section 1.3.

A difficult problem associated with the study of the kinetics of ion-molecule reactions in chemical-ionization mass spectrometry is the estimation of mean residence times of ions. Probably the best solution of this problem is that recently employed by Field [47]. In his work he has studied chemical-ionization processes in both a continuous-extraction, and a pulsed, ion-source. Such a study will give information on mean residence times of the reactant ions, together with, in principle, comparisons with other chemical-ionization experiments. Unfortunately, it was not feasible to obtain ion residence times by a pulse technique in the present work, with the result that it was necessary to use estimates obtained from either the free-fall formula or from ion mobilities.

CHAPTER 2

EXPERIMENTAL

2.1 Chemicals.

The reagent gases methane (Matheson Gas Products; 99.97%) and isobutane (B.O.C.; 99.5%) were used without further purification. The chemicals used in the mass-spectrometric studies were all liquids; these were dried over molecular sieve, type 4A, prior to use. Those having manufacturers' stated purities of 99% or less were distilled at atmospheric pressure after drying.

2.2 The V.G. Micromass 12F mass spectrometer.

The V.G. Micromass 12F mass spectrometer[48] is a 60^{o}, 12.7 cm radius, magnetic sector instrument in which mass analysis is achieved by varying either the strength of the magnetic field (magnet scanning) or the accelerating voltage (voltage scanning). All spectra reported in this work were produced by scanning the magnetic field, the accelerating voltage being maintained constant at 4000 V.

A schematic diagram of the ion-source of the mass spectrometer is given in figure (2.1). The ion-source chamber consists of a cavity (C) milled out of a stainless-steel block (B). An electron-beam is produced by an emission-regulated filament (F) mounted outside the ion-source block.

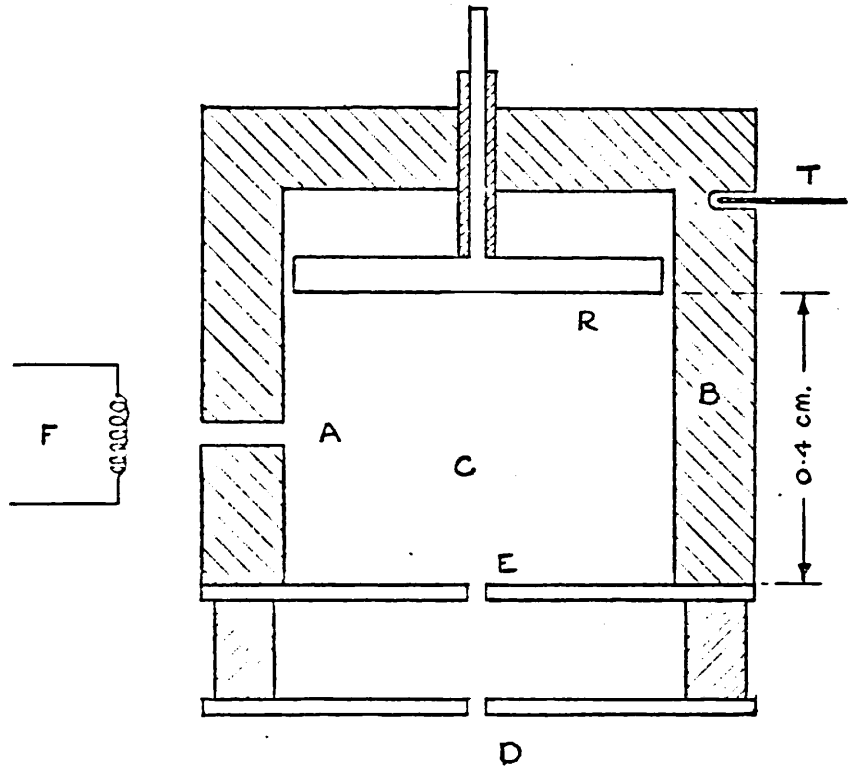

FIGURE (2-1). Schematic diagram of the ion-source of the Micromass 12F spectrometer.

The beam enters the ion-source through a cylindrical aperture (A) of length 2mm and internal diameter 0.5mm*. Ions formed in C leave the ion-source through the ion-exit slit, E. The drift of positive ions towards the exit slit is often assisted by maintaining the potential on the repeller plate (R) positive with respect to the exit-slit plate,E. The ion-exit slit, which is cut in the thin stainless steel plate E, has dimensions of 0.05mm x 5.0mm.

Two further modifications were made to the standard instrument. First, the temperature of the ion-source block, which has a heater embedded in it, was monitored by means of a chromel-alumel thermocouple (T) connected to an electronic thermometer[49]. This enabled temperature measurement to be accurate to $\pm 1^{o}C$. Secondly, the electron-beam collimating magnets, originally fitted to the ion-source, were removed since the presence of magnetic fields in the ion-source is known to give rise to mass-discrimination effects (see section 1.1.D.).

The entire ion-source assembly is contained in an evacuated chamber. The pressure in this chamber was generally lower than 5×10^{-5}torr. Reagent gases and vaporized samples are introduced into the ion-source via ports bored through the ion-source block. These ports are omitted from figure (2.1) for clarity. The reagent-gas-inlet and sample-inlet systems are designed to form gas-tight seals with the ion-source block.

---

* The original electron-entrance aperture was kindly modified for us by the manufacturers to allow higher ion-source gas pressures to be developed.

The Micromass 12F spectrometer has three sample-inlet systems; samples may be introduced into the ion-source from a g.l.c. column, by way of a jet separator, on a direct-insertion probe, or through a septum-inlet system. In the experiments reported in this work all samples were introduced through the septum-inlet system, a schematic diagram of which is given in figure (2.2).

A known volume of volatile liquid sample is injected into the heated, evacuated reservoir (R) and is vaporized. The vapour flows through the heated narrow-bore delivery tube (T) into the ion-source. The flow-rate through the delivery tube is sufficiently slow that there is no measurable change in the total-ion current (see section 1.1.D) and hence in the pressure of sample in the ion-source (see section 2.5), during a period of at least ten minutes after injection of the sample into the reservoir.

Positive ions formed in the ion-source are accelerated by a potential difference of 4000 V applied between plates E and D (see figure (2.1)), and the resulting ion-beam is then analyzed by the magnetic field (see section 1.1.A). The focussed ion-beams, separated according to the differing momenta of the ions, pass through a collector slit and strike the first dynode of a 17-stage electron-multiplier tube. Both the collector and the electron-multiplier are known to introduce mass-discrimination effects into the mass spectrum. To minimize the first of these effects, the collector slit was adjusted to its maximum width (ca.1 mm). The lower instrumental resolution obtained using a wide collector slit did not seriously affect the spectra below m/z $\sim$ 250 a.m.u., and

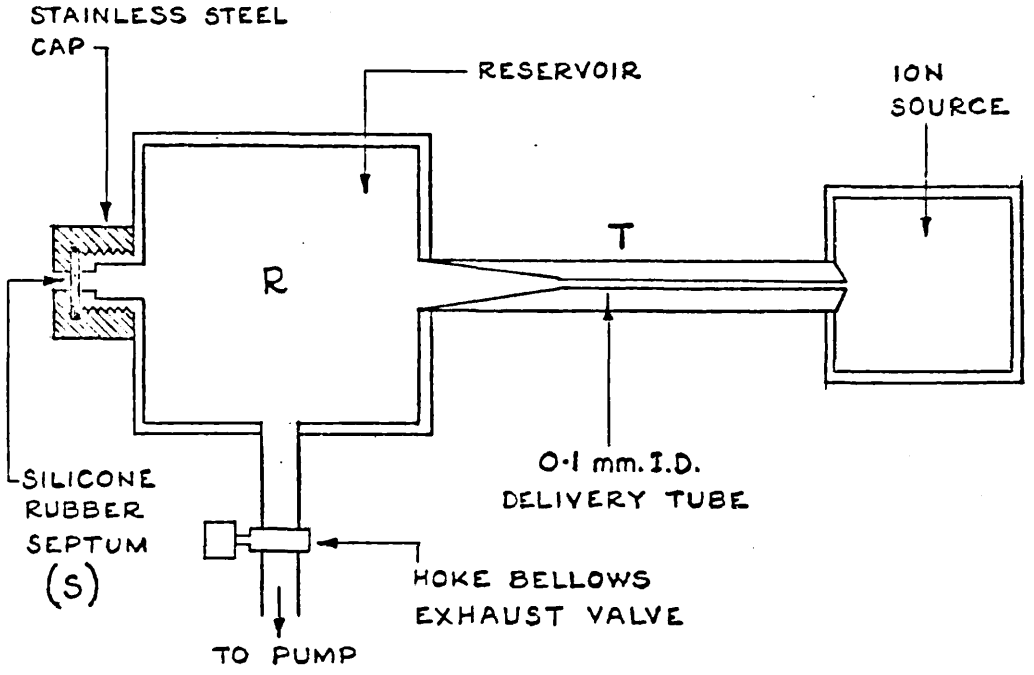

FIGURE (2-2). Schematic diagram of septum-inlet system.

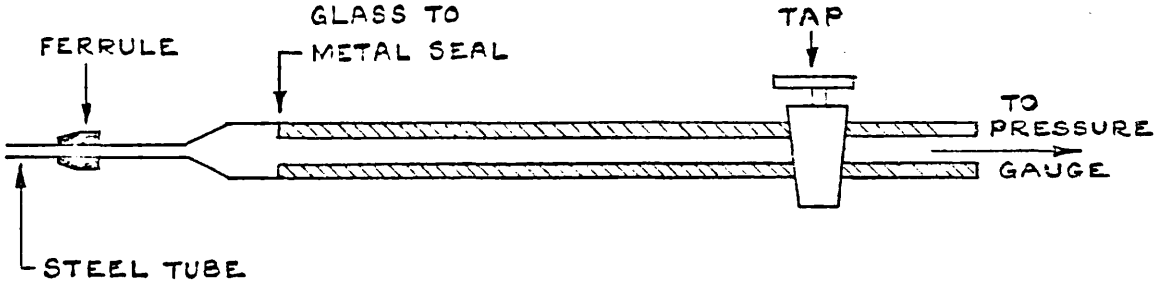

FIGURE (2-3). Probe used to connect pressure gauge to ion-source.

furthermore the samples studied did not produce ions having m/z greater than this value. By comparison, it is difficult to make corrections for mass-discrimination effects arising from the use of an electron-multiplier as a detector. The gain of multiplier tubes is known to depend on not only the mass but also the kinetic energy, and the elemental composition of the ions striking their first dynode [4]. Insufficient data is presently available to allow general corrections for discrimination effects to be made. This problem is discussed further in section 4.2.

The output from the electron multiplier was first amplified then recorded using an oscillograph 3005 recorder [50]. In this instrument three galvanometer mirrors reflect U.V. light onto photo-sensitive paper. The traces produced correspond to three attenuations, x0.01, x0.1 and x1, of the amplified ion-currents. For convenience the galvanometers will be numbered (1), (2), and (3), corresponding to attenuation factors of x0.01, x0.1 and x1.0 respectively.

In succeeding sections it will be assumed that heights of peaks in the mass spectra reflect the abundances of ions in the ion-source. This is an approximation since, at best, it is the areas under the peaks that reflect the ion-abundances. For the mass range covered (<250 a.m.u.) the variation in width of the bases of the peaks was so small that the error introduced by the above assumption is negligible. Peak heights were measured by laying a transparent ruler over the peaks and reading to the nearest 0.5 mm. The maximum relative errors incurred in the

measurement of heights of peaks recorded by galvanometers (1) and (2) were ca. 1%. Although the maximum relative error incurred in the measurement of the height of a peak recorded by galvanometer (3) was as high as 10%, the absolute error was probably not greater than 1% since the peaks themselves were small.

It was found that, for a given amplifier output current, the peak heights recorded by the three galvanometers were not exactly in the expected ratio 1:10:100. A calibration experiment was therefore carried out so that peak heights recorded by galvanometers (1) and (2) could be corrected to the heights that would have been obtained had all the peaks been recorded by galvanometer (3). A signal current was fed into the recorder and the deviations recorded by galvanometers (1) and (2) were measured. This process was repeated with signal currents of various magnitudes over the widest possible range. An exactly similar process was employed to check the deviations recorded by galvanometers (2) and (3) against one another. The data from these experiments were used to obtain equations which enable the peak heights (h_1, h_2) recorded by galvanometers (1) and (2) to be corrected to the value (h_3) which would have been recorded by galvanometer (3):

$$h_3 = 10 \times ((1.071 \pm 0.018)\, h_2 - (0.040 \pm 0.007)) \qquad (2.2\text{-}1)$$

$$h_3 = 100 \times ((0.971 \pm 0.025)\, h_1 - (0.438 \pm 0.008)) \qquad (2.2\text{-}2)$$

Spectra reported in this work were obtained by scanning the magnetic field exponentially from high to low field, ie. such that

$$m = m_o \exp(-t/T) \qquad (2.2\text{-}3)$$

where m is the mass of the ions collected at time t, m_o is the mass of the ions collected initially, and T is the time constant of the scan (ie. the time required to scan one decade of mass units). Differentiation of equation (2.2-3) gives

$$dm = - m_o \exp(-t/T)\, dt/T$$

Therefore

$$dt = Tdm/m \qquad (2.2\text{-}4)$$

Thus the time spent collecting ions of mass m, dt, is dependent upon the reciprocal of the resolution (m/dm) of the instrument, and the time constant T. Since dt is independent of m the heights of the various peaks in a given spectrum may be compared with one another provided mass-discrimination effects are small. Spectra reported herein were recorded using a time constant, T, of 30 sec/decade since the slow scan-rate results in better reproducibility of spectra. The only apparent disadvantage of this slow scanning was that occasionally the sensitivity of the instrument changed <u>during</u> the recording of a spectrum, thus distorting the ratios of peak heights. Allowances for this effect were made by duplicating spectra whenever it was observed that the sensitivity had changed.

2.3 Measurement of pressures of gases in the ion-source.

A. The pressure gauge.

Gas pressures in the ion-source were measured by means of a Bourdon-tube gauge (Texas Instruments, model 144)[51]. The Bourdon tube consists of a quartz spiral, sealed at one end, and contained in an evacuated glass envelope. Gas is introduced into the spiral and causes a torque to be exerted on it. The magnitude of the torque, which is proportional to the pressure of the gas, is measured by means of a mirror attached to the sealed tip of the spiral. A beam of light is reflected from the mirror and detected by a photocell that is able to move in an arc around the tube. Then, providing the tube is suitably calibrated, the movement of the mirror may be directly related to the pressure of the gas in the spiral.

B. Calibration of the pressure gauge.

The pressure gauge was calibrated against the vapour pressures of camphor and of ice. The vapour pressures of these substances over a range of temperatures are known accurately[52].

Camphor was sublimed twice, then freed from volatile impurities such as air and water by a series of freeze-pump-thaw cycles. A tube containing the pure camphor was attached to a gas line connected to the pressure gauge and the system evacuated to a pressure less than 10^{-3} torr (measured by means of a McLeod Gauge).

The tube was immersed in water contained in a Dewar vessel. The temperature of this water-bath was measured by a thermometer that had been calibrated at the National Physical Laboratory. The thermometer was accurate to ± 0.1°C. The water-bath was cooled by adding ice and, when the temperature was steady, the reading on the pressure gauge was recorded. This process was repeated at various temperatures in the range 0.5 to 20.7°C. Ambient temperature was not less than 22°C. The vapour pressure of camphor was obtained from the equation [52]

$$\log_{10} p = \frac{-0.2185A}{T} + B \qquad (2.3\text{-}1)$$

in which A is the molar heat of vaporization of camphor (12800.9 cal $mole^{-1}$), B is a constant (8.7990), and T is the temperature in degrees absolute. The equation gives the vapour pressure, p, in torr. A plot of calculated vapour pressures (p) against readings (G) taken from the pressure gauge was a straight line. Least-squares analysis of the data resulted in the equation

$$p = (0.875 \pm 0.011)\ G + (0.005 \pm 0.002) \qquad (2.3\text{-}2)$$

which enables the gauge readings to be converted to pressure (in torr).

The vapour pressure of camphor at 20°C is approximately 0.2 torr, and the temperature of the solid camphor may not be raised above the temperature of the gas line (ca.22°C) as sublimation occurs. Hence the gauge was able to be calibrated only for pressures in the range 0-0.2 torr by reference to the vapour pressure of camphor. In order to extend the calibrated pressure range of

the gauge, a second calibration was carried out. Distilled deionised water was degassed by a series of freeze-pump-thaw cycles. A tube containing the water was attached to the gas line in place of the tube containing camphor. The tube was now immersed in a slush-bath of known temperature (measured by an accurate thermometer) and the system evacuated as before. By using slush-baths of different compositions a series of gauge readings at various temperatures in the range -28.8°C to -12.8°C were obtained. The vapour pressures of ice at the required temperature were found from tables [52]. Least-squares analysis of the data resulted in equation (2.3-3):

$$p = (0.876 \pm 0.007)\ G + (0.005 \pm 0.007) \qquad (2.3\text{-}3)$$

The pressure range calibrated by reference to the vapour pressure of ice was 0.3 to 1.5 torr. It can be seen that there is good agreement between equations (2.3-2) and (2.3-3).

C. Connection of the pressure gauge to the ion-source.

The pressure gauge was connected to the ion-source by means of a glass probe inserted into the mass spectrometer through the port normally used for the direct-insertion probe. A schematic diagram of this probe is given in figure (2-3)*. The end of the probe which made contact with the ion-source consisted of a narrow metal tube to which was brazed a metal ferrule. This ferrule ensured that a gas-tight seal was made between the probe and the ion-source block. The metal tube was sufficiently long that it penetrated into the cavity C (see figure 2-1). Since,apart

---

* See page 35.

from the tip, the probe was of a glass construction, ion-source pressures could be measured with the mass spectrometer in operation even though the ion-source is then raised to a potential of 4000 V.

2.4 Measurement of ion-abundances: the ion-molecule reactions consequent upon the electron-impact ionization of pure gases.

Ion-molecule reactions consequent upon the electron-impact ionization of the pure gases methane and isobutane were studied with the pressure gauge connected to the ion-source. Prior to the commencement of any experiment the septum in the septum-inlet system (figure 2-2) was replaced to ensure that air did not leak into the ion-source.

A. Methane.

The study of the kinetics of the reaction

$$CH_4^{+\cdot} + CH_4 \longrightarrow CH_5^+ + CH_3^{\cdot} \qquad (2.4\text{-}1)$$

was initially carried out using a repeller voltage of 5.0 V (corresponding to an electric field strength of 12.5 V cm^{-1}), and with an ion-source block temperature of 177 ± 2°C. In the first experiment the electron energy was 50 eV, and the emission current was 50 μA. Anomalous results, were, however, obtained from this experiment (see section 3.1), and a second experiment was carried out in which the electron energy was 500 eV, and the emission current was 10 μA. In these experiments methane was allowed to flow into the ion-source at a steady rate and the pressure was measured using the Bourdon-tube pressure gauge. When the

pressure had attained a constant value, a mass spectrum was recorded as described in section 2.2. The pressure of methane in the ion-source was then changed, and another spectrum recorded. In this way spectra of methane were recorded at various pressures in the range 0 - 0.3 torr. Heights of peaks in the spectra were measured as described in section 2.2, and corrected for the different responses of the galvanometers by use of equations (2.2-1) and (2.2-2) . The relative abundance, at a given methane pressure, of ions having m/z = n was obtained by dividing the height of the appropriate peak by the sum of the heights of all the peaks in the spectrum recorded at the given pressure.

The kinetics of reaction (2.4-1) was also studied using repeller voltages of 1.0, 2.0, 3.0 and 4.1 V. In these experiments the electron energy and emission current were 50 eV and 50 μA respectively, and the temperature of the ion-source block was 177 ± 2°C. The results of these experiments will be discussed in sections 3.1 and 4.1. In section 3.1 it will be seen that the variation of the relative abundances of CH_4^+ and CH_5^+ with methane pressure allows the determination of the rate constant of reaction (2.4-1).

B. Isobutane.

Experiments to study the ion-molecule reactions consequent upon the electron-impact ionization of isobutane were carried out with the repeller voltage adjusted to 2.0 V, corresponding to an electric-field strength of 5 V cm^{-1} in the ion-source. In these experiments the electron energy was

50 eV, and the emission current was 50 μA. The temperature of the ion-source block was 162 ± 2°C. Isobutane was allowed to flow into the ion-source at a steady rate and the pressure was read on the gauge. When the pressure had attained a constant value a mass spectrum was recorded as described in section 2.2. The pressure of isobutane in the ion-source was then changed, and another spectrum recorded. In this way spectra of isobutane were recorded at various pressures in the range 0 - 0.3 torr. Heights of peaks in the spectra were measured as described in section 2.2, and corrected for the different responses of the galvanometers by use of equations (2.2-1) and (2.2-2). The relative abundance, at a given isobutane pressure, of ions having m/z = n was obtained by dividing the height of the appropriate peak by the sum of the heights of all the peaks in the spectrum recorded at the given pressure. The results of these experiments will be discussed in sections 3.2 and 4.1.

2.5 Estimation of pressures in the ion-source due to samples introduced through the septum-inlet system.

A description of the septum-inlet system was given in section 2.2. The sample pressure generated in the ion-source when a few microlitres (<10) of sample was injected into the inlet-system reservoir was too small to be measured directly using the gauge. Hence a method of estimating sample pressures in the ion-source was devised.

For many compounds a sample volume of 15 - 25 μl gave a

small, but measurable, pressure in the ion-source. Graph (2-1) shows that the ion-source pressure generated by four representative compounds increased in direct proportion to the volume of sample injected into the reservoir. For sample volumes in the range 1 to 12 µl the total ion current produced by the electron-impact ionization of a compound was found to be directly proportional to the sample volume, provided the compound did not undergo reactions with the ions produced. Graph (2-2) shows the variation with sample volume of the total ion current generated by the electron-impact ionization of m-xylene, diethyl ether, and 2,2,4 - trimethyl pentane. (These compounds were chosen for their lack of reactivity with the ions produced from them.) The linear relationship between total ion current and sample volume suggests that the amount of sample in the ion-source increases in direct proportion to the sample volume. It was also found that the total ion current did not change during a period of at least 10 minutes after injection, suggesting that the ion-source pressure was constant during a period significantly longer than the time required to produce a mass spectrum. It can be seen that the ion-source pressure per microlitre, and hence per mole, of a sample can be calculated from the pressure measured for a known sample volume in the range 15 - 25 µl. This has been carried out using 18 compounds having a wide range of functional groups, boiling points, densities, and molecular weights. The pressure measurements were actually taken with an accurately known pressure of approximately 0.15 torr of isobutane in the ion-source. Throughout these experiments the temperature of the

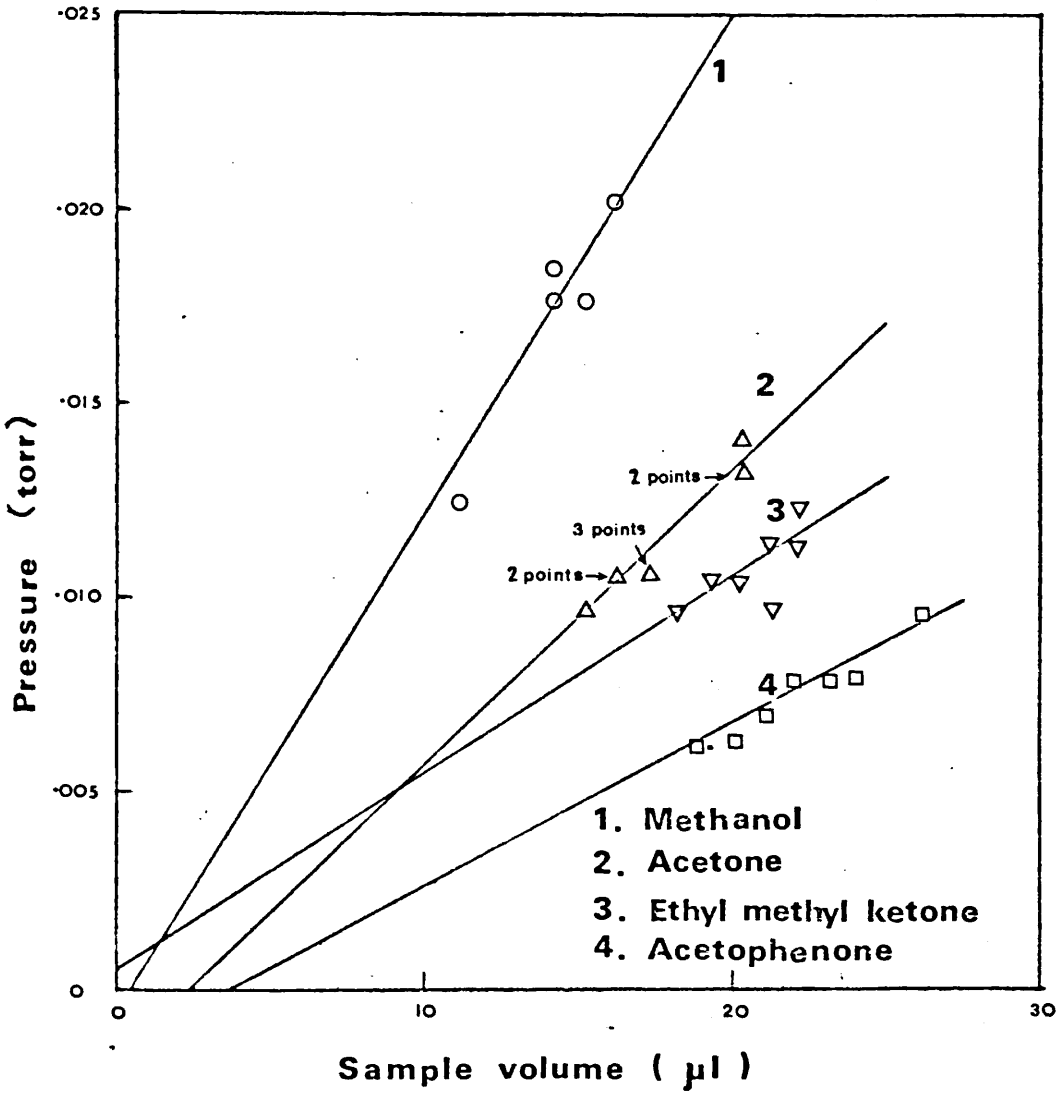

GRAPH (2-1) Plots of ion-source pressure against sample volume.

(Intercepts are within the error limits of (2.3-2)).

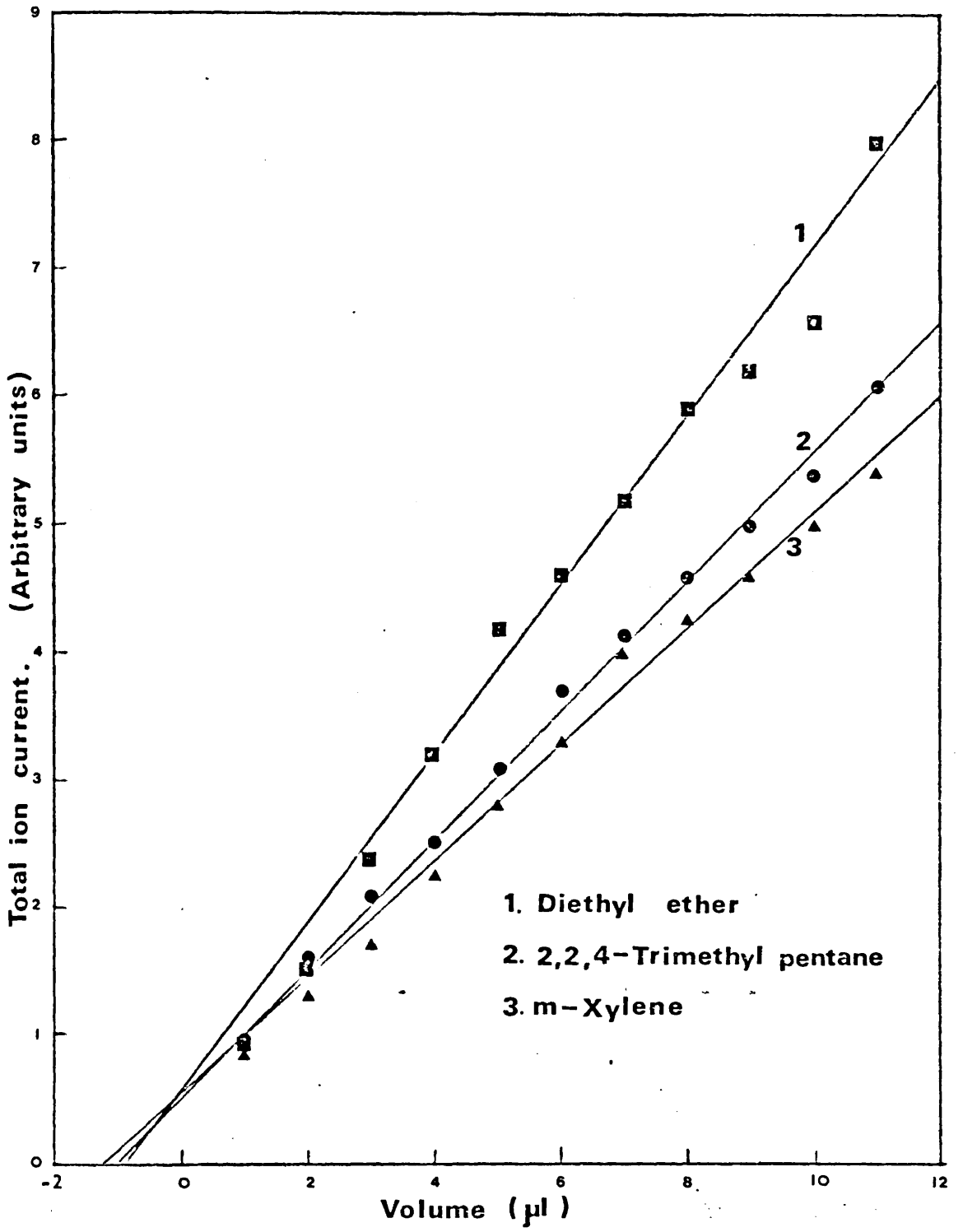

GRAPH (2-2) . Plots of total ion current against sample volume for three compounds.

inlet-system reservoir and delivery tube were maintained at 170 ± 5°C and 130 ± 2°C respectively. Results are given in table (2-1) from which it is apparent that the ion-source pressure per mole generated by each of the compounds is independent of the chemical and physical properties of the compound, and depends only on the molar quantity injected into the reservoir. The mean ion-source pressure per mole was found to be 46.5 ± 1.8 torr.

For the construction of graph (2-2), the sample volume was taken as the volume read directly from the syringe. Since, however, the inlet-system reservoir is permanently evacuated the sample volume actually includes the volume of liquid in the syringe needle. The results show that the volume of the syringe needle is 0.99 ± 0.12 µl. In subsequent experiments the volume of the syringe needle was taken as 1 µl.

2.6 Measurement of ion-abundances in the ion-molecule reactions which give rise to the chemical-ionization mass spectra of organic compounds when isobutane is the reagent gas.

The ion-molecule reactions which give rise to the chemical-ionization mass spectra of various organic compounds (see section 1.2.4) were studied by following changes in the abundances of reactant ions with variation in either the sample pressure, or the pressure of water, carbon tetrachloride, or ethyl methyl ketone introduced in addition to the sample, or, in one case, with variation of the isobutane pressure. Prior to the commencement

Table (2-1)

Ion-source pressures generated by various compounds.

Compound	Molecular weight	Density ρ_4^{20}(g cm^{-3})	Pressure/μl (10^4x torr)	Pressure/mole (torr)
Water	18.02	0.998	27.86±0.94	50.3±1.7
Methanol	32.04	0.791	12.21±0.97	49.4±3.9
Acetonitrile	41.05	0.786	9.18±0.98	47.9±5.1
Ethanol	46.07	0.789	8.42±0.71	49.1±4.1
Acetone	58.08	0.790	6.45±0.28	47.4±2.1
2-Propylamine	59.11	0.889	7.49±0.56	49.8±3.7
Methyl ethyl ketone	72.12	0.805	5.38±0.36	48.2±3.2
Butyraldehyde	72.12	0.817	5.24±0.15	46.2±1.3
Methyl acetate	74.08	0.933	5.69±0.16	45.1±1.3
Diethyl ether	74.12	0.714	5.25±0.40	54.5±4.2
Ethyl acetate	88.12	0.900	4.56±0.29	44.6±2.8
Cyclohexanone	98.15	0.948	4.31±0.35	44.6±3.6
Acetylacetone	100.13	0.972*	4.20±0.11	43.2±1.1
Methyl iso-butyl ketone	100.16	0.798	3.15±0.12	39.5±1.5
m-Xylene	106.17	0.864	3.80±0.48	46.7±5.9
Acetophenone	120.16	1.028	3.48±0.30	40.6±3.5
Benzyl acetate	150.18	1.055	3.16±0.36	44.9±5.1
3-Bromoanisole	187.04	1.456†	3.44±0.15	44.1±1.9

* ρ_4^{25}, ρ_4^{20} not listed.

† Density of 4-Bromoanisole; density of 3-bromoanisole not listed.

of any experiment, the septum in the inlet system (see figure 2-2)) was replaced. In all experiments the electron energy was 50 eV, the emission current was 50 μA, and the repeller voltage was 2 volts, corresponding to an electric-field strength of 5 V cm^{-1} in the ion-source. The temperature of the ion-source block was maintained constant throughout each experiment. Spectra were recorded by scanning the magnetic field from high to low field (see section 2.2).

The heights of peaks in the spectra were measured and normalized with respect to the total ion current as described in section 2.2. Plots of the normalized peak heights (relative abundances) for each of the reactant ions against pressure (see sections 3.3 to 3.5) were used to establish the kinetics and mechanism of the corresponding reactions.

A. Variation of sample pressure.

Experiments in which the sample pressure was varied were commenced by introducing isobutane into the ion-source at a fixed pressure (either ca. 0.1 or ca. 0.2 torr). This pressure was estimated by the method given in section 4.1. The temperatures of the inlet-system reservoir and delivery tube (see figure (2.2)) were adjusted to 170 ± 5°C and 130 ± 2°C respectively. When the isobutane pressure and the temperature of the ion-source block were steady, a known volume of sample was injected into the inlet-system reservoir. The height of a peak corresponding to one of the ions produced from the sample was monitored continuously. When the height of this peak was constant, the spectrum was

recorded as described in section 2.2. The sample was pumped out of the inlet-system reservoir, and a different volume of the sample injected. The above process was repeated with sample volumes up to a maximum volume of 22 µl. Since the maximum volume of the syringe, including the needle, was 11 µl, sample volumes greater than 11 µl required two injections for their introduction. The isobutane pressure was monitored at intervals throughout the experiment. Results obtained from this type of experiment are discussed in sections 3.3 and 4.2.

B. Variation of the pressure of one component of a sample mixture.

It was observed that the presence of impurities in a sample exerted an effect on the relative abundances of ions in a spectrum. Hence experiments were carried out in which the isobutane pressure and the sample pressure were maintained constant while the pressure of water, or carbon tetrachloride, or ethyl methyl ketone, was varied. In these experiments isobutane was first introduced into the ion-source at a fixed pressure (ca. 0.1 torr). The temperatures of the inlet-system reservoir and delivery tube were adjusted to 170 ± 5°C and 130 ± 2°C respectively. When the isobutane pressure and temperature of the ion-source block were steady, a known volume of sample was injected into the inlet-system reservoir. A known volume of one of the three compounds mentioned above was then injected into the reservoir so that both compounds were flowing into the ion-source. When the height of a peak corresponding to one of the ions produced from the sample

had become constant, the spectrum was recorded as described in section 2.2. The compounds were pumped out of the reservoir. The sample was again injected into the reservoir in the same volume as previously, and a new volume of the second compound introduced. The above process was repeated. Volumes of water, carbon tetrachloride, and ethyl methyl ketone were thus varied while the sample volume, hence the pressure of sample in the ion-source, was held constant.

A variation of the above procedure was employed in an additional experiment in which the pressure of anisole was held constant while the pressure of carbon tetrachloride was varied up to the pressure corresponding to 1 µl. In this experiment solutions of various concentrations of carbon tetrachloride in anisole were injected into the reservoir in such volumes that the anisole pressure was always constant. Results obtained from the experiments described above are discussed in sections 3.5 and 4.2.

C. Variation of both isobutane and sample pressures.

An experiment in which the isobutane pressure was varied was commenced by introducing isobutane into the ion-source at a fixed pressure. This pressure was estimated by the method given in section 4.1. The temperatures of the inlet-system reservoir and delivery tube were adjusted to 170 ± 5°C and 130 ± 2°C as before. When the isobutane pressure and the temperature of the ion-source block were steady, a known volume of the sample (acetone) was

injected into the inlet-system reservoir. A spectrum was recorded according to the method given in section 2.2 after checking that the height of one of the peaks in the spectrum of acetone (m/z = 117, see section 3.3.A) was constant. The acetone was pumped out of the inlet-system reservoir, and a different volume of acetone was introduced. The spectrum was again recorded, and the procedure was repeated until spectra of acetone at five different sample pressures, and at the given isobutane pressure, had been recorded. The isobutane pressure was then changed, and the procedure repeated using the same volumes of acetone. Spectra corresponding to the five acetone pressures were recorded for four different isobutane pressures in the range 0.05 to 0.21 torr.

The heights of peaks in the spectra were measured and normalized with respect to the total ion current as described in section 2.2. Comparison of spectra which were recorded at different isobutane pressures was, however, only possible after a second normalization procedure was applied. This procedure is described in section 3.4. Results obtained from this experiment are discussed in section 4.2.

CHAPTER 3

RESULTS

3.1 Determination of the rate constant for the reaction $CH_4^{+\cdot} + CH_4 \longrightarrow CH_5^+ + CH_3^\cdot$: ion residence times.

The reaction between the methane molecular ion-radical and methane gas,

$$CH_4^{+\cdot} + CH_4 \xrightarrow{k} CH_5^+ + CH_3^\cdot \qquad (2.4\text{-}1)$$

has been studied extensively, and values of the rate constant, k, obtained by various workers using a variety of techniques (for example pulsed-ion-source mass spectrometry and ion cyclotron resonance spectrometry) have been summarized by Henchman[38]. From the results it may be deduced that the mean value of k is 12×10^{-10} cm^3 $molecule^{-1}$ sec^{-1}. Furthermore the rate constant has been found to be insensitive to changes in the ion-source field strength[38].

From reaction (2.4-1) it can be seen that the rate of disappearance of $CH_4^{+\cdot}$ is given by

$$-\frac{d[CH_4^{+\cdot}]}{dt} = k[CH_4^{+\cdot}][CH_4]$$

Therefore

$$\log ([CH_4^{+\cdot}]_o / [CH_4^{+\cdot}]) = k[CH_4]\tau$$

where $[CH_4^{+\cdot}]$ is the abundance of $CH_4^{+\cdot}$ ions, $[CH_4^{+\cdot}]_o$ is the initial abundance of $CH_4^{+\cdot}$ ions (i.e., the abundance in the absence of reaction (2.4-1)), $[CH_4]$ is the number density of methane

molecules in the ion-source (vide infra), and τ is the residence time of the $CH_4^{+\cdot}$ ion*. If the heights (I_n) of the peaks having m/z = n in the recorded spectrum may be assumed to reflect accurately the abundances of ions in the ion-source (see sections 1.1.D and 2.4.A.), then

$$\log (I^o_{16}/I_{16}) = k [CH_4] \tau$$

If it be also assumed that reaction (2.4-1) is the only reaction undergone by the $CH_4^{+\cdot}$ ion, and that the product, CH_5^+, does not react with methane , then

$$[CH_4^{+\cdot}]_o = [CH_4^{+\cdot}] + [CH_5^+]$$

and thus

$$I^o_{16} = I_{16}+I_{17}$$

where I_{17} is the abundance of the CH_5^+ ion. Hence

$$\log ((I_{16}+I_{17})/I_{16}) = k[CH_4]\tau \qquad (3.1\text{-}1)$$

The quantity $[CH_4]$, the number density of methane molecules in the ion-source, may be evaluated from the methane pressure by use of the equation of state for an ideal gas

$$[CH_4] = p_{CH_4}/k_BT = p_{CH_4}N \qquad (3.1\text{-}2)$$

where k_B is Boltzmann's constant, T is the absolute temperature (450 K), and $N = 2.146 \times 10^{16}$ molecule cm^{-3} at this temperature. Substitution of equation (3.1-2) into equation (3.1-1) gives

$$\log ((I_{16}+I_{17})/I_{16}) = kN\tau p_{CH_4} \qquad (3.1\text{-}3)$$

---

* The function 'log' refers to Naperian logarithms throughout unless otherwise stated.

The experimental procedure used to study reaction (2.4-1) was described in section 2.4. Data obtained from an experiment in which the electron energy and emission current were set at 500 eV and 10μA respectively, and the repeller-field strength was 12.5 V cm^{-1}, are shown in graph (3.1). From equation (3.1-3), it can be seen that the slope of the line is $kN\tau$. Hence k can be determined provided the ion residence time can be estimated.

There are two methods for the estimation of ion residence times. In the first method it is assumed that under the conditions of the experiment (pressure < 0.3 torr, electric field strength = 12.5 V cm^{-1}), each ion experiences only a few collisions with methane molecules before passing out of the ion-source, and that these collisions do not change the velocity of the ion significantly. If these assumptions are valid then the free-fall formula (equation 3.1-4)) for an ion drifting in an electric field can be used for the estimation of the ion residence time. The free-fall formula is

$$\tau = (2dm/zE)^{\frac{1}{2}} \qquad (3.1\text{-}4)$$

where d is the mean distance travelled by the ion, m and z are respectively the mass and charge of the ion, and E is the electric field strength.

In the second method the effects of collisions are taken into account by invoking ion-mobility considerations. The drift velocity, v, of the ion may be obtained from the equation

$$v = KE \qquad (3.1\text{-}5)$$

where K is the ion-mobility and E is as defined above. If an

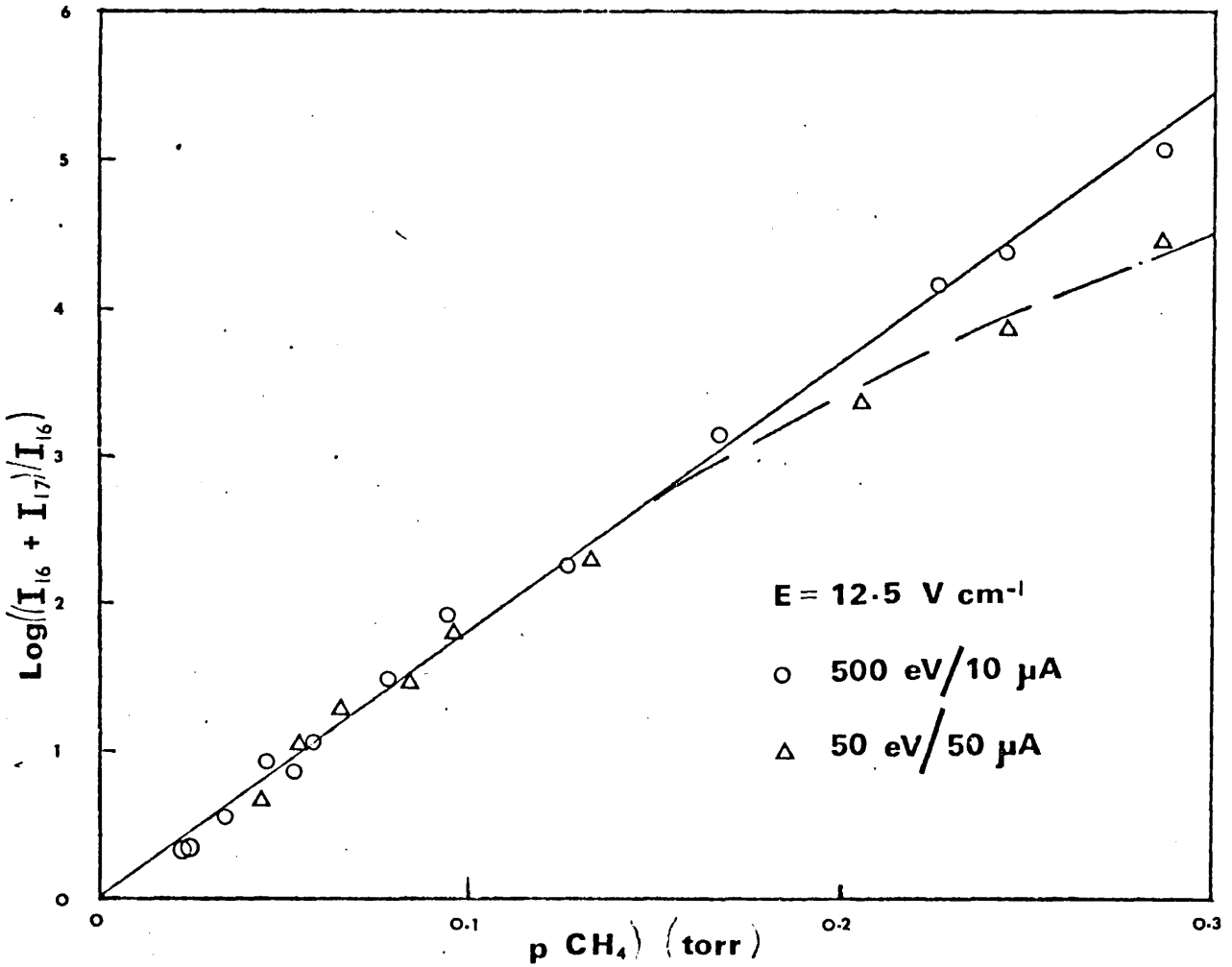

GRAPH (3-1). Kinetic plot for the formation of CH_5^+

experimentally determined value of K is not available, then the reduced mobility, K_o, which is related to K by the equation

$$K = K_o(760/p)(T/273) \qquad (3.1\text{-}6)$$

(in which p is the pressure in torr and T the absolute temperature) can be estimated from the equation given by Ridge and Beauchamp [53].

$$K_o = 13.876/(\alpha\mu)^{\frac{1}{2}} \qquad (3.1\text{-}7)$$

where α is the angle-averaged polarizability (in $\mathring{A}^3$)* of the neutral species and μ is the reduced mass of the reactants (in a.m.u.). Since $\tau = d/v$, it can be seen that the residence time is given by

$$\tau = 273(\alpha\mu)^{\frac{1}{2}} pd/(10546ET) \qquad (3.1\text{-}8)$$

Equation (3.1-8) shows that when the effects of collisions are important the ion residence time is directly proportional to the pressure. Consequently the reaction order with respect to methane will appear greater by one order than it actually is(viz., second order).

The data presented in graph (3-1) suggested that the residence time of CH_4^+ was not dependent on the methane pressure. Thus it was assumed that τ may be estimated from equation (3.1-4). Further justification of this assumption will be given below. The mean distance (d) travelled by an ion in the ion-source was taken to be half the distance from the repeller plate to the ion-exit slit (ie. d = 0.2 cm, see figure (2-1)), so that the estimated mean residence time of CH_4^+ was 7.3×10^{-7} sec.

---

* Polarizabilities are listed in appendix I

The rate constant for reaction (2.4-1) was then found to be 11.6 x 10^{-10} cm^3 $molecule^{-1}$ sec^{-1}, in excellent agreement with results obtained by other workers.

It was stated in section 2.4 that anomalous results were obtained in the study of the kinetics of reaction (2.4-1) when the electron energy and emission current were set at 50 eV and 50μA respectively. The data obtained is also shown in graph (3-1). It can be seen that the values of log $((I_{16}+I_{17})I_{16})$ were low when the pressure was greater than ca.0.15 torr. The effect may be due to comparatively small numbers of electrons penetrating the methane at high pressures, thereby causing reduction of the primary ionization. Since it was found necessary to use a small emission current, it may be that the observed relative ion-abundances are perturbed by thermal-electron-capture processes. The value of the rate constant obtained from this experiment was the same as that given above provided the pressure range was limited to 0-0.15 torr.

Equations (3.1-4) and (3.1-8) can be used to calculate the methane pressure, p_c, for which the residence time calculated from the ion-mobility is equal to that calculated from the free-fall formula. Values of p_c are given for various repeller field strengths in table (3-1).

Table (3-1).

Rate constants for the reaction $CH_4^{+\bullet} + CH_4 \longrightarrow CH_5^+ + CH_3^\bullet$ obtained by assuming that the mean distance travelled by the $CH_4^{+\bullet}$ ion is either 0.2 or 0.4 cm.

Field strength (E) ($V\ cm^{-1}$)	p_c* (torr)	Rate constant for reaction (2.4-1) ($10^{10} \times cm^3\ molecule^{-1}\ sec^{-1}$) d = 0.2 cm.	d = 0.4 cm.
2.5	0.078	15.6 ± 0.4	11.1 ± 0.3
5.0	0.110	14.2 ± 0.5	10.0 ± 0.3
7.5	0.135	12.4 ± 0.3	8.8 ± 0.2
10.25	0.157	10.6 ± 0.3	7.5 ± 0.2
12.5	0.174	11.6 ± 0.2	8.3 ± 0.1

* see text.

The calculation assumes that the mobility of the $CH_4^{+\bullet}$ ion is not perturbed by the presence of symmetric charge-transfer processes. Since the value of τ obtained from the free-fall formula is an effective lower limit to the true mean residence time, lower values of τ obtained from equation (3.1-8) have no physical significance.

A further justification for the use of equation (3.1-4) to obtain a value of the rate constant for reaction (2.4-1) can now be seen: below 0.174 torr (see table (3-1)) the mean residence time cannot be less than 7.3×10^{-7} sec. The fact that the resulting values of log $((I_{16}+I_{17})/I_{16})$ for pressures

greater than 0.174 torr were consistent with the other data was probably fortuitous.

The rate constant for reaction (2.4-1) was also determined using lower repeller field strengths in the ion-source (see graph (3-2)). The values so obtained when the data was treated by the method described above are given in table (3-1). The rate constants obtained using repeller field strengths of 7.5 and 10.25 V cm^{-1} were in good agreement with the values obtained by other workers.[14,15] As the field strength is decreased the probability of the occurrence of collisions in which the ion is deflected backwards (with respect to the electric field) increases, and therefore the effective mean distance (d) travelled by the $CH_4^{+\bullet}$ ion also increases. Values of the rate constant obtained by assuming a mean distance of 0.4 cm (the separation of the repeller plate from the ion-exit-slit) in the calculation of τ suggested that, when E = 2.5 and 5.0 V cm^{-1}, the mean distance travelled by the $CH_4^{+\bullet}$ ions was approximately twice the mean distance travelled when E = 12.5 V cm^{-1}. From the values of p_c listed in table (3-1) it can be seen that the appropriate equation for the evaluation of τ, at all field strengths employed in these experiments, was equation (3.1-4) provided that data was acquired only from the pressure range 0 - ca.0.1 torr.

The agreement between the rate constant for reaction (2.4-1) determined using the Micromass 12F spectrometer with values determined by other workers using a variety of techniques suggested that it is possible to use this commercially available instrument to study the kinetics of ion-molecule reactions.

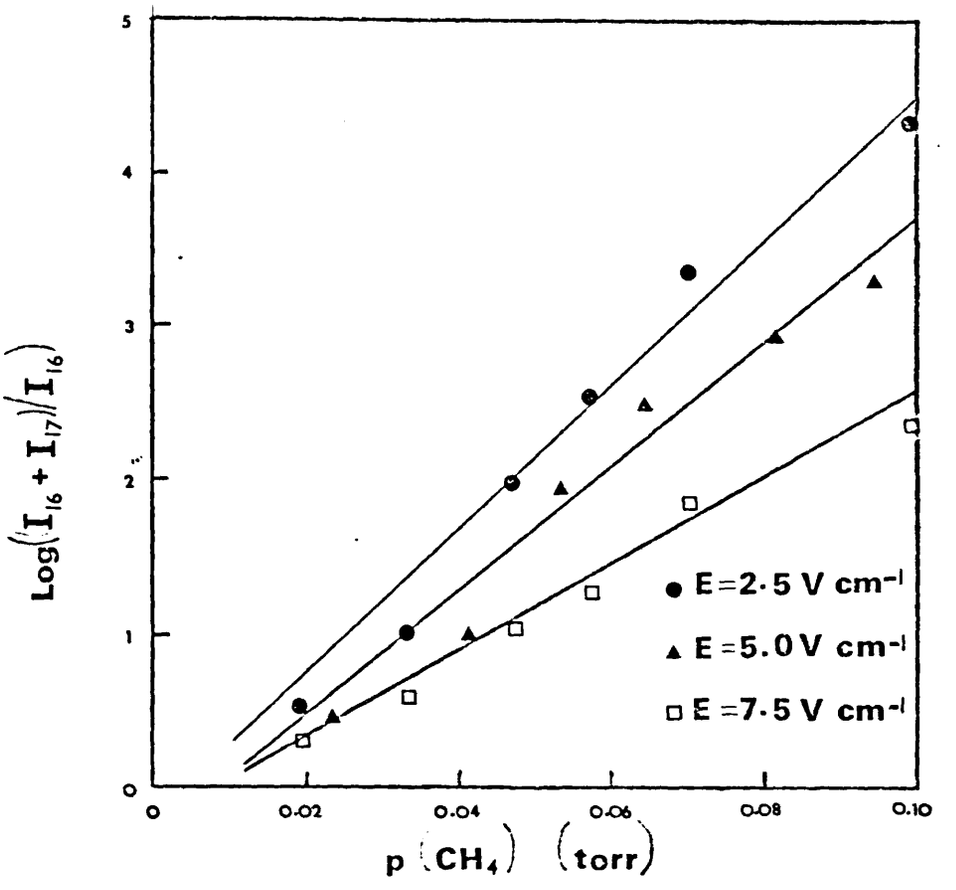

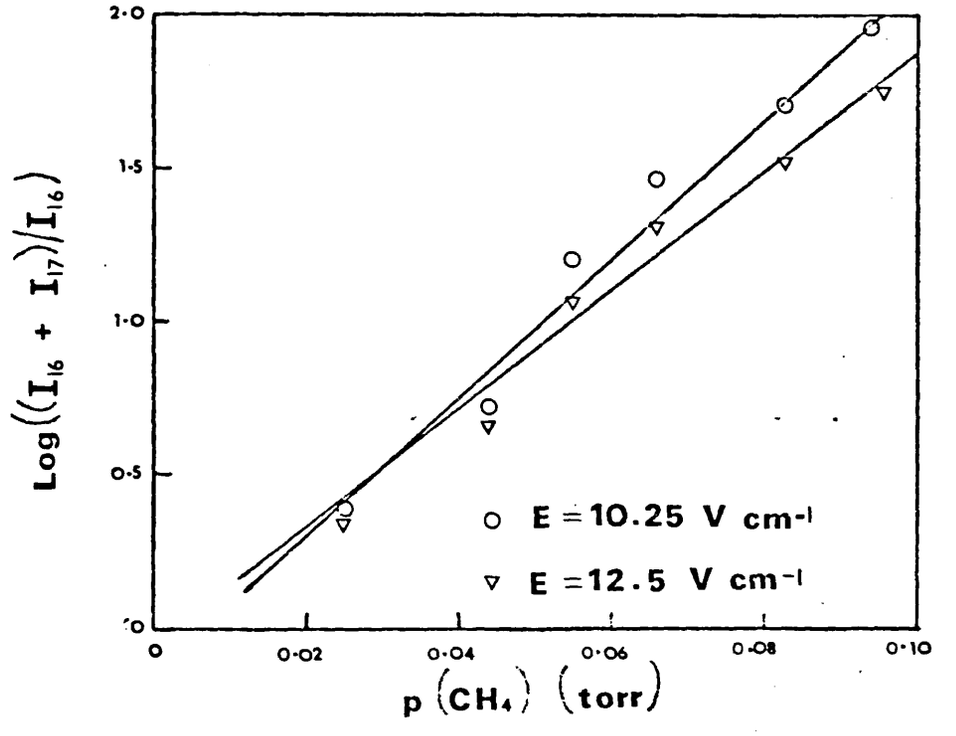

GRAPH (3-2). Kinetic plots for the formation of CH_5^+.

The limitations of the method (discussed in sections 1.1.D and 1.3.B ~~1.1.C~~) may not however influence the value obtained for the rate constant for reaction (2.4-1) significantly, and it should be borne in mind that these limitations may nevertheless influence the value of rate constants obtained for other reactions.

3.2 Reactions of the primary ions from isobutane with isobutane.

The experimental method employed for the study of the reactions of the primary ions from isobutane with isobutane gas was described in section 2.4. The electron-impact ionization of isobutane results in the formation of $C_4H_{10}^{+\cdot}$, which fragments to give the various primary ions. A scheme of possible fragmentation pathways which produce these ions is given overleaf. A peak having m/z = 14.5, and corresponding to the elimination of an ethyl radical from metastable $C_4H_{10}^{+\cdot}$ ions was present in the spectra of isobutane. The presence of this peak suggests that the $C_2H_5^+$ ion(m/z = 29) is formed by the direct elimination of an ethyl radical from the isobutane molecular ion-radical (see section 1.1.A.)

Graph (3-3) shows the variation with isobutane pressure of the relative abundances ($I_n/\sum I$) of all the ions generated from isobutane. The relative abundances of the primary ions decreased as the isobutane pressure was increased, whereas that of the $C_4H_9^+$ ion increased steadily in the pressure range 0 - 0.16 torr, and thereafter remained essentially constant.

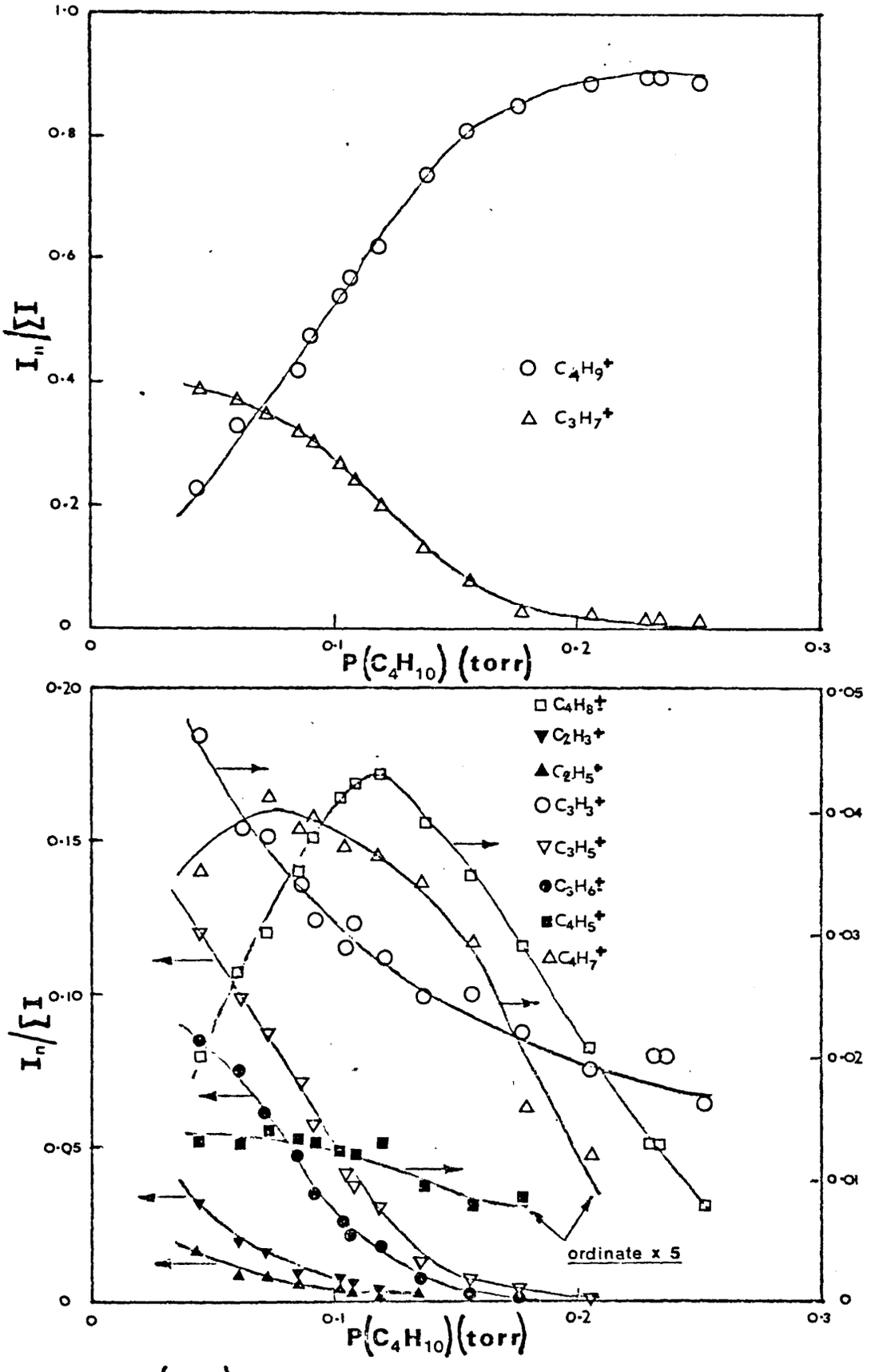

GRAPH (3-3). Variation of relative abundances of isobutane primary ions with pressure

Scheme (3-1)

Possible fragmentation pathways for the formation of the primary ions of isobutane.

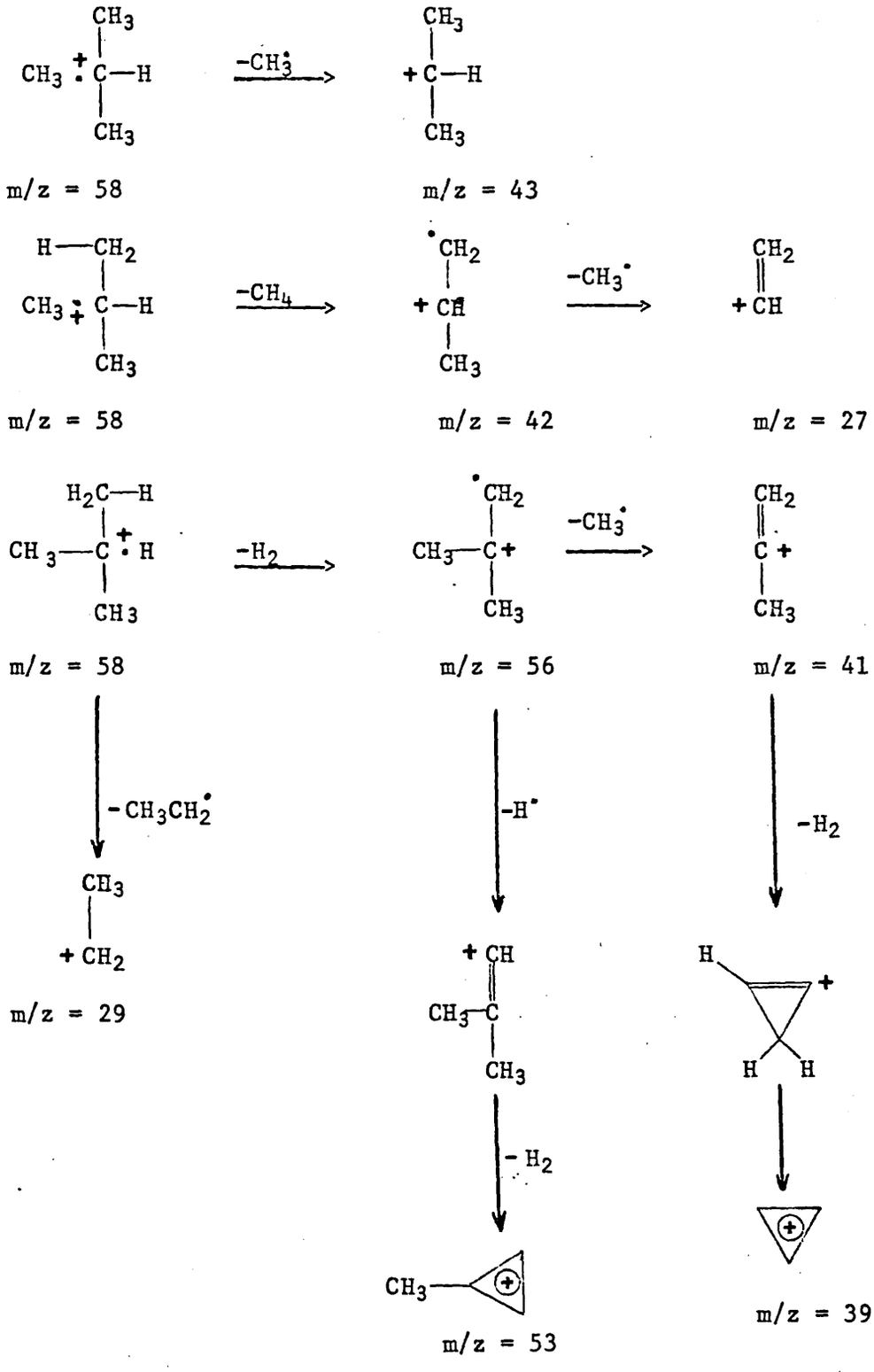

These observations are comparable with those of Field[54], and suggest that the primary ions react with isobutane to form the $C_4H_9^+$ ion. For example

$$C_3H_7^+ + C_4H_{10} \xrightarrow{k_{43}} C_3H_8 + C_4H_9^+ \qquad (3.2\text{-}1)$$

Provided the ion residence times can be estimated, the rates of reactions of this type may be obtained by observing the decreases of relative abundances of each of the primary ions as the isobutane pressure is increased.

Equations (3.1-4) and (3.1-6) can be used to determine the isobutane pressure, p_c, for which values of the mean residence time of a given primary ion, calculated by the two methods discussed in section 3.1, are equal.

When m/z = 43 ($C_3H_7^+$ ion) is used in this calculation it is found that the residence times are equal at 0.044 torr for the field strength (E = 5.0 V cm^{-1}) employed in this experiment. Pressures (p_c) in the range 0.035 - 0.050 torr are obtained when the other primary ions are considered. Thus the residence times of the primary ions are appropriately obtained here using equation (3.1-8), and are expected therefore to be directly proportional to the isobutane pressure (see section 3.1).

From equation (3.2-1)

$$-\frac{d[C_3H_7^+]}{dt} = k_{43}[C_3H_7^+][C_4H_{10}]$$

so that the integrated rate equation for the reaction of the $C_3H_7^+$ is

$$-\log\left([C_3H_7^+]/[C_3H_7^+]_o\right) = k_{43}[C_4H_{10}]\tau \qquad (3.2\text{-}2)$$

where $[C_4H_{10}]$ is the number density of isobutane molecules in the ion source. If the isobutane pressure be denoted by p, then (cf. equation (3.1-2))

$$[C_4H_{10}] = pN \qquad (3.2\text{-}3)$$

Since the residence times of the primary ions are directly proportional to the isobutane pressure, and provided the heights (I_n) of the peaks having m/z = n in the recorded spectrum accurately reflect the abundances of ions in the ion-source, then equation (3.2-2) may be written

$$\log (I_{43}/I_{43}^{o}) = -k_{43}\beta_{43}Np^2 \qquad (3.2\text{-}4)$$

where I_{43}^{o} is the abundance of the $C_3H_7^+$ ion in the absence of reaction (3.2-1) and β_{43} may be calculated from equation (3.1-8)*. Hence a plot of $\log (I_{43}/I_{43}^{o})$ against the square of the isobutane pressure will be a straight line with slope $-k_{43}\beta_{43}N$, provided the reaction is bimolecular. As a value of I_{43}^{o} was inaccessible, it was necessary to plot the logarithm of the relative ion abundance ($\log (I_{43}/\sum I)$, where $\sum I$ is the total ion current) against the square of the pressure. Since equation (3.2-4) can be written in the form

$$\log (I_{43}/\sum I) - \log (I_{43}^{o}/\sum I^{o}) = - k_{43}\beta_{43}Np^2 \qquad (3.2\text{-}5)$$

where $I_{43}^{o}/\sum I^{o}$ is the relative abundance of $C_3H_7^+$ in the absence of reaction (3.2-1) (ie. the relative abundance in the electron-impact mass spectrum of isobutane), it can be seen that the plot of $\log (I_{43}/\sum I)$ against the square of the pressure will also be a straight line with slope $-k_{43}\beta_{43}N$.

---

*$\beta_{43} = 273(\alpha\mu)^{1/2} pd/1054 ET$

Equations similar to (3.2-5) can be developed for the reactions of all the primary ions with isobutane. The general equation is

$$\log (I_n/\sum I) - \log (I_n^o/\sum I^o) = - k_n \beta_n N p^2 \qquad (3.2\text{-}6)$$

Kinetic plots for the disappearance of the primary ions are given in graph (3-4) from which it is apparent that most of the primary ions undergo simple bimolecular reactions with isobutane. The most notable exception is the $C_4H_8^+$ ion for which the plot is linear only in the pressure range 0.15 - 0.30 torr. For increases in pressure in the range 0 - 0.15 torr more $C_4H_8^+$ ions were produced than were consumed by reaction with isobutane*. This behaviour cannot as yet be explained. Graph (3-4) also shows that neither the $C_4H_7^+$ ions, nor the $C_3H_3^+$ ions, obeyed the simple bimolecular rate law at low pressure.

Rate constants of the reactions of the primary ions with isobutane are listed in table (3-2). This table also contains the pressure ranges over which the simple bimolecular rate law is valid, and the intercepts at zero pressure obtained from the kinetic plots. Both sets of figures are required for the method of estimating isobutane pressure given in section 4.1.

---

* See equation (1.1-16)

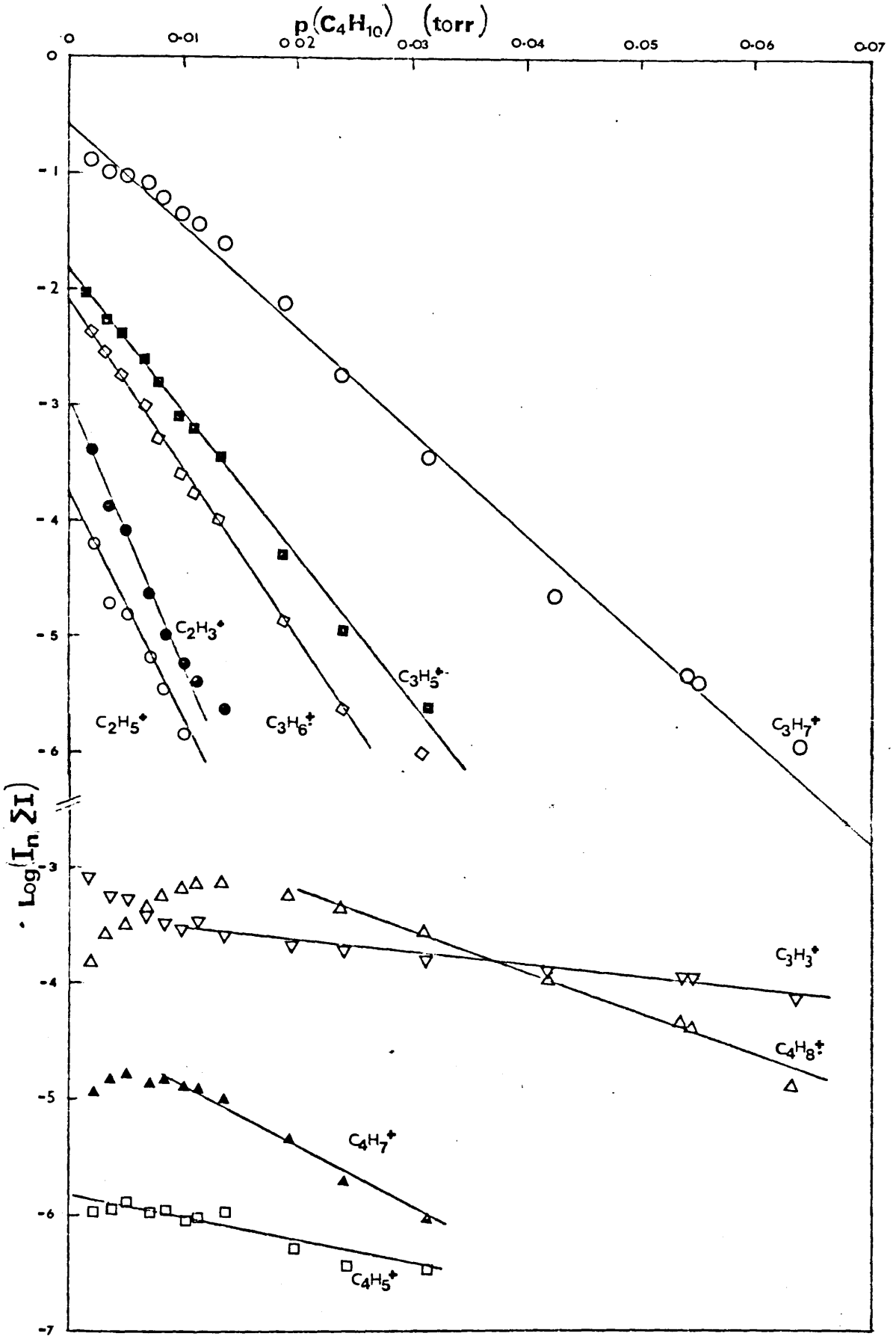

GRAPH (3-4). Kinetic plots for reactions of the isobutane primary ions with isobutane

Table (3-2).

Rate constants of the reactions of the primary ions from isobutane with isobutane.

Ion	m/z	Rate constant (10^{11} x cm^3 $molecule^{-1}$ sec^{-1})	Intercept at zero pressure*	Pressure range over which the bimolecular rate law is valid. (torr)
$C_2H_3^+$	27	15.4 ± 1.1	-3.22 ± 0.12	0.04 - 0.10
$C_2H_5^+$	29	14.0 ± 1.0	-3.92 ± 0.09	0.04 - 0.12
$C_3H_3^+$	39	0.73 ± 0.06	-3.42 ± 0.03	0.08 - 0.30
$C_3H_5^+$	41	8.05 ± 0.30	-1.94 ± 0.08	0.04 - 0.20
$C_3H_6^{+\cdot}$	42	9.28 ± 0.42	-2.21 ± 0.09	0.04 - 0.17
$C_3H_7^+$	43	6.22 ± 0.16	-0.49 ± 0.08	0.08 - 0.30
$C_4H_5^+$	53	1.77 ± 0.26	-5.74 ± 0.05	0.07 - 0.16
$C_4H_7^+$	55	3.94 ± 0.39	-4.20 ± 0.14	0.10 - 0.18
$C_4H_8^{+\cdot}$	56	2.37 ± 0.18	-2.41 ± 0.13	0.16 - 0.30

* see equation (3.2-6)

Table (3-3).

Relative abundances of ions produced from two ketones at selected low and high sample pressures.

Compound (M)	Isobutane pressure (torr)	Temp. (°C)	Sample pressure (torr)	Relative ion-abundances†				
				$M^{+\cdot}$	MH^+	$MC_3H_5^+$	$MC_3H_7^+$	M_2H^+
Acetone	0.108	176	1.9×10^{-3}	?*	0.135	<0.001	<0.001	0.002
			1.2×10^{-2}	?*	0.457	0.017	0.010	0.371
Ethyl methyl ketone	0.109	175	2.1×10^{-3}	0.002	0.191	0.002	<0.001	0.004
			1.1×10^{-2}	0.012	0.385	0.027	0.016	0.441

† Abundances have been corrected for ^{13}C isotopes.

* See text.

3.3 The chemical-ionization mass spectra of selected compounds: changes of relative ion-sbundances with variation of sample pressure.

The chemical-ionization mass spectra of various compounds with isobutane as the reagent gas are described in this section. The compounds were selected from the following classes of compound: ketones, nitriles, anisoles, and alcohols. The spectra of carbon tetrachloride and of water are also described. It will be shown that the relative abundances of ions in isobutane chemical-ionization mass spectra are dependent upon the amount of sample present in the ion-source.

A. Ketones

Chemical-ionization mass spectra of two ketones, acetone and ethyl methyl ketone, were recorded as described in section 2.2. The pressure of the reagent gas, isobutane, was maintained constant at ca.0.1 torr. The temperature of the ion-source block was 176 $\pm 2^{o}$C. Sample pressures were varied by varying the volume of sample injected into the inlet-system reservoir (see section 2.6.A) so that spectra were obtained for pressures corresponding to sample volumes up to 22µl.

The principal ions produced from these ketones are listed in table (3-3). Relative abundances of the ions are given for two selected sample pressures, ca.2 x 10^{-3} torr and ca.1 x 10^{-2} torr. These pressures represent the low and high regions of the

pressure range. It can be seen from table (3-3) that the major peaks in the spectra of these compounds (M) corresponded to the protonated sample molecule (MH^+) and the proton-bound dimer ion (M_2H^+). The overall reactions which produce these ions may be written as

$$RH^+ + M \longrightarrow R + MH^+ \qquad (3.3\text{-}1)$$

$$MH^+ + M \longrightarrow M_2H^+ \qquad (3.3\text{-}2)$$

in which RH^+ represents an ion derived from isobutane (see section 3.2). The mechanism of the protonation reaction is, however, more complicated than is suggested by reaction (3.3-1) and will be discussed at length in chapter 4.

Mass spectral peaks corresponding to the decomposition of metastable ions (hereinafter referred to as 'metastable peaks') were found in the spectra of both ketones (see table(3-11) at the end of section 3.3). It was found that these peaks corresponded to the elimination of a sample molecule (M) from the proton-bound dimer ions (M_2H^+). This suggests that the lifetime of the M_2H^+ species was of the order of the residence times of these ions in the ion-source (ca. 10 μsec). It is interesting to note that the collision-induced decomposition of proton-bound dimer ions is also a slow process [17].

Peaks corresponding to the molecular ion-radical $M^{+\cdot}$, were found in the spectra of ethyl methyl ketone, although their relative abundance remained small over the entire range of sample pressures (see table (3-3)). It was not possible to ascertain whether a similar ion was formed from acetone as the peak would be obscured by the peak corresponding to the

$^{13}C\,^{12}C_3H_9^+$ ion. The $M^{\cdot+}$ ions could result from either electron-impact ionization of sample molecules, or be produced by charge-transfer reactions, viz.,

$$RH^+ + M \longrightarrow RH^{\cdot} + M^{\cdot+} \qquad (3.3\text{-}3)$$

Since the spectra of aromatic compounds, eg. the anisoles (vide infra), contained molecular ions in relative abundances which were much larger than would be expected from the direct electron-impact ionization of the sample molecules, it seems fairly likely that the molecular ions in the spectra of the ketones were produced by charge-transfer reactions. It is not possible to deduce from the experimental data which of the reactant ions, RH^+, undergo reaction (3.3-3).

The spectra of both acetone and ethyl methyl ketone contained peaks corresponding to ions having m/z = m+41 and m/z = m+43, where m is the molecular weight of the ketone. These ions may be formed by the association reactions

$$M + C_3H_5^+ \longrightarrow MC_3H_5^+ \qquad (3.3\text{-}4)$$

$$M + C_3H_7^+ \longrightarrow MC_3H_7^+ \qquad (3.3\text{-}5)$$

or, in the case of $MC_3H_5^+$, by the reaction

$$M + C_4H_9^+ \longrightarrow [MC_4H_9^+] \longrightarrow MC_3H_5^+ + CH_4 \qquad (3.3\text{-}6)$$

It is interesting to note that the $MC_4H_9^+$ ion did not occur to any significant extent in the spectra of either of the ketones.

Ions having m/z = 99 (m+41) and m/z = 101 (m+43) could, in principle, be produced in the spectrum of acetone by decomposition of the $(CH_3.CO.CH_3)_2H^+$ ion. Thus,

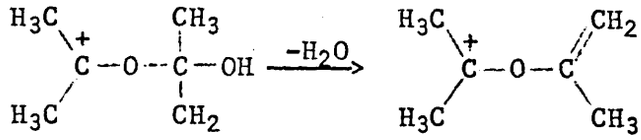

(3.3-7)

m/z = 99

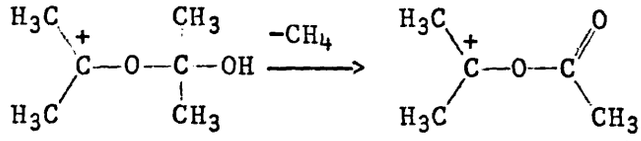

(3.3-8)

m/z = 101

It can be seen from table (3-3) that the $(CH_3.CH_2.CO.CH_3)_2H^+$ ion did not undergo reactions similar to (3.3-7) and (3.3-8) since ions having m/z = 127 and m/z = 129 were not present in the spectrum.

Since the natural abundance of the ^{13}C isotope in carbon is 1.1%, and since the natural abundances of isotopes of hydrogen and oxygen are very small, the number of carbon atoms present in an ion containing only carbon, hydrogen, and oxygen atoms may be ascertained from the ratio

$$\frac{I_{n+1}}{I_n+I_{n+1}} = 0.011x \qquad (3.3\text{-}9)$$

where I_i is the abundance of the ion having m/z = i, and x is the number of carbon atoms present. Use of equation (3.3-9) showed that the ion having m/z = 101 formed from acetone contained six carbon atoms, suggesting that reaction (3.3-8) did not occur. This approach could not be applied to the ion having m/z = 99 since the products of both reactions (3.3-4) and (3.3-7) each

contain six carbon atoms. Reaction (3.3-7) does, however, seem unlikely as water was not eliminated from the M_2H^+ ion formed from ethyl methyl ketone.

The relative abundances of all the ions generated from isobutane decreased as the sample pressure was increased. It will be shown in section 4.2 that information on the kinetics and mechanism of reaction (3.3-1) is obtained if the function $\log (I_n/I_n^o)$ (where I_n is the relative abundance of the reactant ion, RH^+, having m/z = n and I_n^o is the relative abundance of this ion in the absence of sample) is plotted against sample pressure. Accordingly, graph (3-5) shows examples of the ways in which $\log (I_n/I_n^o)$ (for n = 57 and n = 39, corresponding to the $C_4H_9^+$ and $C_3H_3^+$ ions respectively) varied with pressure of ethyl methyl ketone. It is apparent that the variation of $\log (I_n/I_n^o)$ with sample pressure was either linear or somewhat resembled a parabola. The continuous lines in graph (3-5) were calculated from the mathematical expressions which resulted from kinetic analysis of the reaction mechanisms proposed in section 4.2. It will be seen from the results described below that the variation with sample pressure of $\log (I_n/I_n^o)$, for all reactant ions and all compounds studied, assumed one of the two forms illustrated in graph (3-5). Table (3-4) lists the reactant ions (RH^+) for which reaction with the ketones resulted in a linear decrease of $\log (I_n/I_n^o)$ with sample pressure. The significance of these results will be discussed in section 4.2.

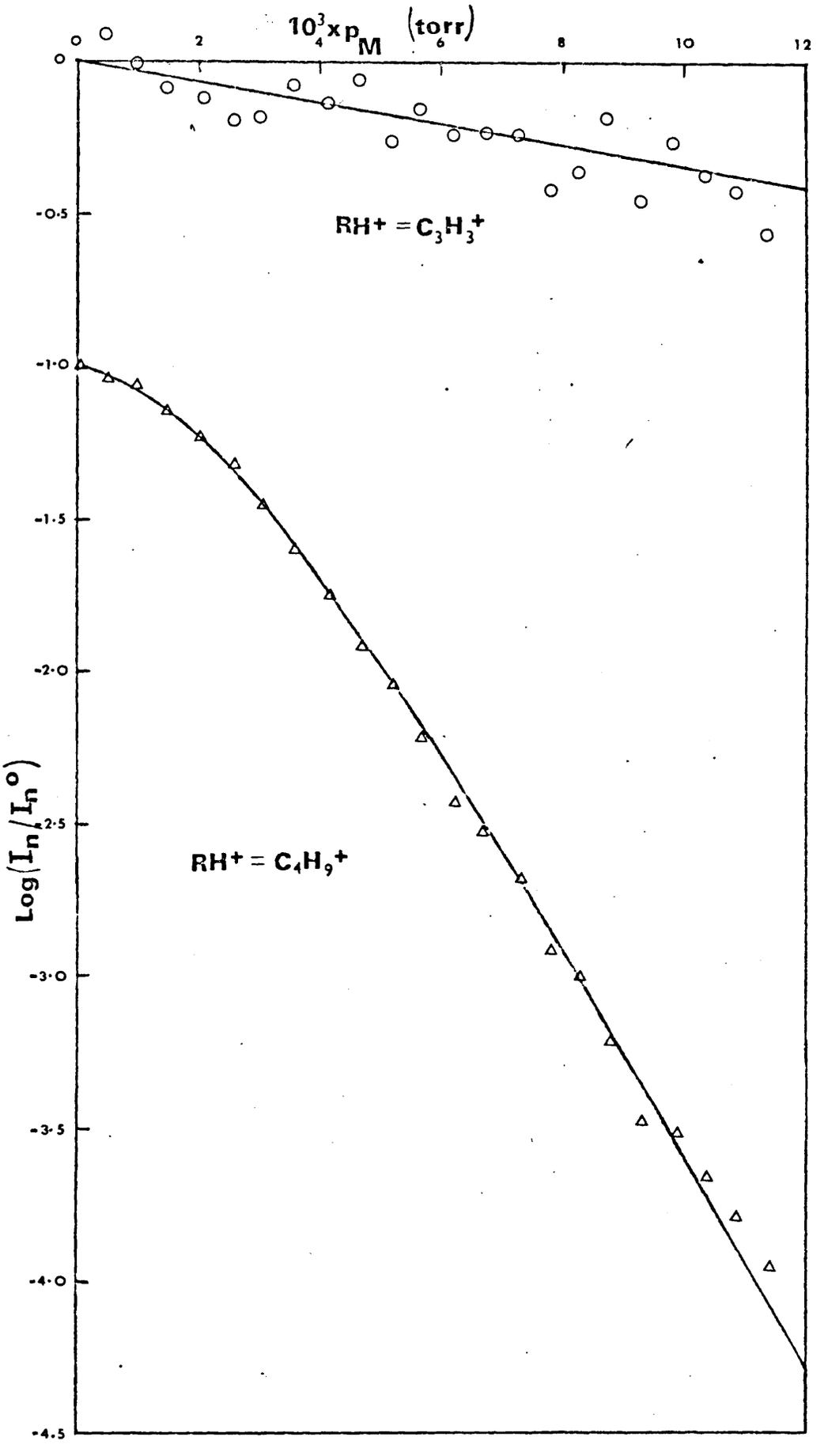

GRAPH (3 - 5) . Kinetic plots for the reactions of ethyl methyl ketone (M) with 2 reactant ions, RH^+.

Table (3-4).

Reactant ions for which reaction with the ketones resulted in a linear decrease of log (I_n/I_n^o) with sample pressure.

Compound	Reactant ions (RH^+)	
Acetone	$C_3H_3^+$	$C_4H_5^+$
Ethyl methyl ketone	$C_3H_3^+$	$C_4H_5^+$

B. Nitriles.

Chemical-ionization mass spectra of the five aliphatic nitriles listed in table (3-5) were recorded as described in section 2.2, sample pressures being varied according to the method given in section 2.6.A. The isobutane pressure was maintained constant at ca. 0.1 torr. The temperature of the ion-source block was 174 ± 2°C.

The principal ions produced from these nitriles are listed in table (3-5), which shows the relative ion-abundances at selected low and high sample pressures. Once again it was found that the major peaks in the spectra corresponded to the protonated sample molecule (MH^+) and the proton-bound dimer ion (M_2H^+) which were presumably produced by reactions (3.3-1) and (3.3-2) respectively.

Table (3-5).
Relative abundances of ions produced from various nitriles at selected low and high sample pressures.

Compound (M)	Isobutane pressure (torr)	Temp. (°C)	Sample pressure (torr)	Relative ion-abundances †						
				MH^+	$MC_3H_3^+$	$MC_3H_5^+$	$MC_3H_7^+$	$MC_4H_9^+$	M_2H^+	M_2H^+-HCl
Acetonitrile	0.100	174	1.8×10^{-3}	~0.04*	<0.001	<0.001	<0.001	<0.001	<0.001	-
			1.2×10^{-2}	0.462	<0.001	0.001	0.005	0.013	0.097	
Propionitrile	0.100	174	2.0×10^{-3}	~0.10*	0.001	0.001	<0.001	<0.001	0.002	
			1.1×10^{-2}	0.388	<0.003	0.032	0.001	0.064	0.223	-
Butyronitrile	0.104	174	2.1×10^{-3}	0.100	0.001	0.002	<0.001	0.004	0.003	
			1.2×10^{-2}	0.221	0.008	0.041	0.004	0.079	0.399	-
2-Chloro-propionitrile	0.103	174	1.8×10^{-3}	0.029	-	<0.001	-	<0.001	<0.001	0.001
			1.2×10^{-2}	0.295		0.011		0.002	0.103	0.013
2-Bromo-propionitrile	0.105	174	2.2×10^{-3}	0.019	-	<0.001	-	<0.001	<0.001	-
			1.2×10^{-2}	0.135		0.004		0.004	0.010	

† Abundances have been corrected for ^{13}C isotope, and chlorine and bromine isotopes where appropriate.
* Accurate measurement was not possible as a reactant ion had the same m/z as MH^+; abundances were obtained by subtracting approximate reactant-ion abundances from the observed abundances.

Metastable peaks corresponding to the decomposition of M_2H^+ ions occurred in the spectra of all the nitriles (see table (3-11) at the end of section 3.3), suggesting that the proton-bound dimer ions formed from the nitriles have lifetimes that are of the order of the ion-residence times (cf. ketones). The spectra of 2-chloropropionitrile and 2-bromopropionitrile also contained peaks which resulted from the decomposition of metastable $MC_3H_5^+$ ions

$$MC_3H_5^+ \longrightarrow MH^+ + C_3H_4 \qquad (3.3\text{-}10)$$

where the neutral product is assumed to be either allene or cyclopropene. The absence of metastable peaks corresponding to reaction (3.3-10) from the spectra of acetonitrile, propionitrile, and butyronitrile suggested that the $MC_3H_5^+$ ions formed from these compounds were more stable than those formed from the 2-halopropionitriles.

In addition to $MC_3H_5^+$ ions, the spectra of acetonitrile, propionitrile, and butyronitrile also contained ions having m/z = m+39, m+43, and m+57, where m is the molecular weight of the sample molecule. These ions are assumed to be $MC_3H_3^+$, $MC_3H_7^+$, and $MC_4H_9^+$ respectively. The $MC_3H_3^+$ and $MC_3H_7^+$ ions were not detected in the spectra of the 2-halopropionitriles, and the relative abundances of $MC_4H_9^+$ ions formed from these compounds were much lower than the relative abundances formed from acetonitrile, propionitrile, and butyronitrile.

The relative abundances of all the ions generated from isobutane decreased as the sample pressure was increased.

Table (3-6).

Reactant ions for which reaction with the nitriles resulted in a linear decrease of log (I_n/I_n^o) with sample pressure.

Compound	Reactant ions (RH^+)	Comments
Acetonitrile	$C_3H_3^+$, $C_4H_5^+$	Molecular weight = 41 - Behaviour of $C_3H_6^+$ could not be studied
		Molecular weight = 55 - Behaviour of $C_4H_8^+$ could not be studied
Propionitrile	$C_3H_3^+$	Data for $C_4H_5^+$, $C_4H_7^+$ badly scattered.
Butyronitrile	$C_2H_5^+$, $C_3H_3^+$, $C_4H_5^+$	Data for $C_2H_3^+$ badly scattered.
2-Chloropropionitrile	$C_2H_5^+$, $C_3H_3^+$, $C_4H_5^+$	Data for $C_3H_7^+$ badly scattered.
2-Bromopropionitrile	$C_2H_5^+$, $C_2H_5^+$, $C_3H_3^+$, $C_3H_5^+$ $C_3H_6^+$, $C_4H_5^+$, $C_4H_7^+$, $C_4H_8^+$	

Illustrative plots of log (I_n/I_n^o) (see section 3.3.A) against pressure of acetronitrile are given in graph (3-6). The continuous lines in graph (3-6) were calculated from the mathematical expressions which resulted from kinetic analysis of the reaction mechanisms proposed in section 4.2 Table (3-6) lists the reactant ions for which reaction with each of the nitriles resulted in a linear decrease of log (I_n/I_n^o) with sample pressure. For the other reactant ions the decrease of log (I_n/I_n^o) was of the curved form illustrated by the variation of log (I_{56}/I_{56}^o) with pressure of acetonitrile (graph 3-6)). The significance of these results will be discussed in section 4.2.

C. Alcohols.

Chemical-ionization mass spectra of the alcohols listed in tables (3-7) and (3-8) were recorded as described in section 2.2. The isobutane pressure was maintained constant at ca. 0.1 torr throughout each experiment. The temperature of the ion-source block was 175 ± 2°C in all experiments except those carried out with methanol, 1-propanol, and 2-propanol, in which the temperature was 167 ± 2°C. Sample pressures were varied as described in section 2.6.A. For convenience in the following discussion the alcohols are divided into two groups: alkyl alcohols, and halogen-containing alcohols.

The principal ions produced from the alkyl alcohols are listed in table (3-7) which shows the relative ion-abundances at

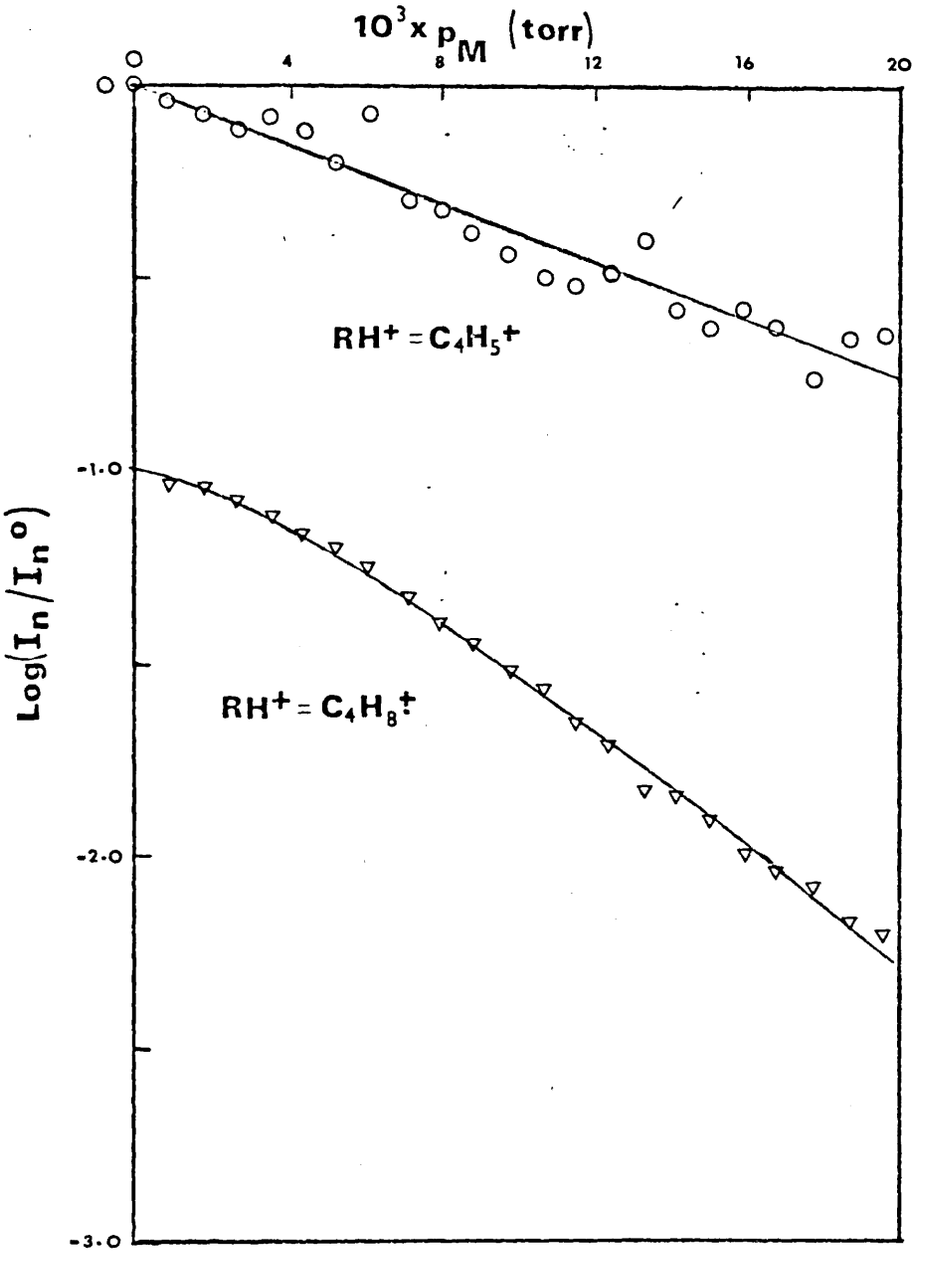

GRAPH (3-6). Kinetic plots for the reactions of acetonitrile (M) with 2 reactant ions, RH^+.

Table (3-7)

Relative abundances of ions produced from various alcohols at selected low and high sample pressures.

Compound (R_1OH)	Isobutane pressure (torr)	Temp. (^oC)	Sample pressure (torr)	Relative ion-abundances†								
				CH_3O^+	$C_3H_5O^+$	R_1^+	R_1O^+	$R_1OH_2^+$	$R_1O^+-H_2O$	$R_1O^+-H_2$	$(R_1OH)R_1^+$	$(R_1OH)_2H^+$
	0.110	167	2.3×10^{-3}	(R_1O^+)			<0.001	0.015	-	-	<0.001	<0.001
			1.1×10^{-2}		-	-	0.001	0.200			0.006	0.011
1-Propanol	0.110	167	2.5×10^{-3}		($R_1OH_2^+$)		<0.001	0.018			<0.001	0.001
			1.2×10^{-2}	-		-	0.012	0.121	-	-	0.009	0.164
2-Propanol	0.111	166	2.4×10^{-3}	-	($R_1OH_2^+$)	-	<0.001	0.034	-	-	<0.001	<0.001
			2.1×10^{-2}				0.012	0.169			0.039	0.126
1-Pentanol	0.099	174	1.3×10^{-3}	-	-	0.027	<0.001	<0.001	0.002	-	<0.001	<0.001
			8.2×10^{-3}			0.302	0.008	0.005	0.015		0.001	0.009
2-Pentanol	0.110	174	1.3×10^{-3}	-	0.002	0.028	0.001	0.003	<0.001	0.002	<0.001	<0.001
			$8.1\text{-}10^{-3}$		0.009	0.357	0.013	0.044	0.007	0.026	0.004	0.037
3-Pentanol	0.099	174	1.3×10^{-3}	<0.001	0.002	0.031	0.001	0.004	0.002	<0.001	<0.001	<0.001
			8.2×10^{-3}	0.001	0.009	0.375	0.012	0.058	0.008	0.007	0.003	0.048
1-Hexanol	0.100	174	1.1×10^{-3}	-	<0.001	0.022	<0.001	0.002	<0.001	-	-	<0.001
			8.1×10^{-3}		0.001	0.290	0.003	0.010	0.015			0.008
2-Hexanol	0.098	174	1.1×10^{-3}	<0.001	<0.001	0.042	0.002	0.002	<0.001	<0.001	-	<0.001
			8.2×10^{-3}	0.011	0.013	0.414	0.023	0.018	0.011	0.002		0.001
3-Hexanol	0.098	174	1.1×10^{-3}	-	<0.001	0.038	0.003	0.003	<0.001	<0.001	-	<0.001
			8.2×10^{-3}		0.009	0.402	0.044	0.027	0.009	0.003		0.035

Abundances have been corrected for ^{13}C isotope.

Table (3-7) continued

Compound	Isobutane pressure (torr)	Temp. (^{o}C)	Sample pressure (torr)	Relative ion-abundances				
				$R_1O^+ - CH_3OH$	$R_1OH_2^+ - CH_3OH$	$R_1OH^{+\cdot} - H_2O$	$R_1OH^{+\cdot}$	$(R_1OH)_2H^+ - C_2H_5OH$
2-Propanol	0.111	166	2.4×10^{-3}					<0.001
			1.1×10^{-2}	-	-	-	-	0.020
3-Pentanol	0.099	174	1.3×10^{-3}					<0.001
			8.2×10^{-3}	-	-	-	-	0.007
1-Hexanol	0.100	174	1.1×10^{-3}	0.001	0.001	0.001	0.001	-
			8.1×10^{-3}	0.005	0.002	0.007	0.003	
2-Hexanol	0.097	174	1.1×10^{-3}	<0.001	<0.001	<0.001	<0.001	-
			8.2×10^{-3}	0.007	0.006	0.007	0.002	
3-Hexanol	0.098	174	1.1×10^{-3}	<0.001	<0.001	<0.001	<0.001	-
			8.2×10^{-3}	0.008	0.008	0.004	0.002	

† Abundances have been corrected for ^{13}C isotope.

selected low and high sample pressures. In the spectra of methanol, 1-propanol, and 2-propanol, the major peaks corresponded to the $R_1OH_2^+$ and $(R_1OH)_2H^+$ ions (ie. MH^+ and M_2H^+ ions respectively). Minor peaks corresponded to ions formed by elimination of water from the $(R_1OH)_2H^+$ species, and ions produced by hydride-transfer reactions:

$$RH^+ + R_1OH \longrightarrow RH_2 + R_1O^+ \qquad (3.3\text{-}11)$$

The $(R_1OH)_2H^+$ species formed from 2-propanol gave rise to an ion of low relative abundance by elimination of ethanol. This rather surprising reaction occurred with only one other alcohol: 3-pentanol.

The spectra of the pentanols and hexanols were dominated by peaks corresponding to the alkyl ions (R_1^+) formed in the reactions

$$RH^+ + R_1OH \longrightarrow R + R_1OH_2^+ \qquad (3.3\text{-}12)$$

$$R_1OH^+ \longrightarrow R_1^+ + H_2O \qquad (3.3\text{-}13)$$

The largest of the minor peaks in the spectra of 1-pentanol and 1-hexanol corresponded to ions produced by the elimination of water from the ionic product (R_1O^+) of reaction (3.3-11). For example,

$$C_5H_{11}O^+ \longrightarrow C_5H_9^+ + H_2O \qquad (3.3\text{-}14)$$

Of the minor peaks in the spectra of 2- and 3-pentanol and 2- and 3-hexanol, however, those having somewhat larger abundances corresponded to the $R_1OH_2^+$ and $(R_1OH)_2H^+$ ions. Nevertheless the spectra of the pentanols and the hexanols differed in several ways. Whereas the $(R_1OH)_2H^+$ ions formed from the pentanols underwent elimination of water to a small extent, a similar

reaction was not observed with the hexanols. On the other hand, certain ion types were formed from the hexanols which were not found in the spectra of any of the other alcohols studied. Both the $R_1OH_2^+$ and the R_1O^+ ions formed from the hexanols underwent elimination of methanol (see table (3-7)). Furthermore the spectra of the hexanols contained ions presumably produced by charge transfer reactions,

$$RH^+ + C_6H_{13}OH \longrightarrow C_6H_{13}OH^{\ddagger\cdot} + RH^{\cdot} \quad (3.3\text{-}15)$$

and the products of these reactions underwent elimination of water

$$C_6H_{13}OH^{\ddagger\cdot} \longrightarrow C_6H_{12}^{\ddagger\cdot} + H_2O \quad (3.3\text{-}16)$$

The spectrum of 3-hexanol contained three ions (m/z = 113,115 and 120) to which compositions could not be assigned.

Metastable peaks corresponding to the elimination of a sample molecule from the M_2H^+ ions were found in the spectra of methanol, 1-propanol, and 2-propanol (see table(3-12) at the end of section 3.3).

The spectra of the pentanols contained metastable peaks which corresponded to the elimination of ethylene from the alkyl ion (R_1^+ in reaction (3.3-13)) subsequent to the loss of water from the protonated alcohol:

$$C_5H_{11}^+ \longrightarrow C_3H_7^+ + C_2H_4 \quad (3.3\text{-}17)$$

Similarly, the spectra of the hexanols contained metastable peaks corresponding to the elimination of propylene from the $C_6H_{13}^+$ ion:

$$C_6H_{13}^+ \longrightarrow C_3H_7^+ + C_3H_6 \quad (3.3\text{-}18)$$

It will be noticed that the ionic products of reactions

(3.3-17) and (3.3-18) have the same mass-to-charge ratio m/z = 43) as one of the reactant ions formed from isobutane. Therefore the occurrence of these reactions was inferred only from the metastable peaks, since the 'daughter' ions could not be observed directly.

The principal ions produced from the halohydrins ($X.CH_2.CH_2.OH$) and from 2,2,2-trifluorothanol are listed in table (3-8); this shows the relative ion-abundances at selected low and high sample pressures. It can be seen that the spectra of the halohydrins changed in a fairly systematic way as the atomic number of the halogen-atom substituent increased. The major peaks in the spectrum of each of 2-fluoro, 2-chloro, and 2-bromoethanol corresponded to the MH^+ and M_2H^+ ions, although their relative abundances tended to decrease in the order X = F>Cl>Br, becoming minor peaks in the spectrum of 2-iodoethanol. Concomitantly, the relative abundance of the $X.CH_2.CH_2^+$ ion, produced from the reaction

$$X.CH_2.CH_2.OH_2^+ \longrightarrow X.CH_2.CH_2^+ + H_2O \qquad (3.3\text{-}19)$$

increased in the order X = F<Cl<Br<I, while the relative abundance of the $HO.CH_2.\ CH_2^+$ ion, produced from the reaction

$$X.CH_2.CH_2.OH_2^+ \longrightarrow HO.CH_2.CH_2^+ + HX \qquad (3.3\text{-}20)$$

decreased in the order X = F>Cl>Br>I.

Compositions could not be assigned to the ions having m/z = 328 and m/z = 200 observed in the spectrum of 2-iodoethanol, although the latter may be formed from the former by elimination of a molecule of HI. Ions having m/z = 170 and m/z = 184

Table (3-8)

Relative abundances of ions produced from various halogeno-alcohols at selected low and high sample pressures.

Compound (XCH_2CH_2OH or M)	Isobutane pressure (torr)	Temp, (°C)	Sample pressure (torr)	Relative ion-abundances †						
				$HOCH_2^+$	$HOCH_2CH_2^+$	$XCH_2CH_2^+$	MH^+	$(MC_4H_9^+-HX-H_2O)$	$MC_3H_7^+$	$MC_4H_9^+$
2-Fluoroethanol	0.114	175	1.6×10^{-3}	<0.001	<0.001	<0.001	0.010	<0.001	<0.001	<0.001
			1.2×10^{-2}	0.002	0.016	0.002	0.108	0.002	0.001	0.001
2-Chloroethanol	0.115	175	1.4×10^{-3}	<0.001	<0.001	0.001	0.010	-	-	-
			1.2×10^{-2}	0.001	0.013	0.008	0.137			
2-Bromoethanol	0.115	175	1.7×10^{-3}	-	0.001	0.004	0.010	-	-	-
			1.2×10^{-2}		0.010	0.039	0.065			
2-Iodoethanol	0.117	175	1.8×10^{-3}	-	<0.001	0.006	0.001	-	-	-
			1.2×10^{-2}		0.008	0.052	0.009			

	M_2H^+-2HX	$(M_2H^+-HX-H_2O)$	(M_2H^+-HX)	$(M_2H^+-H_2O)$	M_2H^+	(M_3H^+-2HX)	M_3H^+
2-Fluoroethanol	<0.001	<0.001	<0.001		<0.001	<0.001	<0.001
	0.011	0.006	0.006	-	0.112	0.005	0.001
2-Chloroethanol	<0.001	-	<0.001	<0.001	<0.001	-	-
	0.001		0.004	0.001	0.058		
2-Bromoethanol	<0.001	<0.001	<0.001	<0.001	<0.001		
	0.001	0.003	0.008	0.022	0.016	-	-
2-Iodoethanol					<0.001		
	-	-	-	-	0.001	-	-

	$HOCH_2^+$	$((CF_3CH_2OH)H^+-HF)$	$(CF_3CH_2OH)H^+$	$((CF_3CH_2OH)_2H^+-2HF)$	$(CF_3CH_2OH)_2H^+$
2,2,2-Trifluoro ethanol	0.109	166	2.6×10^{-3}	<0.001	<0.001	0.001	<0.001	<0.00L
			1.2×10^{-2}	0.002	0.001	0.006	0.001	0.003

† Abundances have been corrected for ^{13}C isotope.

(formed from this compound) may correspond to $C_3H_7I^{+\cdot}$ and $C_4H_9I^{+\cdot}$. These ions could be formed either by direct association of the reactant ions (RH^+) with free iodine atoms formed by the thermal decomposition of 2-iodoethanol, or may have been produced by the reactions

$$RH^+ + I.CH_2.CH_2.OH \longrightarrow RHI^{+\cdot} + {}^{\cdot}CH_2.CH_2.OH \qquad (3.3\text{-}21)$$

where RH^+ is either $C_3H_7^+$ or $C_4H_9^+$.

One of the larger minor peaks in the spectrum of 2-iodoethanol has m/z = 300 (see table (3.8)). This mass-to-charge ratio suggested that the ion was the product of association of $ICH_2CH_2OH_2^+$ and free iodine atoms. Furthermore, substitution of values of I_{300} and I_{301} into equation (3.3-9) confirmed that the ion contains two carbon atoms. It seems, then, that the ion possessed the structure

$$ICH_2CH_2OH\cdots H^+\cdots I$$

and was probably formed by a reaction analogous to one of those proposed above for the formation of the $RHI^{+\cdot}$ species.

It can be seen from table (3-8) that the relative abundances of ions produced from 2,2,2-trifluoroethanol were very low, as might be expected from a molecule containing three strongly electron-withdrawing substituents (cf. CCl_4, below). The MH^+ and M_2H^+ ions were responsible for the major peaks in the spectrum.

Metastable peaks corresponding to the elimination of a sample molecule from the M_2H^+ ions were found in the spectra of 2-fluoroethanol and 2-chloroethanol (see table(3.12) at the end of section 3.3). Additionally, the spectrum of 2-fluoroethanol

contained a metastable peak which corresponded to the elimination of a molecule of acetylene from the ion formed after the elimination of both HF and H_2O from the M_2H^+ ion, the ionic product being the MH^+ ion. Metastable peaks were not detected in the spectra of 2-bromoethanol, 2-iodoethanol, or 2,2,2-trifluoroethanol.

Spectra of all the alcohols show that the relative abundances of all the ions generated from isobutane decreased as the sample pressure was increased. Illustrative plots of $\log (I_n/I_n^o)$ (see section 3.3.A) against pressure of two of the alcohols are given in graphs (3-7) and (3-8). The continuous lines in graphs (3-7) and (3-8) were calculated from the mathematical expressions which resulted from kinetic analysis of the reaction mechanisms proposed in section 4.2. Table (3-9) lists the reactant ions for which reaction with the nitriles resulted in a linear decrease of $\log (I_n/I_n^o)$ with sample pressure. For the other reactant ions the decrease of $\log(I_n/I_n^o)$ was of the curved form illustrated, for example, by the variation of $\log (I_{43}/I_{43}^o)$ with pressure of 3-pentanol (graph (3-7)). The significance of the above results will be discussed in section 4.2.

D. Anisoles.

Chemical-ionization mass spectra of anisole, the 3- and 4-methyl-anisoles, and the 3- and 4-fluoro-anisoles were recorded as described in section 2.2. Sample pressures were varied according to the method given in section 2.6.A. The temperature of the ion-source block was 175 ± 2°C.

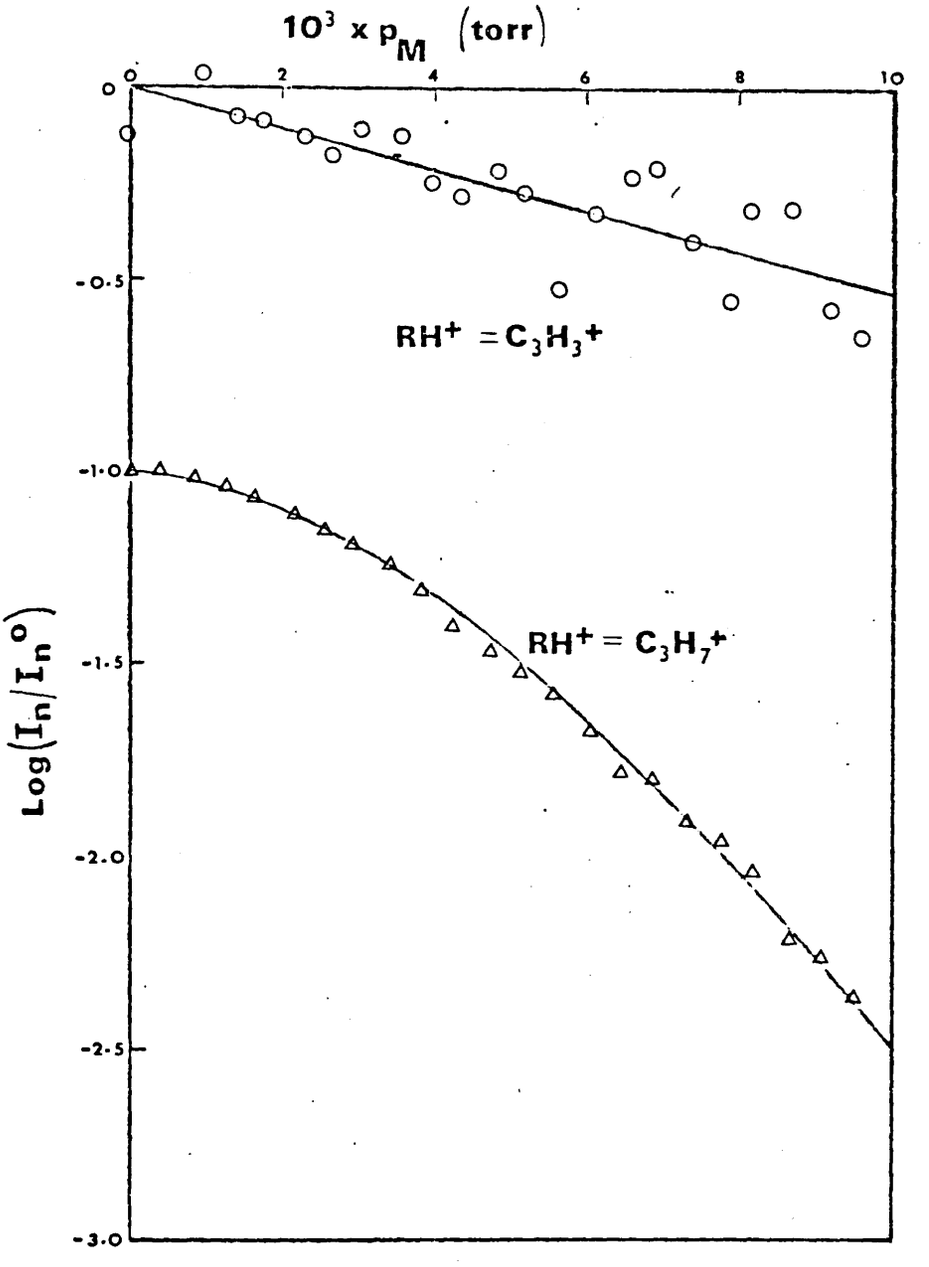

GRAPH (3-7) . Kinetic plots for the reactions of 3-pentanol (M) with 2 reactant ions, RH^+ .

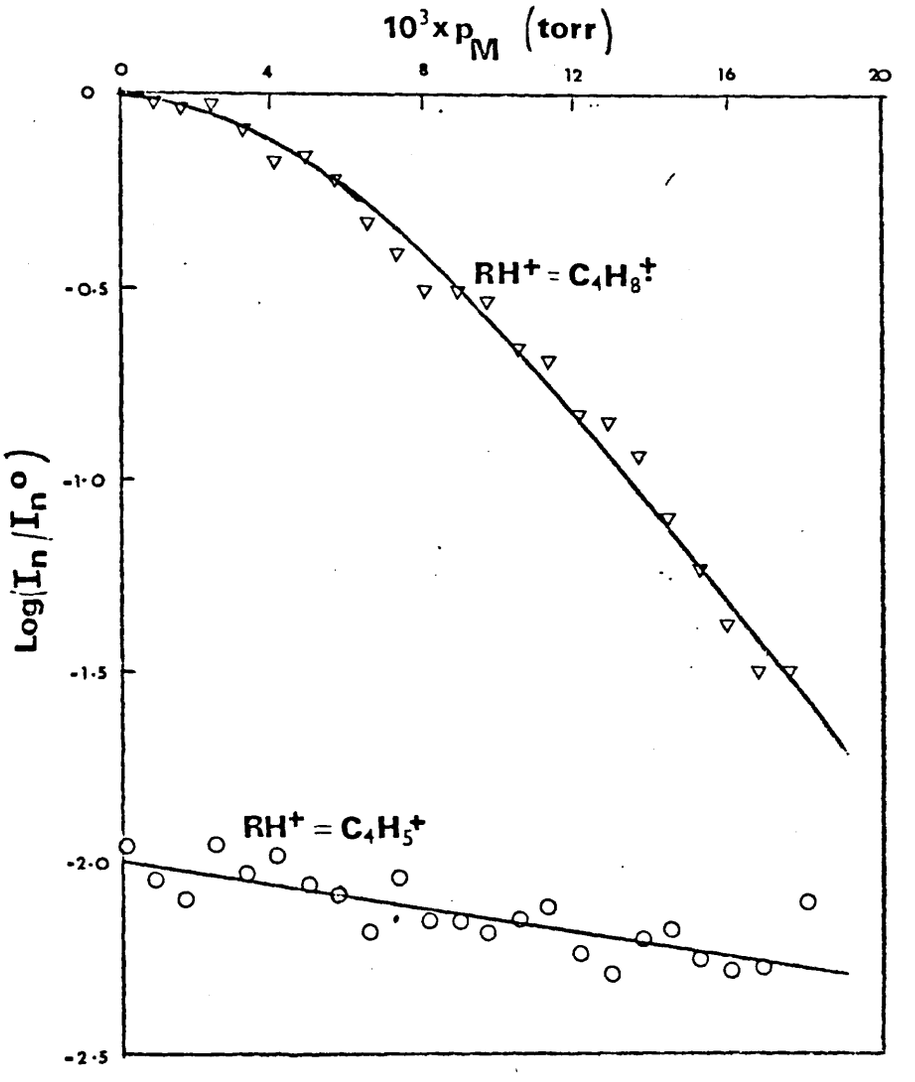

GRAPH (3-8). Kinetic plots for the reactions of 2-fluoroethanol (M) with 2 reactant ions, RH^+.

Table (3-9)

Reactant ions for which reaction with the alcohols resulted in a linear decrease of $\log (I_n/I_n^{\circ})$ with sample pressure.

Compound	Reactant ions (RH^+)	Comments
Methanol	$C_2H_3^+$, $C_2H_5^+$, $C_3H_3^+$, $C_4H_5^+$, $C_4H_7^+$	
1-Propanol	$C_2H_3^+$, $C_2H_5^+$, $C_3H_3^+$, $C_4H_5^+$, $C_4H_7^+$	
2-Propanol	$C_2H_3^+$, $C_2H_5^+$, $C_3H_3^+$, $C_4H_5^+$, $C_4H_7^+$	
1-Pentanol	$C_2H_3^+$, $C_2H_5^+$, $C_3H_3^+$, $C_3H_6^{\ddagger}$, $C_4H_5^+$, $C_4H_7^+$	Data for $C_3H_5^+$ badly scattered.
2-Pentanol	$C_2H_3^+$, $C_2H_5^+$, $C_3H_3^+$, $C_3H_6^{\ddagger}$, $C_4H_5^+$, $C_4H_7^+$	
3-Pentanol	$C_2H_5^+$, $C_3H_3^+$, $C_4H_5^+$	Data for $C_2H_3^+$ badly scattered.
1-Hexanol	$C_2H_3^+$, $C_2H_5^+$, $C_3H_3^+$, $C_4H_5^+$, $C_4H_7^+$	Data for $C_3H_5^+$, $C_3H_6^{\ddagger}$ badly scattered.
2-Hexanol	$C_2H_3^+$, $C_2H_5^+$, $C_3H_3^+$, $C_4H_5^+$, $C_4H_7^+$	Data for $C_3H_5^+$, $C_3H_6^{\ddagger}$ badly scattered.
3-Hexanol	$C_2H_3^+$, $C_2H_5^+$, $C_3H_3^+$, $C_3H_5^+$, $C_3H_6^{\ddagger}$, $C_4H_5^+$, $C_4H_7^+$	
2-Fluoroethanol	$C_2H_3^+$, $C_2H_5^+$, $C_2H_3^+$, $C_3H_5^+$, $C_3H_6^{\ddagger}$ $C_4H_5^+$, $C_4H_7^+$	
2-Chloroethanol	$C_2H_3^+$, $C_2H_5^+$, $C_3H_3^+$, $C_3H_5^+$, $C_3H_6^{\ddagger}$ $C_4H_5^+$, $C_4H_7^+$, $C_4H_8^{\ddagger}$, $C_4H_9^+$	
2-Bromoethanol	ALL	
2-Iodoethanol	ALL	
2,2,2-Trifluoro-ethanol	ALL	

In these experiments the isobutane pressure was ca.0.24 torr. At this pressure the relative abundance of $C_4H_9^+$ ion in the isobutane spectrum is ca.0.90. Thus reactions of ions other than $C_4H_9^+$ with the anisoles do not make a significant contribution to the production of the spectra, and will be omitted from the following discussion.

The principal ions produced from the five anisoles are listed in table (3-10), which shows the relative ion-abundances at selected low and high sample pressures. It can be seen from the table that the major peaks in the spectra corresponded to the $M^{+\cdot}$ and MH^+ ions. The $M^{+\cdot}$ ions were probably produced by charge-transfer reactions (cf.reaction (3.3-3)) since the formation of these ions by direct electron-impact ionization of sample molecule is unlikely when isobutane is present at a pressure of ca.0.2 torr. As the $C_4H_9^+$ ion was essentially the only reactant ion present, the charge-transfer reactions may be written as

$$M + C_4H_9^+ \longrightarrow M^{+\cdot} + C_4H_9^{\cdot} \qquad (3.3\text{-}22)$$

although the neutral product may subsequently decompose, for example by loss of a hydrogen atom or a methyl radical. This reaction was in competition with the proton-transfer reaction (reaction 3.3-23) which produced the other major peak in the spectra of each of the anisoles.

$$M + C_4H_9^+ \longrightarrow MH^+ + C_4H_8 \qquad (3.3\text{-}23)$$

Graph (3-9) shows the variation of the ratio $I_{MH^+}/(I_{M^{+\cdot}} + I_{MH^+})$ with sample pressure. For anisole and the two fluoro-substituted anisoles, the ratio increased with increasing sample

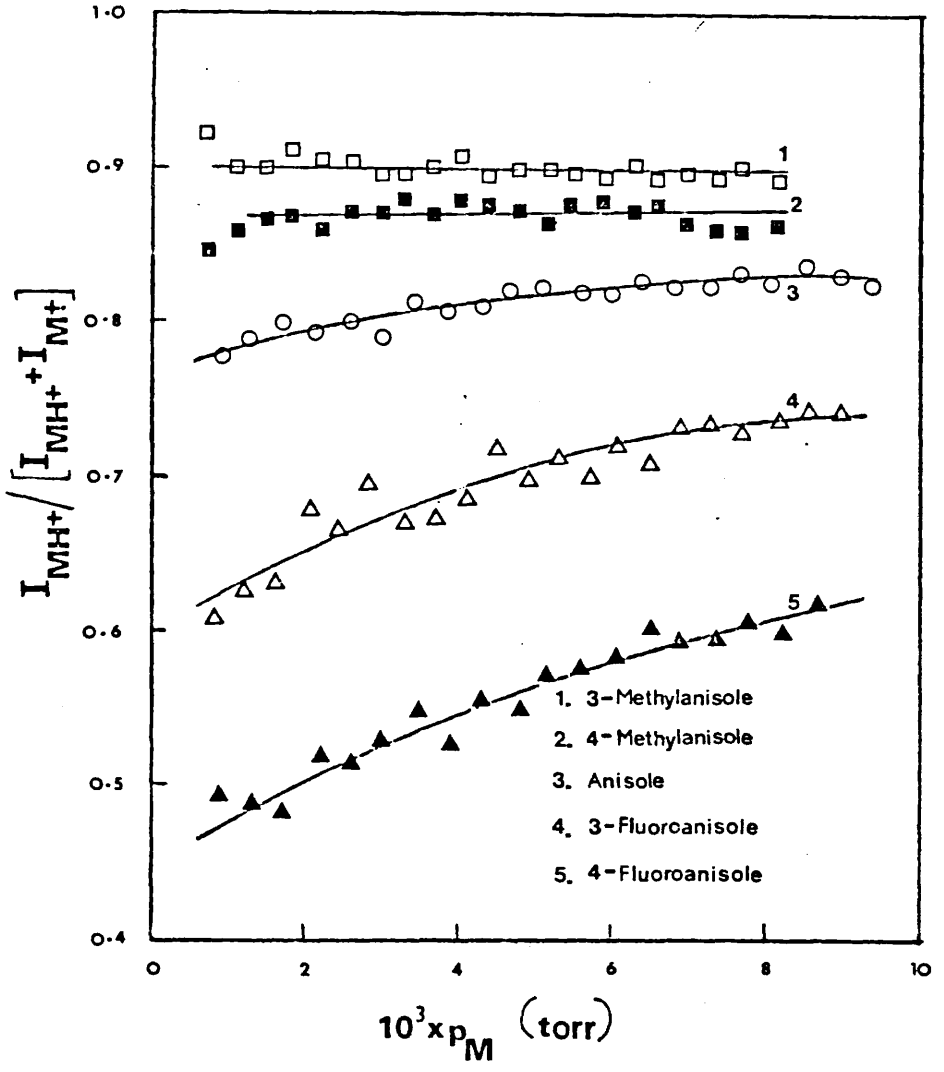

GRAPH (3-9) . Plots of $I_{MH^+}/[I_{MH^+}+I_{M^+}]$ against pressure of various anisoles (M) .

pressure, whereas, for the two methyl-substituted anisoles, it remained constant. These results will be discussed in section 4.3.A.

Ions having m/z = m+15, m+41, m+43, and m+57 were also present in the spectra, although their relative abundances were generally small. Ions having m/z = m+57 were presumably formed by the association reactions

$$M + C_4H_9^+ \longrightarrow MC_4H_9^+ \qquad (3.3\text{-}24)$$

Elimination of propene and methane from this ion would then give the species having m/z = m+15 and m/z = m+41, respectively.

$$MC_4H_9^+ \longrightarrow MCH_3^+ + C_3H_6 \qquad (3.3\text{-}25)$$

$$MC_4H_9^+ \longrightarrow MC_3H_5^+ + CH_4$$

The ion having m/z = m+43 could not be formed by a reaction of the type (3.3-4) since the increase of the relative abundance of $MC_3H_7^+$ with sample pressure was considerably greater than the decrease of the relative abundance of the $C_3H_7^+$ ion. Furthermore, the elimination of a neutral CH_2 species from the $MC_4H_9^+$ ion

$$MC_4H_9^+ \longrightarrow MC_3H_7^+ + CH_2 \qquad (3.3\text{-}27)$$

seems inherently unlikely, so that the origin of this ion remains obscure.

It can be seen from table (3-10) that M_2H^+ ions were formed only from the two para-substituted anisoles. Furthermore the relative abundance of these ions remained small even at the highest sample pressure. No metastable peaks were observed in the spectra of any of the anisoles.

The spectra of the anisoles showed that the relative abundance of the $C_4H_9^+$ ion decreased as the sample pressure was increased. Graph (3-10) shows the way in which log (I_{57}/I_{57}^o) varied with pressure of 4-methylanisole. Similar curves were obtained for the variation of log (I_{57}/I_{57}^o) with pressure of the other anisoles. The continuous line in graph (3-10) was calculated from the mathematical expression which resulted from the kinetic analysis of one of the reaction mechanisms proposed in section 4.2.

E. Miscellaneous compounds.

(i) Carbon Tetrachloride.

Chemical-ionization mass spectra of carbon tetrachloride were recorded for sample pressures in the range $0 - 4 \times 10^{-3}$ torr. The isobutane pressure was maintained constant at 0.10 torr, and the temperature of the ion-source block was 174 ± 2°C.

The CCl_3^+ ion was the only ion produced from carbon tetrachloride by reaction with the isobutane reactant ions. This ion was presumably the product of chloride-abstraction reactions:

$$RH^+ + CCl_4 \longrightarrow RHCl + CCl_3^+ \qquad (3.3\text{-}28)$$

The relative abundances of all the reactant ions except $C_3H_6^+$ and $C_4H_8^+$ were found to decrease linearly as the sample pressure was increased. Graph (3-11) shows that variation of log (I_{57}/I_{57}^o) with pressure of carbon tetrachloride. The significance of these results is discussed in section 4.2.

(ii) Water.

Chemical-ionization mass spectra of water were recorded

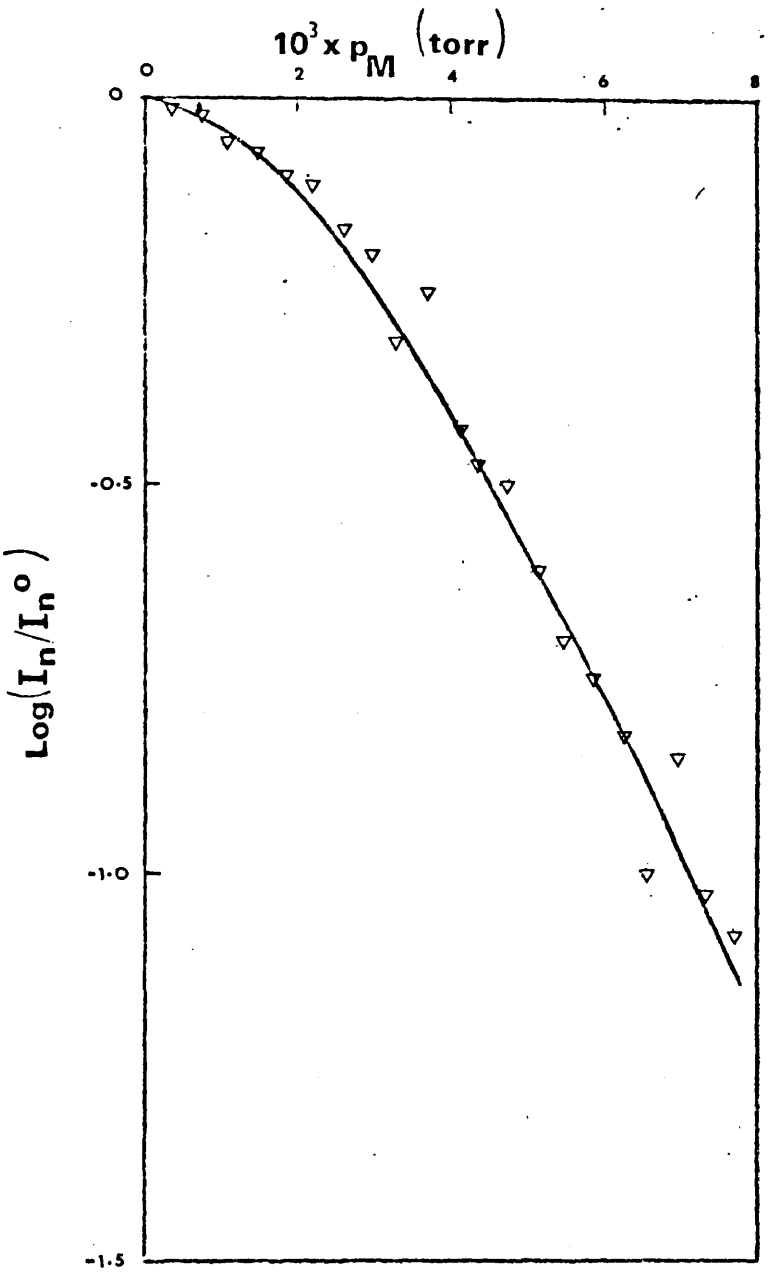

GPAPH (3-10). Kinetic plot for the reaction of 4-methylanisole with $C_4H_9^+$.

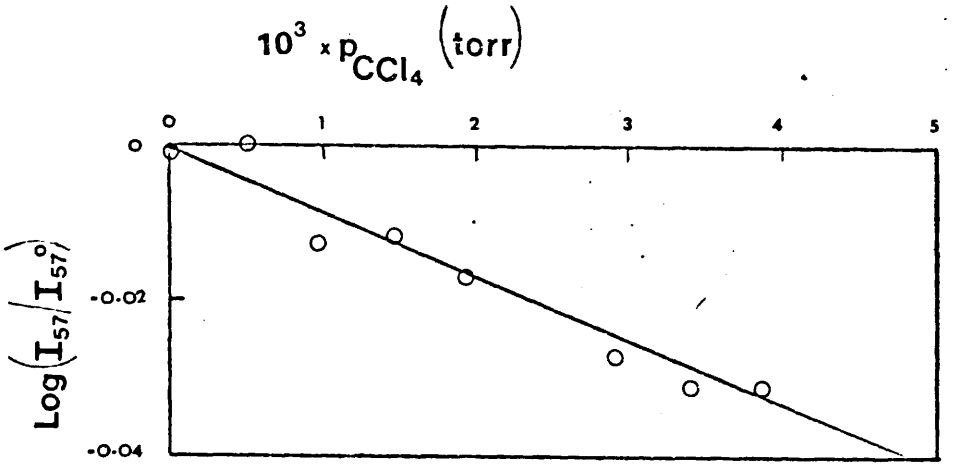

GRAPH 3-11. Kinetic plot for the reaction between carbon tetrachloride and $C_4H_9^+$.

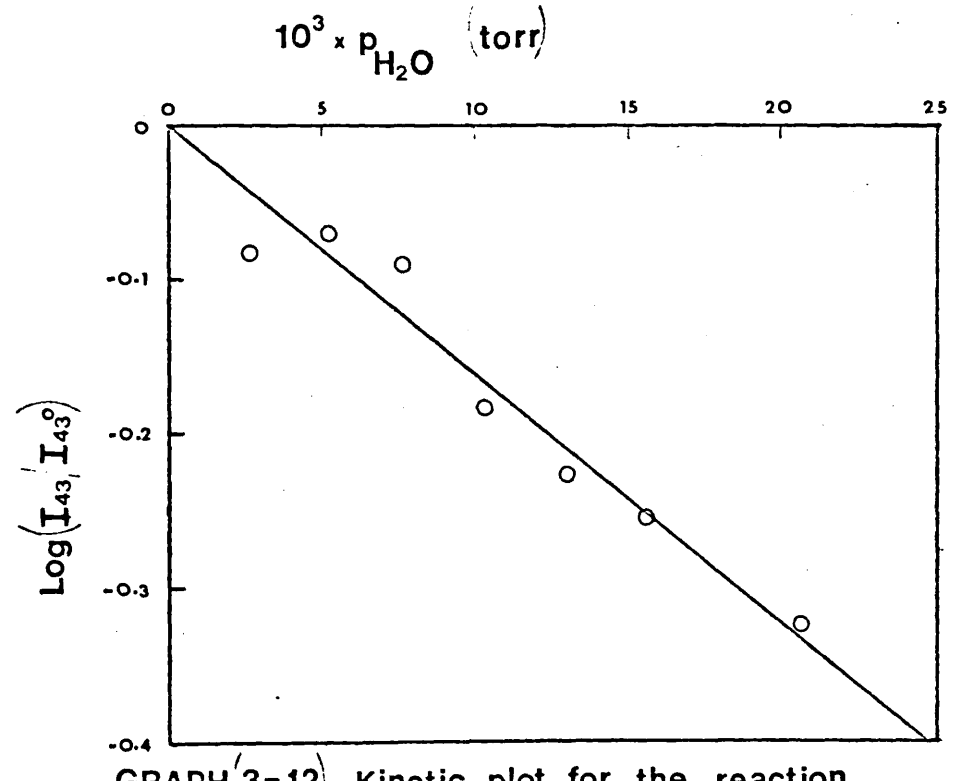

GRAPH 3-12. Kinetic plot for the reaction between water and $C_3H_7^+$.

for sample pressures in the range 0 - 2.1 x 10^{-2} torr. The isobutane pressure was maintained constant at 0.09 torr, and the temperature of the ion-source block was 175 ± 2°C.

Ions having m/z = 19 (H_3O^+) and m/z = 37 ($(H_2O)_2H^+$) were the only product ions detected in the spectra. These ions were presumably produced by the reactions:

$$RH^+ + H_2O \longrightarrow R + H_3O^+ \qquad (3.3\text{-}29)$$

$$H_3O^+ + H_2O \longrightarrow (H_2O)_2H^+ \qquad (3.3\text{-}30)$$

The relative abundances of all the reactant ions except $C_4H_9^+$ were found to decrease linearly as the sample pressure was increased. Graph (3-12) shows the variation of log (I_{43}/I_{57}^0) with pressure of water. The significance of these results is discussed in section 4.2.

Table (3-10).

Relative abundances of ions produced from the anisoles at selected low and high sample pressures.

Compound (M)	Isobutane pressure (torr)	Temp. (°C)	Sample pressure (torr)	Relative ion-abundances †						
				M^+	MH^+	MCH_3^+	$MC_3H_5^+$	$MC_3H_7^+$	$MC_4H_9^+$	M_2H^+
Anisole	0.240	175	1.3×10^{-3}	0.003	0.029	0.002	<0.001	0.002	0.003	
			9.0×10^{-3}	0.074	0.375	0.013	0.009	0.014	0.027	
3-Fluoroanisole	0.230	175	1.2×10^{-3}	0.006	0.013	-	<0.001	<0.001	<0.001	
			9.0×10^{-3}	0.055	0.164		0.008	0.013	0.007	
4-Fluoroanisole	0.240	175	1.3×10^{-3}	0.008	0.008	-	<0.001	<0.001	<0.001	<0.001
			9.1×10^{-3}	0.068	0.112		0.008	0.009	0.002	0.002
3-Methylanisole	0.236	175	1.1×10^{-3}	0.007	0.055	<0.001	<0.001	<0.001	<0.001	
			8.1×10^{-3}	0.042	0.394	0.002	0.005	0.009	0.006	
4-Methylanisole	0.240	175	1.1×10^{-3}	0.008	0.041	<0.001	<0.001	<0.001	<0.001	<0.001
			7.7×10^{-3}	0.082	0.506	0.003	0.006	0.009	0.005	0.002

† Abundances have been corrected for ^{13}C isotope

Table (3-11)

Metastable peaks in the spectra of ketones and nitriles.

Compound (M)	Observed m/z	Calculated m/z	Assignments*
Acetone	29.71	29.75	$M_2H^+ \longrightarrow MH^+ + M$
Ethyl methyl ketone	36.75	36.75	$M_2H^+ \longrightarrow MH^+ + M$
Acetonitrile	21.18	21.25	$M_2H^+ \longrightarrow MH^+ + M$
Propionitrile	28.27	28.25	$M_2H^+ \longrightarrow MH^+ + M$
Butyronitrile	35.34	35.25	$M_2H^+ \longrightarrow MH^+ + M$
2-Chloropropionitrile	45.27	45.25	$^{35}M_2H^+ \longrightarrow {}^{35}MH^+ + {}^{35}M$
		44.75	$^{35}M{}^{37}MH^+ \longrightarrow {}^{35}MH^+ + {}^{37}M$
	46.46	46.76	$^{35}M{}^{37}MH^+ \longrightarrow {}^{37}MH^+ + {}^{35}M$
		46.25	$^{37}M_2H^+ \longrightarrow {}^{37}MH^+ + {}^{37}M$
2-Chloropropionitrile	62.26	62.31	$^{35}MC_3H^+ \longrightarrow {}^{35}MH^+ + C_3H_4$
	64.27	64.12	$^{37}MC_3H_5^+ \longrightarrow {}^{37}MH^+ + C_3H_4$
2-Bromopropionitrile	67.07	67.25	$^{79}M_2H^+ \longrightarrow {}^{79}MH^+ + {}^{79}M$
		66.75	$^{79}M{}^{81}MH^+ \longrightarrow {}^{79}MH^+ + {}^{81}M$
	68.20	68.76	$^{79}M{}^{81}MH^+ \longrightarrow {}^{81}MH^+ + {}^{79}M$
		68.25	$^{81}M_2H^+ \longrightarrow {}^{81}MH^+ + {}^{81}M$
2-Bromopropionitrile	103.22	103.20	$^{79}MC_3H_5^+ \longrightarrow {}^{79}MH^+ + C_3H_4$
	105.00	105.09	$^{81}MC_3H_5^+ \longrightarrow {}^{81}MH^+ + C_3H_4$

* The symbol ^nM for a compound containing chlorine or bromine signifies that the molecule contains a chlorine or bromine isotope having atomic mass = n.

Table (3-12).

Metastable peaks in the spectra of alcohols.

Compound (M)	Observed m/z	Calculated m/z	Assignment*
Methanol	16.57	16.75	$M_2H^+ \longrightarrow MH^+ + M$
1-Propanol	30.65	30.75	
2-Propanol	30.80	30.75	
1-Pentanol	25.91	26.04	
2-Pentanol	26.05	26.04	
3-Pentanol	25.88	26.04	
1-Hexanol	21.70	21.75	
2-Hexanol	21.66	21.75	
3-Hexanol	21.73	21.75	
2-Fluoroethanol	32.77	32.75	$M_2H^+ \longrightarrow MH^+ + M$
	46.44	46.43	$MC_2H_3^+ \longrightarrow MH^+ + C_2H_2$ (see text)
2-Chloroethanol	40.80	40.75	$^{35}M_2H^+ \longrightarrow {}^{35}MH^+ + {}^{35}M$
		42.26	$^{35}M^{37}MH^+ \longrightarrow {}^{37}MH^+ + {}^{35}M$
		40.25	$^{35}M^{37}MH^+ \longrightarrow {}^{35}MH^+ + {}^{27}M$
		41.75	$^{37}M_2H^+ \longrightarrow {}^{37}MH^+ + {}^{37}M$

* The symbol ^{n}M for 2-chloroethanol signifies that the molecule contains the chlorine isotope having atomic mass = n.

3.4 The effects of variation of the pressures of isobutane and acetone on the chemical-ionization mass spectrum of acetone.

The effects of variation of both the isobutane pressure and the acetone pressure on the chemical-ionization mass spectrum of acetone were investigated by the method described in section 2.6.C. The temperature of the ion-source block was 175 ± 2°C. The five acetone pressures and four isobutane pressures employed in this experiment are listed in table (3-13). Spectra recorded at different isobutane pressures, but with a fixed acetone pressure, may be compared only after the reactions of the primary ions from isobutane with isobutane itself have been taken into account. If the relative abundance of, for example, the $C_4H_9^+$ ion at a given isobutane pressure, p, be denoted by $I_{57}^{o}(p)$when there is no acetone present, and by $I_{57}(p)$ when acetone is present, then the effect of variation of isobutane pressure upon the reaction

$$CH_3.CO.CH_3 + C_4H_9^+ \longrightarrow (CH_3.CO.CH_3)H^+ + C_4H_8 \qquad (3.4\text{-}1)$$

may be determined by evaluating the function $\log (I_{57}(p)/I_{57}^{o}(p))$ for the various pressures of acetone and of isobutane used in the experiment. This normalization procedure will be rationalized in section 4.2.B. Results are presented in table (3-13) from which it can be seen that the value of the function decreased as both the isobutane pressure, and the acetone pressure, increased. The calculated values of $\log (I_{57}(p)/I_{57}^{o}(p))$ given in the table were obtained from a curve-fitting procedure which is also discussed in section 4.2.B.

Table (3-13).

Variation of log $(I_{57}(p)/I^{o}_{57}(p))$ with acetone and isobutane pressure.

Acetone pressure (10^3x torr)	Isobutane pressure (torr)	-log $(I_{57}(p)/I^{o}_{57}(p))$ (observed)	-log $(I_{57}(p)/I^{o}_{57}(p))$ (calculated)
3.2	0.056	0.097	0.130
	0.098	0.071	0.234
	0.164	0.307	0.405
	0.206	0.560	0.521
5.1	0.056	0.272	0.293
	0.098	0.393	0.519
	0.164	0.878	0.887
	0.206	1.181	1.129
7.0	0.056	0.514	0.495
	0.098	0.789	0.875
	0.164	1.537	1.483
	0.206	1.930	1.880
8.9	0.056	0.839	0.729
	0.098	1.274	1.281
	0.164	2.147	2.164
	0.206	2.739	2.736
10.1	0.056	1.082	0.894
	0.098	1.583	1.574
	0.164	2.612	2.655
	0.206	3.302	3.352

The normalization procedure may not be applied to reactant ions other than $C_4H_9^+$ since the relative abundances of these ions are very small at high isobutane pressures with the consequence that the determination of the value of log $(I_n(p)/I_n^o(p))$ is then subject to large errors.

It is apparent from table (3-14) that, for a given acetone pressure, the sum of the relative abundances of the ions derived from reactions with acetone increased as the isobutane pressure was increased. Furthermore the relative abundance of the $(CH_3CO.CH_3)_2H^+$ ion increased as both the isobutane pressure and the acetone pressure were increased. The changes in the relative abundance of the $(CH_3.CO.CH_3)H^+$ ion are more complicated owing to the reaction of this ion with acetone molecules (reaction 3.3-2). The results presented in table (3-13) will be discussed further in section 4.2.B.

3.5 The chemical-ionization mass spectra of mixtures.

The experimental procedure used to determine the effects of variation of pressure of one component of a two-component sample mixture upon the chemical-ionization mass spectrum was described in section 2.6.B. Mixtures investigated by this method are listed in table (3-15) together with the isobutane pressures and ion-source block temperatures employed in each experiment.

Table (3-14).

Relative abundances of ions produced from acetone: variation with isobutane pressure.

Acetone pressure (10^3x torr)	Isobutane pressure (torr)	Relative ion-abundances†				
		MH^+	$MC_3H_5^+$	$C_3H_7^+$	M_2H^+	Sum
3.2	0.056	0.151	0.001	-	-	0.152
	0.098	0.216	0.002	-	0.005	0.223
	0.164	0.296	0.002	-	0.031	0.329
	0.206	0.342	0.002	-	0.060	0.404
5.1	0.056	0.305	0.002	-	0.002	0.309
	0.098	0.395	0.004	-	0.027	0.426
	0.164	0.442	0.004	-	0.123	0.569
	0.206	0.434	0.003	-	0.207	0.644
7.0	0.056	0.440	0.004	0.002	0.009	0.455
	0.098	0.510	0.009	0.001	0.071	0.591
	0.164	0.461	0.006	0.001	0.274	0.742
	0.206	0.372	0.006	0.002	0.419	0.799
8.9	0.056	0.551	0.009	0.004	0.025	0.589
	0.098	0.561	0.010	0.002	0.146	0.719
	0.164	0.380	0.010	0.002	0.436	0.828
	0.206	0.253	0.006	0.003	0.614	0.876
10.1	0.056	0.595	0.012	0.006	0.047	0.660
	0.098	0.545	0.012	0.004	0.210	0.771
	0.164	0.311	0.011	0.004	0.548	0.874
	0.206	0.187	0.009	0.004	0.700	0.900

† Abundances have been corrected for ^{13}C isotope.

Table (3-15).

Compounds used in the studies of the chemical-ionization mass spectra of mixtures.

First Component	Second Component	Isobutane pressure (torr)	Temp. (°C)
Anisole	Water	0.113	175 ± 2
Acetone	Water	0.105	174 ± 2
Anisole	Carbon tetrachloride	0.089	174 ± 2
4-Fluoroanisole	Carbon tetrachloride	0.112	174 ± 2
Acetone	Carbon tetrachloride	0.102	163 ± 3
Acetone	Ethyl methyl ketone	0.135	178 ± 3

It was stated in section 3.3.E that both water and carbon tetrachloride effect only very small changes in the spectrum of isobutane. Thus it might be expected that the chemical-ionization mass spectrum of a mixture of, for example, acetone and carbon tetrachloride would be not very different from the spectrum of pure acetone. This, however, was not the case: the presence of carbon tetrachloride caused marked changes in the spectrum of acetone. Firstly, the relative abundances of ions produced from acetone increased. Secondly, the spectrum of the mixture contained ions which were not present in the spectrum of either acetone or carbon tetrachloride alone.

Increases of the relative abundances of product ions occurred with all the mixtures studied. Furthermore, spectra

of mixtures of anisole with carbon tetrachloride and of 4-fluoroanisole with carbon tetrachloride contained ions which were not present in the spectra of these pure compounds (vide infra).

Tables (3-16) and (3-17) show that relative abundances of product ions in the spectra of acetone, anisole, and 4-fluoroanisole both alone and in the presence of either water or carbon tetrachloride. The effects of the presence of water and carbon tetrachloride on the spectrum of acetone were studied at several acetone pressures.

As the relative abundances of product ions increased, so the relative abundances of ions generated from isobutane decreased. Examples of the changes of relative abundances of reactant ions observed when the pressure of one component of the mixture was varied while the pressure of the other was held constant are given in graphs (3-13) and (3-14). These graphs consist of plots of the function log (I_n/I_n^o), where I_n^o is the abundance of ions having m/z = n in the absence of any sample, against pressure of either water or carbon tetrachloride. It is apparent that log (I_n/I_n^o) decreased linearly as the pressure of the second component of the mixture was increased, although in some cases there was a comparatively large, non-linear decrease of the function in the low-pressure region. Table (3-18) shows the cases in which this latter behaviour was observed. For certain ions the function log (I_n/I_n^o) was found to approach a limiting value as the pressure of water was increased (see graph (3-14)).

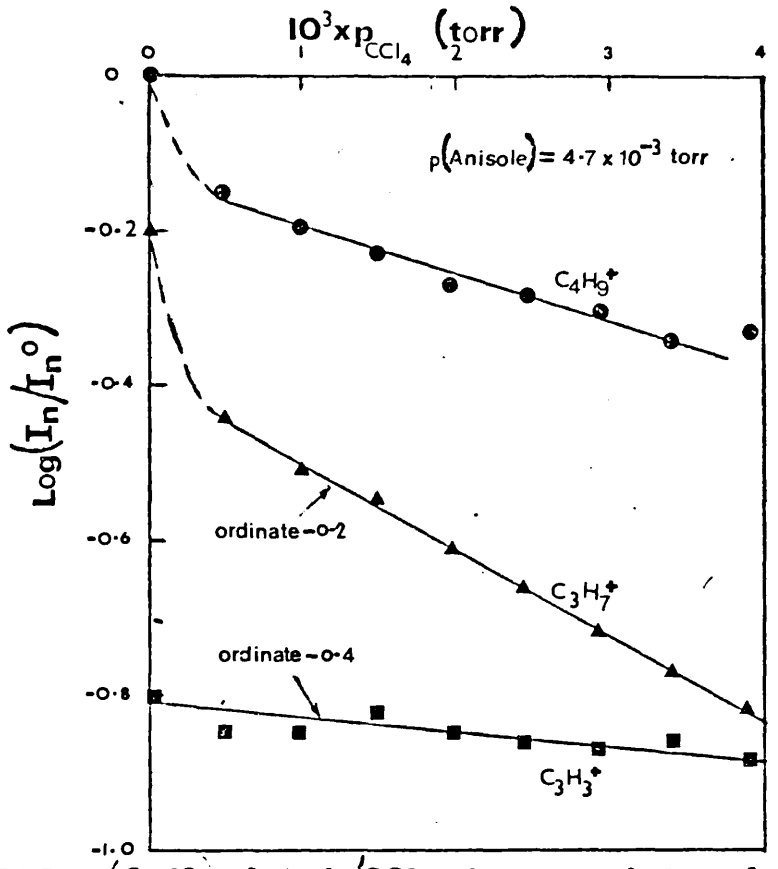

GRAPH (3-13) Anisole/CCl_4 mixture variation of $\log(I_n/I_n^o)$ with pressure of CCl_4.

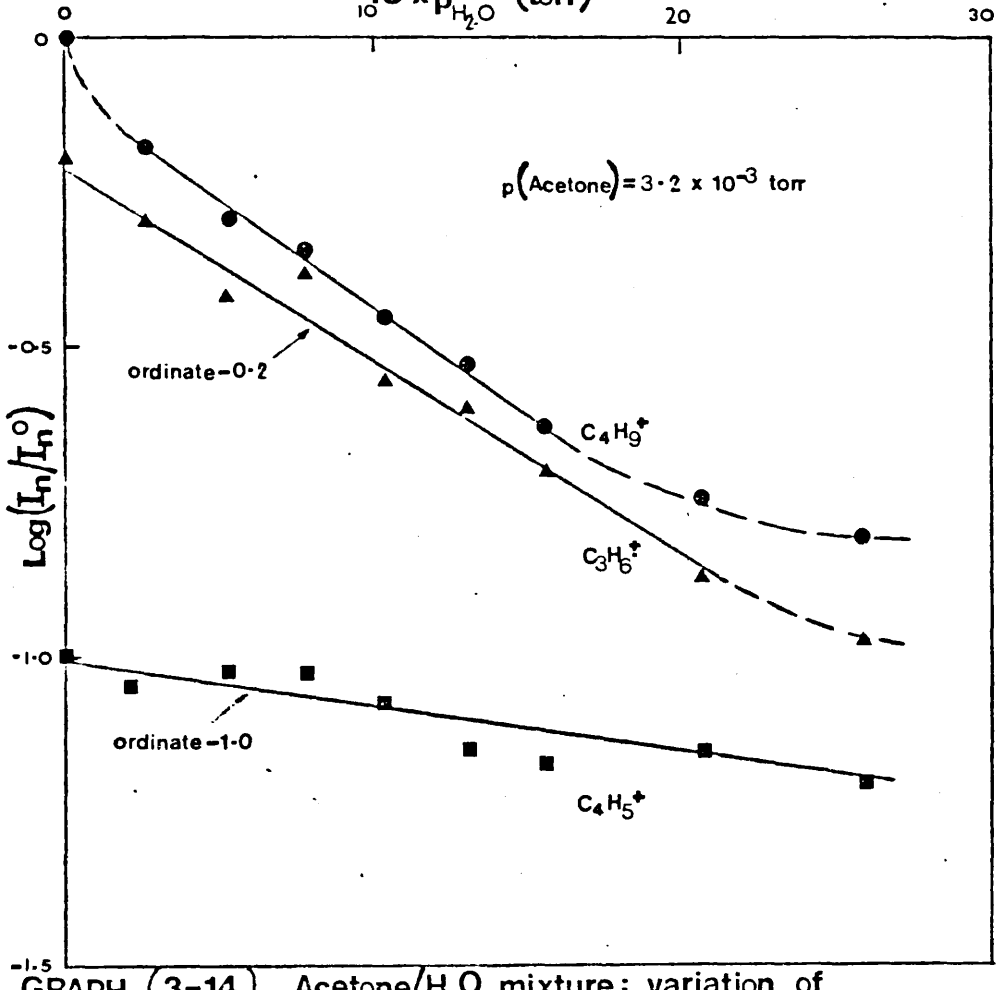

GRAPH (3-14). Acetone/H_2O mixture: variation of $\log(I_n/I_n^o)$ with pressure of H_2O.

Table (3-16)

Relative abundances of ions produced from mixtures of acetone with carbon tetrachloride and water.

First Component of mixture (M)	Pressure of M (10 x torr)	Second Component of mixture (T)	Pressure of T (10 x torr)	Relative ion-abundances †					
				MH^+	$MC_3H_5^+$	$MC_3H_7^+$	M_2H^+	$M_2C_3H_5^+$	M_3H^+
Acetone	1.3	CCl_4	0	0.068	0.001	-	0.001	-	-
			3.9	0.155	0.002		0.012		
	2.5		0	0.174	0.003	-	0.005	-	-
			3.9	0.284	0.005		0.045		
	3.8		0	0.282	0.005	-	0.017	< 0.001	< 0.001
			3.9	0.367	0.009		0.010	0.001	0.001
	5.1		0	0.379	0.007	< 0.001	0.034	< 0.001	< 0.001
			3.9	0.406	0.013	0.001	0.169	0.002	0.002
Acetone	3.2	H_2O	0	0.230	0.001	< 0.001	0.006	-	-
			15.5	0.525	0.005	0.001	0.056		
	7.0		0	0.525	0.005	0.001	0.065	-	-
			15.5	0.559	0.012	0.002	0.239		

† Abundances have been corrected for ^{13}C isotope.

Table (3-17).

Relative abundances of ions produced from mixtures of anisole and 4-fluoroanisole with carbon tetrachloride, and from a mixture of anisole with water.

First Component of mixture (M)	Pressure of M (10^3x torr)	Second Component of mixture (T)	Pressure of T (10^3x torr)	Relative ion-abundances†						
				M^+	MH^+	$MC_3H_5^+$	$MC_3H_7^+$	$MC_4H_9^+$	$M.CCl_3^+$	$M.CCl_3^+$-HCl
Anisole	4.7	CCl_4	0	0.050	0.145	0.009	0.006	0.001	–	–
			3.9	0.125	0.271	0.018	0.010	0.003	0.013	0.005
4-Fluoro-anisole	4.8	CCl_4	0	0.040	0.079	0.006	0.003	–	–	–
			4.3	0.108	0.219	0.014	0.009		0.020	0.015
Anisole	4.7	H_2O	0	0.043	0.125	0.008	0.007	0.002	–	–
			15.5	0.129	0.404	0.023	0.017	0.007		

† Abundances have been corrected for ^{13}C isotope, and chlorine isotopes where appropriate.

Table (3-18).

Spectra of mixtures: reactant ions for which log (I_n/I_n^o) underwent a non-linear decrease with low pressures of water or carbon tetrachloride.

First component of mixture	Pressure of first component (torr)	Second Component	Ions
Anisole	4.7×10^{-3}	Water	$C_2H_3^+$, $C_3H_5^+$, $C_3H_6^+$, $C_3H_7^+$, $C_4H_7^+$, $C_4H_8^+$, $C_4H_9^+$
Acetone	3.2×10^{-3}	Water	$C_4H_8^+$, $C_4H_9^+$
Anisole	4.7×10^{-3}	Carbon tetrachloride	$C_3H_5^+$, $C_3H_6^+$, $C_3H_7^+$, $C_4H_5^+$, $C_4H_7^+$, $C_4H_8^+$, $C_4H_9^+$
4-Fluoroanisole	4.8×10^{-3}	Carbon tetrachloride	$C_2H_5^+$, $C_3H_5^+$, $C_3H_6^+$, $C_3H_7^+$, $C_4H_5^+$, $C_4H_8^+$, $C_4H_9^+$
Acetone	1.3×10^{-3}	Carbon tetrachloride	
	2.5×10^{-3}	Carbon tetrachloride	NONE
	3.8×10^{-3}	Carbon tetrachloride	
	5.1×10^{-3}	Carbon tetrachloride	

The spectra of the mixture of anisole with carbon tetrachloride contained two groups of peaks which were not present in the spectra of either pure anisole or pure carbon tetrachloride. One group consisted of ions with m/z = 225, 227,229, and 231. The heights of the peaks relative to one another suggested that the corresponding ions contained three chlorine atoms. These ions were accordingly identified as adducts of anisole with CCl_3^+ ions. The other group of peaks consisted of ions with m/z = 189,191, and 193. The heights of the peaks relative to one another similarly suggested that the corresponding ions contained two chlorine atoms. The ions were identified as the products obtained when a molecule of hydrogen chloride is eliminated from the anisole-CCl_4 adduct. If the CCl_3^+ ion added to the ortho-position of anisole, then the elimination reaction may proceed with ring-closure:

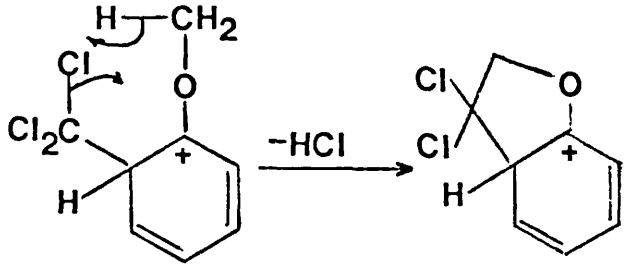

(3.5-1)

Reaction (3.5-1) is analogous to the reaction proposed by Field[55] for the elimination of acetic acid from the adduct formed from benzyl acetate and the $C_4H_9^+$ ion. Peaks corresponding to the adduct formed from 4-fluoroanisole and the CCl_3^+ ion, and to the product obtained by elimination of HCl from this species, were found in the spectrum of mixture of 4-fluoroanisole with carbon tetrachloride.

Spectra of the mixture of acetone with carbon tetrachloride also contained ions which were not present in the spectrum of either pure acetone or pure carbon tetrachloride (vide supra). These ions had m/z = 175 and m/z = 157. They were identified as $(CH_3.CO.CH_3)_3H^+$ and $(CH_3.CO.CH_3)_2C_3H_5^+$, and were presumably formed by the reactions:

$$(CH_3.CO.CH_3)_2H^+ + CH_3.CO.CH_3 \longrightarrow (CH_3.CO.CH_3)_3H^+ \qquad (3.5\text{-}2)$$

$$(CH_3.CO.CH_3)C_3H_5^+ + CH_3.CO.CH_3 \longrightarrow (CH_3.CO.CH_3)_2C_3H_5^+ \qquad (3.5\text{-}3)$$

Unlike the observations with the anisoles, no peaks corresponding to an adduct between acetone and the CCl_3^+ ions were found in the spectra.

Changes of the relative abundances of ions produced from acetone when ethyl methyl ketone was added were difficult to evaluate since the $(CH_3.CO.CH_3)H^+$ ion reacts with ethyl methyl ketone:

$$(CH_3.CO.CH_3)H^+ + CH_3.CH_2.CO.CH_3 \longrightarrow (CH_3.CO.CH_3)(CH_3.CH_2.CO.CH_3)H^+ \qquad (3.5\text{-}4)$$

It was possible, however, using the following method, to evaluate changes of the relative abundances of the isobutane reactant ions which were effected by a mixture of the two ketones, but not by either acetone or ethyl methyl ketone separately. Firstly, from an experiment in which the only sample was ethyl methyl ketone, the variation of, for example, log (I_{57}/I_{57}^o)* with sample pressure was obtained (see section 3.3.A.). Secondly, from the experiment in which the pressure of acetone (3.16×10^{-3} torr) was held constant while the pressure of ethyl

* I_{57} is the relative abundance of $C_4H_9^+$ in the absence of sample.

methyl ketone was varied, the variation of log $(I'_{57}/\sum I)$ with pressure of ethyl methyl ketone was obtained. ~~This~~ These data ~~was~~ were normalized with respect to the relative abundance of $C_4H_9^+$ (I'^{o}_{57}) when acetone was present at the above pressure, but in the absence of ethyl methyl ketone. Values of the function L_{57}, where

$$L_{57} = \log (I'_{57}/I'^{o}_{57}) - \log (I_{57}/I^{o}_{57}) \qquad (3.5\text{-}5)$$

were used to ascertain the change of the relative abundance of $C_4H_9^+$ ion effected by the mixed sample over ~~the~~ and above the changes brought about by the two ketones separately. The method is not restricted to the $C_4H_9^+$ reactant ion. Values of L_n, where n is the mass-to-charge ratio of the ion, were obtained for all the isobutane reactant ions.

Examples of the variation of L_n with pressure of ethyl methyl ketone are given in graph (3-15). For pressures of ethyl methyl ketone in the range 0 - ca. 1.6×10^{-3} torr, and for various values of n, the function L_n decreased linearly with increasing pressure, but above 1.6×10^{-3} torr L_n usually approached a limiting value. The behaviour of the $C_4H_5^+$ ion was exceptional: L_{53} decreased linearly over the entire pressure range.

Finally, as was mentioned above, with some of the mixtures there was a comparatively large, non-linear decrease of log (I_n/I^{o}_n) when low pressures of either water or carbon tetrachloride were present (see graphs (3-13) and (3-14)). In the case of the anisole/CCl_4 mixture an experiment was carried out in which the pressure of carbon tetrachloride was varied

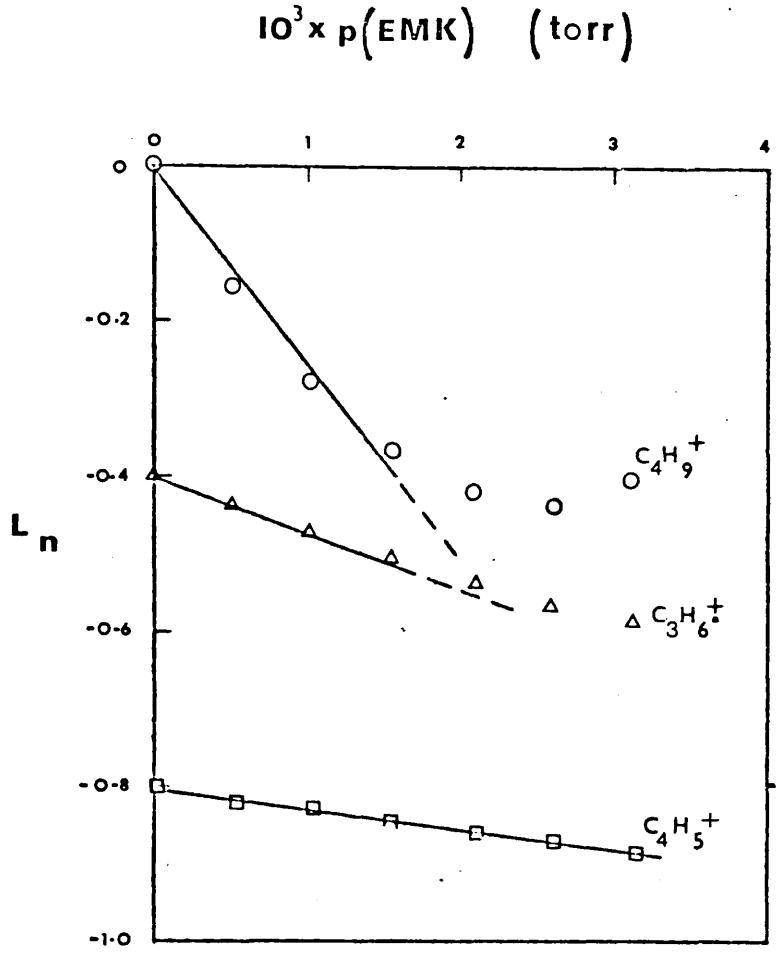

GRAPH (3-15). Acetone/ethyl methyl ketone mixture; variation of L_n (n=42, 53, 57) with pressure of ethyl methyl ketone.

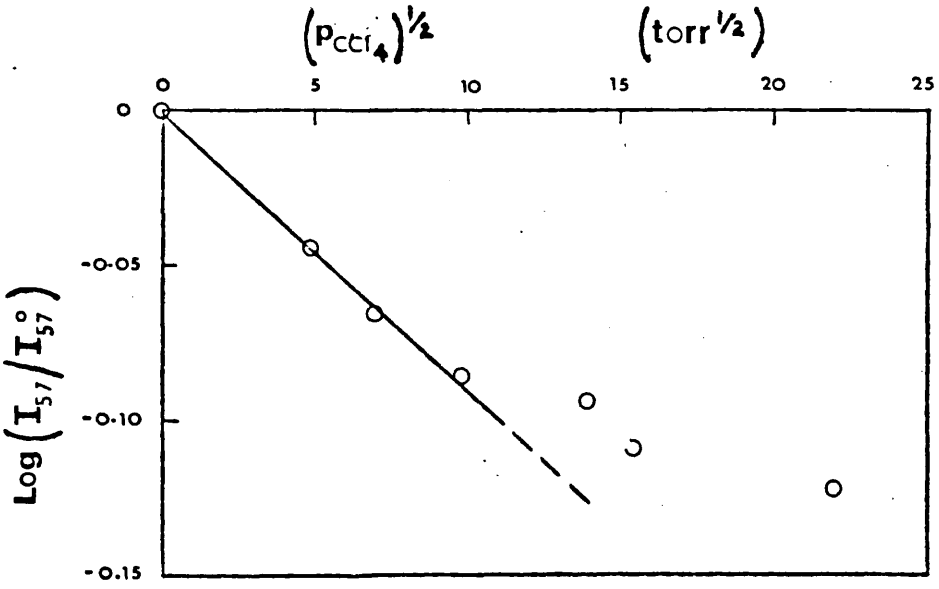

GRAPH (3-16) Anisole/CCl_4 mixture variation of $\log(I_{57}/I_{57}^\circ)$ with $(p_{CCl_4})^{1/2}$

between 0.0 and 4.8×10^{-4} torr (see section 2.6). This was done in an attempt to obtain more information on the initial (non-linear) decrease of log (I_n/I_n^o). Graph (3-16) shows the variation of log (I_{57}/I_{57}^o) with the square root of pressure of carbon tetrachloride. It is apparent from the graph that log (I_{57}/I_{57}^o) varied linearly with this function of pressure up to a pressure of ca.1×10^{-4} torr. Similar behaviour was observed with the $C_3H_7^+$ and $C_4H_8^{+\cdot}$ ions, but scatter of the data precluded any definite conclusions being drawn from the plots for the other ions.

The significance of all the above results will be discussed in section 4.2.C.

CHAPTER 4

DISCUSSION

4.1 A novel method of estimation of ion-source pressures of the reagent gases methane and isobutane.

It was shown in section 3.4 that in the spectrum of acetone obtained using isobutane as reagent gas the relative abundances of ions produced from the acetone are affected by the isobutane pressure. It will become apparent from the discussion given in section 4.2 that it is likely that the relative abundances of ions produced from any compound will be affected by the isobutane pressure to a greater or lesser extent. Comparison of isobutane chemical-ionization mass spectra is therefore only meaningful if the isobutane pressure is known, and it is unfortunate that most commercial chemical-ionization mass spectrometers are not fitted with gauges that measure the pressure of the reagent gas in the ion-source. Simple, routine methods of estimation of reagent-gas pressure, that do not require a pressure gauge to be fitted to the ion-source, will therefore be of general use. One such method, which is based upon a knowledge of the rate constants of the reactions of the primary ions with reagent gas, is now described with reference to the two most commonly used reagent gases, methane and isobutane.

A. Methane.

The rate constant for reaction (2.4-1)

$$CH_4^{+\bullet} + CH_4 \longrightarrow CH_5^+ + CH_3^\bullet \qquad (2.4\text{-}1)$$

has been found to be $k = 11.6 \times 10^{-10}$ cm^3 molecule^{-1} sec^{-1} (see section 3.1). A knowledge of this rate constant gives access to a very simple method of estimating the pressure of methane in the ion-source of a mass spectrometer, provided the residence time, τ, of the $CH_4^{+\bullet}$ ion can be estimated, and provided the assumptions made in the derivation of equation (3.1-3) are valid.

Equation (3.1-3) may be written in the form

$$p_{CH_4} = (1/kN\tau)\log((I_{16}+I_{17})/I_{16}) \qquad (4.1\text{-}1)$$

where p_{CH_4} is measured in torr. From this equation it is apparent that, if τ can be estimated, it is necessary only to obtain values of I_{16} and I_{17} in order to determine the pressure of methane in the ion-source.

It has been demonstrated that, provided a repeller-field strength greater than 10 V cm^{-1} is employed, equation (3.1-4) may be used for the estimation of τ. In this equation, in which τ is related to the mass-to-charge ratio of the ion, the electric field strength (E), and the mean distance (d) travelled by the ion, the latter is taken as half the distance between the repeller plate and the ion-exit slit.

In view of the anomalous results obtained in the study of the kinetics of reaction (2.4-1) when the electron energy was 50 eV (see section 3.1), it is recommended that a suitably large value of electron energy ($\sim$500 eV) be established during all pressure determinations. In contrast, it is important that the number

density of electrons in the ion-source be kept small as it seems that electron-capture processes perturb the observed relative abundances. Hence it is recommended that the emission current should be maintained at the lowest possible value during the estimation of methane pressures. Adherence to the above conditions makes the estimation of methane pressures a very simple procedure: the peak heights, I_{16} and I_{17}, corresponding to the ions $CH_4^{+\cdot}$ and CH_5^+ are measured from the methane spectrum and substituted in equation (4.1-1) together with the appropriate values of k and τ.

B. Isobutane.

The rate constants of the reactions of the primary ions from isobutane with isobutane were given in table (3-2) (section 3.2). These rate constants may be used in a manner similar to that described for methane to give an estimation of the pressure of isobutane in the ion-source of a mass spectrometer.

Equation (3.2-5) can be written in the form

$$p^2 = (1/k_n\beta_n N)\left[\log(I_n^{\circ}/\sum I^{\circ}) - \log(I_n/\sum I)\right] \qquad (4.1\text{-}2)$$

where p is the isobutane pressure in torr, and β_n may be calculated from equation (3.1-8). Values of the intercepts at zero pressure, $\log (I_n^{\circ}/\sum I^{\circ})$, were obtained from the kinetic plots given in graph (3-4) (section 3.2), and are listed in table (3-2). It is apparent from equation (4.1-2) that the isobutane pressure can be determined fairly simply by evaluating $I_n/\sum I$ (for a given ion) from the isobutane spectrum,

and substituting the value into the equation together with the values of the appropriate rate constant and intercept at zero pressure. Furthermore the pressure estimated using a given ion can be checked by comparing the estimate with that determined by reference to a different ion.

Now, having obtained a value of the rate constant for the reaction of $C_3H_7^+$ with isobutane, the experimental values of log $(I_{43}/\sum I)$, can be substituted in equation (4.1-2) to give estimates of $I_{43}^{\circ}/\sum I^{\circ}$ appropriate to each isobutane pressure employed in the experiment. If these estimates be divided by values of the function $(I_{43}+I_{57})/\sum I$, also evaluated at the appropriate isobutane pressure, then the figures obtained represent the extent to which the $C_4H_9^+$ ion is formed from the $C_3H_7^+$ ion. These results are given in table (4-1) and show that, on average, 80% of the relative abundance of $C_4H_9^+$ is formed from the $C_3H_7^+$ ion. Hence the initial abundance of $C_3H_7^+$ ion is given approximately by

$$I_{43}^{\circ}/\sum I^{\circ} = 0.80(I_{43}+I_{57})/\sum I \qquad (4.1\text{-}3)$$

Equation (3.2-4) may now be written in the form

$$\log (0.8) + \log((I_{43}+I_{57})/I_{43}) = k_{43}\beta_{43}Np^2 \qquad (4.1\text{-}4)$$

which shows that there should be a linear correlation of log $((I_{43}+I_{57})/I_{43})$ with the square of the isobutane pressure. The appropriate plot is given in graph (4-1) from which it is apparent that equation (4.1-4) is obeyed. The value of k_{43} obtained by this method was $(6.42 \pm 0.13) \times 10^{-11}$ cm^3 molecule^{-1} sec^{-1}, in excellent agreement with the value obtained in

Table (4-1)

Fraction of abundance of the $C_4H_9^+$ ion formed from the $C_3H_7^+$ ion.

Isobutane pressure (torr)	$\frac{I_{43}\sum I}{(I_{43}+I_{57})\sum I^{o}}$	
0.044	0.76	
0.060	0.77	
0.072	0.83	
0.085	0.85	
0.090	0.82	
0.103	0.86	
0.107	0.86	
0.117	0.86	
0.137	0.80	
0.154	0.67	
0.177	0.68	
0.206	0.55	
0.232	0.80	
0.234	0.82	
0.252	1.07	Mean value = 0.80± 0.11

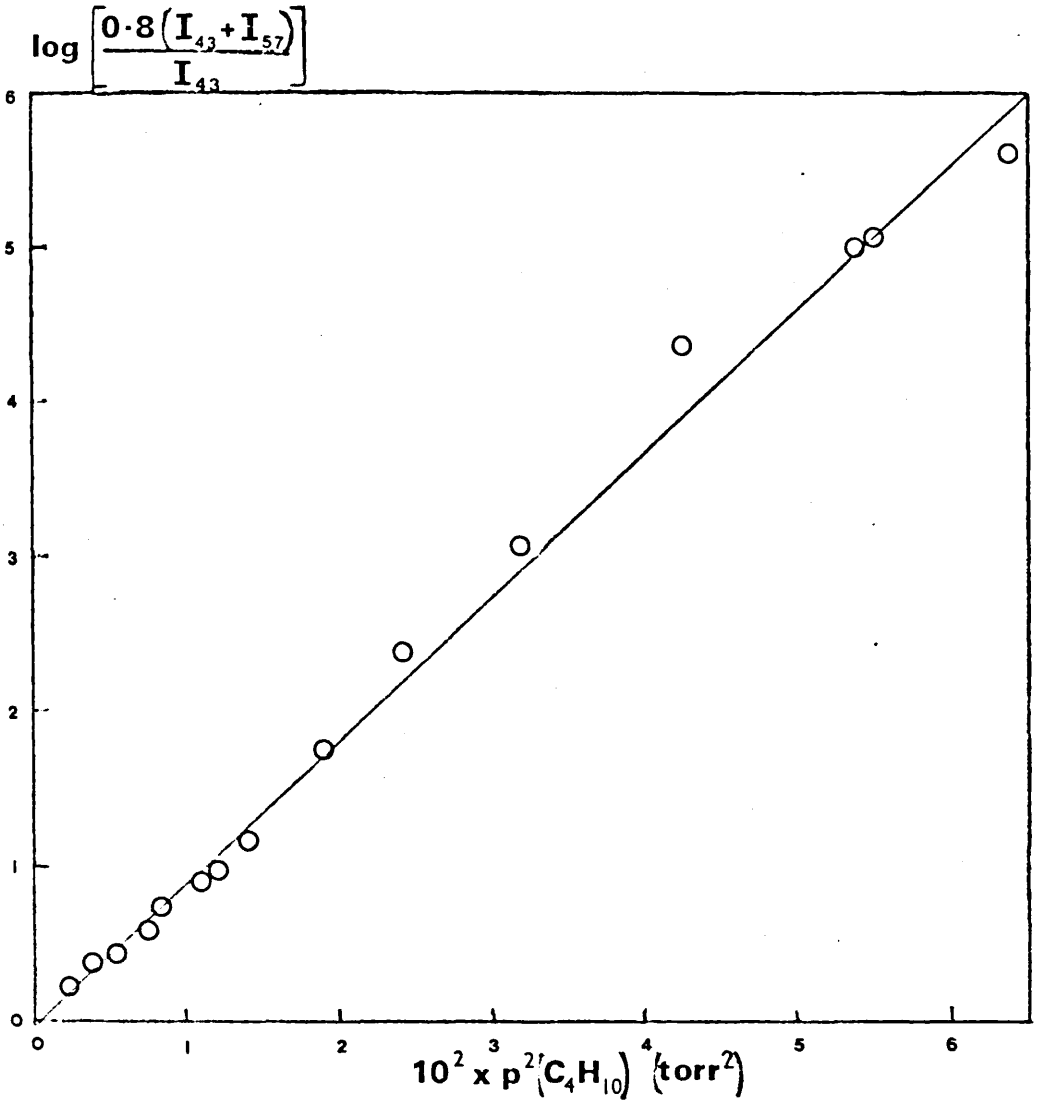

GRAPH (4-1). Kinetic plot for the reaction of $C_3H_7^+$ with isobutane.

section 3.2 (see table 3-2)).

Estimation of the ion-source pressure of isobutane is thus straightforward since it is necessary to measure only two peak heights (I_{43} and I_{57}) in the isobutane spectrum and substitute these measured values in equation (4.1-4) together with the values of k_{43} and β_{43}.

In summary, the methods of estimation of either methane or isobutane pressures in the ion-source discussed above are simple, rapid, and can be performed without modification of the mass spectrometer. It is therefore to be hoped that these methods will prove to be of value to those analysts regularly engaged in chemical-ionization mass spectrometry.

4.2 Mechanisms of the ion-molecule reactions which give rise to chemical-ionization mass spectra when isobutane is the reagent gas.

In the experiments described in section 3.3 it was found that the relative abundances of the isobutane reactant ions decreased as the sample pressure was increased. The function $\log (I_n/I_n^{\circ})$ (where I_n is the relative abundance of the reactant ions, RH^+, having m/z = n, and I_n° is the relative abundance of this ion in the absence of sample) was found to decrease in one of two ways: either linearly with sample pressure, as, for example, in the case of $C_4H_5^+$ when acetonitrile is the sample, or in the curved form exemplified by the case of $C_4H_9^+$ again with acetonitrile as the sample (see graph 3-6)). If the reactant ion, RH^+, generated from isobutane undergoes a simple bimolecular reaction with a sample

$$RH^+ + M \xrightarrow{k_o} \text{products} \qquad (4.2\text{-}1)$$

then it would be expected that $\log (I_n/I_n^{\circ})$ would decrease linearly as the sample pressure increased, as can be seen from the following kinetic analysis. The rate equation for reaction (4.2-1) is

$$-\frac{d[RH^+]}{dt} = k_o[M][RH^+]$$

Hence

$$\log ([RH^+]/[RH^+]_o) = k_o[M]\tau$$

where $[RH^+]_o$ is the initial concentration of the RH^+ ion, and τ is the residence time of this ion. If the heights (I_n) of the

peaks in the recorded spectra accurately reflect the abundances of ions having m/z = n, then

$$\log (I_n/I_n^{\circ}) = -k_o[M]\tau \qquad (4.2\text{-}2)$$

By using an equation analogous to equation (3.1-2), equation (4.2-2) may be written in the form

$$\log (I_n/I_n^{\circ}) = -k_o N\tau p_M \qquad (4.2\text{-}3)$$

from which it is apparent that $\log (I_n/I_n^{\circ})$, varies linearly with sample pressure, p_M, and that the slope of the line is proportional to the rate constant of reaction (4.2-1).

Thus it is possible that the reactions for which $\log (I_n/I_n^{\circ})$ decreased linearly with sample pressure are simple bimolecular reactions. However, it will be shown below that an alternative mechanism is also possible for these reactions which nevertheless results in a linear variation of $\log (I_n/I_n^{\circ})$ with sample pressure.

It has been assumed that the decrease of the relative abundance of the reactant ion was due solely to reaction of the ion with the sample. This assumption is not valid if the sample is able to catalyse the reaction between the reactant ion and isobutane (hence decrease further the relative abundance of RH^+), or alternatively, if the reactant-ion residence time is significantly altered by the presence of sample molecules. Since the primary ions from isobutane appear to undergo simple bimolecular reactions with isobutane gas (see section 3.2), catalysis of these reactions by another compound is unlikely. Changes of the reactant-ion residence time may occur, however,

as the maximum sample pressures employed in the experiments were generally ca.0.01 torr, corresponding to 10% of the isobutane pressure*. It will be assumed that if there are changes in the residence times, these are reflected in changes in the rate constants that are within the error limits of the latter (vide infra).

It will be shown below that the mechanism of reactions for which the plots of the decrease of log (I_n/I_n°) are curved involve several elementary reactions. For example, consideration of the data for the variation of log (I_{57}/I_{57}°) with the pressure of ethyl methyl ketone (see graph 3-5) shows that this variation is approximately linear for sample pressures in the range 7.5×10^{-3} to 11.5×10^{-3} torr. This suggests that the overall kinetics of the reaction approximate to second order when the sample pressure is comparatively high. On the other hand, below ca.3×10^{-3} torr the function resembles a parabola, suggesting that a plot of log (I_{57}/I_{57}°) against the square of the sample pressure should be a straight line. Graph (4-2) shows that this behaviour is also observed. Hence the overall kinetics of the reaction approximate to third order when the sample pressure is low, and the curves shown in the graphs in section 3.3 correspond to transitions from third- to second-order kinetics of reaction. This behaviour will be rationalized

---

* In the flowing-afterglow technique (see section 1.3) the pressure of source gas is generally <0.2% of that of the buffer gas.

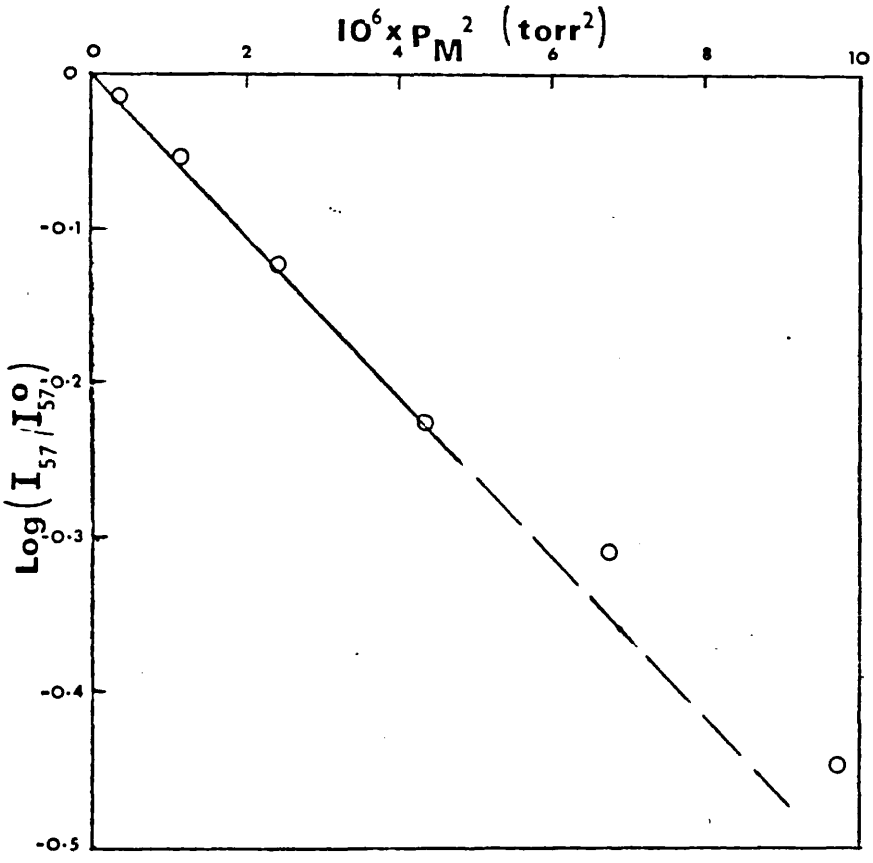

GRAPH (4-2). Plot of $\log\left(I_{57}/I_{57}^{o}\right)$ against square of the pressure of ethyl methyl ketone.

in the succeeding sections.

A. Significance of changes in the overall kinetic order of the reactions with variation of sample pressure.

The change from overall third-order to overall second-order kinetics of the reactions (vide supra) can be explained by postulating that these reactions proceed via a comparatively long-lived complex which may undergo either unimolecular decomposition to reactants, or else collision-induced decomposition to products. Since the only molecules available to take part in the collision-induced decomposition are those of isobutane and the sample, the reaction scheme may be written as

$$RH^+ + M \underset{k_{-1}}{\overset{k_1}{\rightleftharpoons}} MRH^{+*} \qquad (4.2\text{-}4)$$

$$MRH^{+*} + M \xrightarrow{k_2} \text{Products} \qquad (4.2\text{-}5)$$

$$MRH^{+*} + C_4H_{10} \xrightarrow{k_3} \text{Products} \qquad (4.2\text{-}6)$$

It is apparent from the tables given in section 3.3 that, for many compounds, the principal ionic product of reactions (4.2-5) and (4.2-6) is the MH^+ ion. For the reaction between the $C_3H_7^+$ ion and acetone, for example, (4.2-5) may be written as

$$(CH_3.CO.CH_3)C_3H_7^{+*} + CH_3.CO.CH_3 \longrightarrow (CH_3.CO.CH_3)H^+ + C_3H_6 + CH_3.CO.CH_3^* \qquad (4.2\text{-}7)$$

in which it is assumed that the collision energy is entirely removed by the third-body molecule (here acetone)†.

† This is purely for convenience in writing the equation: recent work [57] has shown that excess energy is usually removed from an ion by a stepwise process.

An alternative product of reactions (4.2-5) and(4.2-6) is an association ion. For example

$$(CH_3.CO.CH_3)C_3H_7^{+*} + CH_3.CO.CH_3 \longrightarrow (CH_3.CO.CH_3)C_3H_7^{+} + CH_3.CO.CH_3^{*} \qquad (4.2\text{-}8)$$

Other products are possible when the sample is an alcohol or an anisole. In the case of alcohols, products apparently formed by the loss of water or a hydrogen halide (see tables(3-7) and (3-8)) from the MH^+ species may, in fact, be formed in reactions (4.2-5) and (4.2-6):

$$(R_1OH)C_4H_9^{+*} + R_1OH \longrightarrow R_1^{+} + C_4H_9OH + R_1OH^{*} \qquad (4.2\text{-}9)$$

(This reaction is somewhat similar to the reaction proposed by Field [56] for the production of the benzyl ion in the chemical-ionization mass spectrum of benzyl acetate). Finally, the formation of $M^{+\cdot}$ ions from, for example, the anisoles, may also occur via reactions (4.2-4) to (4.2-6). For example

$$C_6H_5.O.CH_3 + C_4H_9^{+} \longrightarrow (C_6H_5.O.CH_3)C_4H_9^{+*} \qquad (4.2\text{-}10)$$

$$(C_6H_5.O.CH_3)C_4H_9^{+*} + C_6H_5.O.CH_3 \longrightarrow C_6H_5.O.CH_3^{+\cdot} + C_4H_9^{\bullet} + C_6H_5.O.CH_3 \qquad (4.2\text{-}11)$$

together with a similar reaction in which isobutane acts as the third-body. However, $M^{+\cdot}$ may also be produced by a reaction that does not involve the formation of a collision complex. Indeed it is possible that $M^{+\cdot}$ is formed by both routes. This added complication is discussed further in section 4.3.A, but here it will be assumed that $M^{+\cdot}$ is formed only via the collision complex.

From equations (4.2-4) to (4.2-6) it can be seen that

$$\frac{d[MRH^{+*}]}{dt} = k_1[M][RH^+] - (k_{-1} + k_2[M] + k_3[C_4H_{10}])[MRH^{+*}]$$

so that application of the Bodenstein steady-state hypothesis to the collision complex gives

$$[MRH^{+*}] = \frac{k_1[M][RH^+]}{k_{-1} + k_2[M] + k_3[C_4H_{10}]}$$

now since the rate of reaction of RH^+ is given by

$$\frac{-d[RH^+]}{dt} = k_1[M][RH^+] - k_{-1}[MRH^{+*}]$$

it follows that

$$\frac{-d[RH^+]}{dt} = k_1[M][RH^+]\left(\frac{k_2[M] + k_3[C_4H_{10}]}{k_{-1} + k_2[M] + k_3[C_4H_{10}]}\right)$$

Integration of this equation then gives

$$-\log\left(\frac{[RH^+]}{[RH^+]_o}\right) = k_1[M]\tau\left(\frac{k_2[M] + k_3[C_4H_{10}]}{k_{-1} + k_2[M] + k_3[C_4H_{10}]}\right) \qquad (4.2\text{-}12)$$

in which τ is the ion residence time, and $[RH^+]_o$ is the concentration of RH^+ in the absence of sample. Provided the heights (I_n) of peaks in the spectra accurately reflect the relative abundance of reactant ions with m/z = n, then equation (4.2-12) may be written

$$-\log\left(\frac{I_n}{I_n^o}\right) = k_1[M]\tau\left(\frac{k_2[M] + k_3[C_4H_{10}]}{k_{-1} + k_2[M] + k_3[C_4H_{10}]}\right) \qquad (4.2\text{-}13)$$

It will be shown in section 4.2.B that $k_2[M] >> k_3[C_4H_{10}]$ when acetone is the sample.

If this condition is valid for any sample, then

$$- \log \left(\frac{I_n}{I_n^{\,o}}\right) = \frac{k_1 k_2 [M]^2 \tau}{k_{-1} + k_2 [M]} \qquad (4.2\text{-}14)$$

By using an equation analogous to (3.1-2) equation (4.2-14) may be written in the form

$$- \log \left(\frac{I_n}{I_n^{\,o}}\right) = \frac{k_1 k_2 N^2 \tau p_M^2}{k_{-1} + k_2 N p_M} \qquad (4.2\text{-}15)$$

where p_M is the sample pressure. The observed behaviour of the function $\log (I_n/I_n^{\,o})$ can now be rationalized. According to equation (4.2-15) $\log (I_n/I_n^{\,o})$ varies linearly with p_M^2 when the sample pressure is low, whereas for high sample pressures the function varies linearly with p_M.

Rearrangement of equation (4.2-15) gives

$$- \log \left(\frac{I_n}{I_n^{\,o}}\right) = \frac{(k_1 k_2 / k_{-1}) N^2 \tau p^2_M}{1 + (k_2/k_{-1}) N p_M} \qquad (4.2\text{-}16)$$

in which the rate constant for the formation of the collision complex, k_1, and the ratio of rate constants k_2/k_{-1} can be seen to be accessible from the coefficients of p_M^2 and p_M. These coefficients were determined by fitting a curve of the appropriate functional form to the experimental data for each compound. Details of the computational method for the curve fitting are given in appendix II. The graphs in section 3.3 show the data obtained for the reactions of various compounds with various ions, together with their fitted curves. It is apparent from these graphs that, in general, curves of the functional form of equation (4.2-16) give excellent fits to the data. This success

substantiates the mechanism set out in reactions (4.2-4) to (4.2-6).

From equation (4.2-16) it can be seen that if $(k_2/k_{-1})Np_M >> 1$ then log (I_n/I_n°) will vary linearly with sample pressure. This condition is valid either for high sample pressures (vide supra), or for low sample pressures provided $k_2 >> k_{-1}$, but in both these cases equation (4.2-16) becomes indistinguishable from equation (4.2-3). Thus in the instances for which it was observed that log (I_n/I_n°) varied linearly with sample pressure, it was not possible, from this evidence alone, to deduce whether the reaction proceeds via a complex or not.

Values of the rate constants, k_1, for the formation of the collision complex between the compounds discussed in section 3.3 and the isobutane reactant ions, as deduced from the curve-fitting procedure outlined above, are listed in tables (4-2) to (4-5). Also included there are the rate constants obtained from simple plots in which log (I_n/I_n°)varied linearly with sample pressure, although the rate constants may correspond to reactions other than the formation of a collision complex*. Values of the ratio k_2/k_{-1} are given in table (4-6) and (4-7). All these rate constants are discussed in section 4.2.D and 4.2.E.

The mechanism proposed in equations (4.2-4) to (4.2-6) suggest that the free-energy changes that occur during the reactions take a form similar to that shown in figure (4-1)

---

* The values of these rate constants are underlined in the tables.

Table (4-2)

Rate constants for the formation of collision complexes between the C_4 reactant ions and various ketones, nitriles, and anisoles.

Compound	Temp. (°C)	Isobutane pressure (torr)	k_1 (10^{10}x cm^3 molecule^{-1} sec^{-1})†			
			$C_4H_9^+$	$C_4H_8^+$	$C_4H_7^+$	$C_4H_5^+$
Acetone	176	0.108	23.08 ± 0.82	20.0 ± 1.1	11.47 ± 0.59	2.84 ± 0.16
Ethyl methyl ketone	175	0.109	21.02 ± 0.22	24.08 ± 0.24	9.80 ± 0.17	2.83 ± 0.17
Acetonitrile	174	0.100	4.81 ± 0.05	5.09 ± 0.06	7.94 ± 0.13	2.54 ± 0.15
Propionitrile	174	0.100	12.01 ± 0.25	M	S	S
Butyronitrile	174	0.104	14.90 ± 0.24	18.53 ± 0.38	18.24 ± 0.35	3.03 ± 0.22
2-Chloropropionitrile	174	0.103	6.11 ± 0.24	4.36 ± 0.19	1.10 ± 0.18	1.55 ± 0.19
2-Bromopropionitrile	174	0.105	7.67 ± 0.49	0.67 ± 0.07	0.54 ± 0.11	0.61 ± 0.18
Anisole	175	0.240	2.47 ± 0.09			
3-Fluoroanisole	175	0.230	1.04 ± 0.04			
4-Fluoroanisole	175	0.240	0.99 ± 0.03			
3-Methylanisole	175	0.236	4.94 ± 0.22			
4-Methylanisole	175	0.240	8.24 ± 0.32			

S: Computation was not carried out as experimental data was badly scattered.
M: Reactant ion was obscured by the MH^+ ion.
† Underlined values were obtained from plots in which log (I_n/I_n^o) varied linearly with sample pressure over the entire range (see text).

Table (4-3)

Rate constants for the formation of collision complexes between the C_3 and C_2 reactant ions and various ketones and nitriles.

Compound	Temp. (°C)	Isobutane Pressure (torr)	$k_1(10^{10}$x cm^3 molecule^{-1} sec^{-1}) †					
			$C_3H_7^+$	$C_3H_6^+$	$C_3H_5^+$	$C_3H_3^+$	$C_3H_5^+$	$C_2H_3^+$
Acetone	176	0.108	9.75±0.48	12.41±0.45	12.34±0.40	0.43±0.05	23.99±0.97	12.08±0.39
Ethyl methyl ketone	175	0.109	15.91±0.20	14.51±0.34	13.09±0.21	0.50±0.07	7.00±0.87	9.81±0.44
Acetonitrile	174	0.100	11.35±0.25	M	6.83±0.24	0.74±0.15	5.22±0.16	7.07±0.29
Propionitrile	174	0.100	22.85±0.19	9.49±0.20	18.16±0.22	0.71±0.10	S	S
Butyronitrile	174	0.104	21.89±0.23	15.91±0.32	24.60±0.38	0*	6.31±0.62	S
2-Chloropropio-nitrile	174	0.103	S	11.60±0.55	12.09±0.82	0.08±0.05	3.98±0.28	6.26±0.71
2-Bromopropio-nitrile	174	0.105	7.45±0.69	1.33±0.31	2.06 0.17	0*	1.99±0.22	1.64±0.23

S: Computation was not carried out as data was badly scattered.
M: Reactant ion was obscured by the MH^+ ion.

* The experimental method did not permit the determination of rate constants lower than ca.10^{-12} cm^3 molecule^{-1} sec^{-1}.

† Underlined values were obtained from plots in which log (I_n/I_n^o) varied linearly with sample pressure over the entire range (see text).

Table (4-4).

Rate constants for the formation of collision complexes between the C_4 reactant ions and various alcohols.

Compound	Temp. (°C)	Isobutane pressure (torr)	k_1 (10^{10} x cm^3 molecule^{-1} sec^{-1}) †			
			$C_4H_9^+$	$C_4H_8^+$	$C_4H_7^+$	$C_4H_5^+$
Methanol	167	0.110	1.54 ± 0.05	2.51 ± 0.13	0.64 ± 0.06	0.69 ± 0.08
1-Propanol	167	0.110	4.49 ± 0.21	11.84 ± 0.37	3.54 ± 0.25	2.35 ± 0.11
2-Propanol	166	0.111	9.27 ± 0.43	9.97 ± 0.33	3.59 ± 0.19	2.35 ± 0.10
1-Pentanol	174	0.099	10.29 ± 0.36	11.08 ± 0.79	0*	2.21 ± 0.11
2-Pentanol	174	0.110	11.53 ± 0.21	14.28 ± 0.33	2.59 ± 0.16	2.55 ± 0.18
3-Pentanol	174	0.099	26.11 ± 0.88	30.91 ± 0.92	12.15 ± 0.48	3.40 ± 0.25
1-Hexanol	174	0.100	7.13 ± 0.31	7.74 ± 0.70	0*	1.36 ± 0.21
2-Hexanol	174	0.097	6.89 ± 0.45	12.92 ± 0.45	4.32 ± 0.24	2.14 ± 0.36
3-Hexanol	174	0.098	16.04 ± 0.27	15.91 ± 0.39	0.32 ± 0.33	2.68 ± 0.38
2-Fluoroethanol	175	0.114	2.15 ± 0.08	5.38 ± 0.18	2.03 ± 0.11	0.87 ± 0.15
2-Chloroethanol	175	0.115	1.00 ± 0.26	1.41 ± 0.06	1.03 ± 0.08	0.57 ± 0.17
2-Bromoethanol	175	0.115	0.79 ± 0.03	0.78 ± 0.07	0.58 ± 0.12	0.33 ± 0.15
2-Iodoethanol	175	0.117	0.60 ± 0.04	0.48 ± 0.04	0.22 ± 0.10	0.03 ± 0.15
2,2,2-Trifluoroethanol	166	0.109	0*	0.05 ± 0.05	0.75 ± 0.19	0.35 ± 0.15

* The experimental method did not permit the determination of rate constants lower than approximately 10^{-12} cm^3 molecule^{-1} sec^{-1}.

† Underlined values were obtained from plots in which log (I_n/I_n^o) varied linearly with sample pressure over the entire range (see text).

Table (4-5).

Rate constants for the formation of collision complexes between the C_3 and C_2 reactant ions and various alcohols.

Compound	Temp. (°C)	Isobutane pressure (torr)	$k_1(10^{10}$x cm^3 molecule^{-1} sec^{-1}) †					
			$C_3H_7^+$	$C_3H_6^+$	$C_3H_5^+$	$C_3H_3^+$	$C_2H_5^+$	$C_2H_3^+$
Methanol	167	0.110	6.60 ± 0.25	4.50 ± 0.15	3.78 ± 0.12	0.30 ± 0.25	2.39 ± 0.07	2.82 ± 0.12
1-Propanol	167	0.110	7.08 ± 0.23	11.04 ± 0.34	6.57 ± 0.17	0.29 ± 0.06	4.74 ± 0.16	3.83 ± 0.15
2-Propanol	166	0.111	6.62 ± 0.24	11.50 ± 0.16	10.20 ± 0.25	0.29 ± 0.05	4.41 ± 0.23	3.45 ± 0.15
1-Pentanol	174	0.099	18.6 ± 1.6	3.72 ± 0.34	S	0.66 ± 0.07	0*	2.37 ± 0.63
2-Pentanol	174	0.110	12.79 ± 0.29	5.75 ± 0.22	7.82 ± 0.35	0.54 ± 0.05	0.05 ± 0.19	3.32 ± 0.31
3-Pentanol	174	0.099	23.31 ± 0.73	12.84 ± 0.33	20.02 ± 0.52	0.77 ± 0.11	0*	S
1-Hexanol	174	0.100	12.8 ± 1.7	S	S	0.34 ± 0.11	2.56 ± 0.26	0.61 ± 0.53
2-Hexanol	174	0.097	24.42 ± 0.98	S	S	0.85 ± 0.12	4.74 ± 0.05	1.97 ± 0.50
3-Hexanol	174	0.098	11.35 ± 0.26	7.23 ± 0.45	7.28 ± 0.27	0.93 ± 0.15	4.42 ± 0.42	3.30 ± 0.36
2-Fluoroethanol	175	0.114	13.51 ± 0.23	3.83 ± 0.13	4.49 ± 0.11	0.45 ± 0.04	2.20 ± 0.24	2.85 ± 0.23
2-Chloroethanol	175	0.115	4.80 ± 0.21	2.50 ± 0.12	2.77 ± 0.14	0.10 ± 0.06	1.63 ± 0.25	0.87 ± 0.28
2-Bromoethanol	175	0.115	2.78 ± 0.13	1.78 ± 0.13	2.15 ± 0.18	0.03 ± 0.06	0.77 ± 0.28	0.60 ± 0.25
2-Iodoethanol	175	0.117	0.56 ± 0.85	0.16 ± 0.14	0.34 ± 0.10	0*	1.42 ± 0.27	0.43 ± 0.25
2,2,2-Trifluoroethanol	166	0.109	0.95 ± 0.06	1.88 ± 0.19	1.77 ± 0.19	0.37 ± 0.10	2.79 ± 0.24	3.31 ± 0.24

S: Computation was not carried out as data was badly scattered.

* The experimental method did not permit the determination of rate constants lower than ca.10^{-12} cm^3 molecule^{-1} sec^{-1}.

† Underlined values were obtained from plots in which log (I_n/I_n°) varied linearly with sample pressure over the entire range (see text).

Table (4-6)

Rate-constants ratios (k_2/k_{-1}) for decomposition reactions of collision complexes formed from reactant ions and various ketones, nitriles, and anisoles*.

Compound	k_2/k_{-1} (10^{10} x cm^3 $molecule^{-1}$)							
	$C_4H_9^+$	$C_4H_8^{+\cdot}$	$C_4H_7^+$	$C_3H_7^+$	$C_3H_6^{+\cdot}$	$C_3H_5^+$	$C_2H_5^+$	$C_2H_3^+$
Acetone	5.88±0.95	11.63±0.83	12.5 ±1.9	243 ± 48	10.93±0.93	7.7 ±0.49	2.28±0.67	5.16±0.42
Ethyl methyl ketone	12.8 ±1.3	10.56±0.96	16.1 ±2.0	14.6 ±1.6	10.9 ±1.9	7.8 ±1.2	24.7 ±5.1	5.5 ±1.9
Acetonitrile	9.71±0.40	9.96±0.50	2.74±0.24	24.37±0.32	MW	20.30±0.91	21.22±0.75	27.74±0.69
Propionitrile	3.44±0.23	MW	S	9.00±0.38	19.77±0.56	3.99±0.75	S	S
Butyronitrile	4.41±0.21	4.02±0.26	3.48±0.49	10.20±0.59	3.31±0.40	2.01±0.33	L	S
2-Chloropropionitrile	2.18±0.42	3.53±0.58	L	S	2.54±0.18	2.50±0.27	L	6.61±2.1
2-Bromopropionitrile	0.71±0.18	L	L	4.6±2.3	L	L	L	L
Anisole	26.3±1.4							
3-Fluoroanisole	36.3±3.8							
4-Fluoroanisole	12.8±1.3							
3-Methylanisole	9.1±1.1							
4-Methylanisole	5.57±0.96							

S: Computation was not carried out as experimental data was badly scattered.
MW: Reactant ion was obscured by a product ion (MH^+).
L: The function log (I_n/I_n^o) varied linearly with sample pressure.
* Temperatures and isobutane pressures are listed in table (4-2).

Table (4-7)

Rate-constant ratios (k_2/k_{-1}) for decomposition reactions of collision complexes formed from reactant ions and various alcohols *

Compound	k_2/k_{-1} (10^{15} x cm^3 $molecule^{-1}$					
	$C_4H_9^+$	$C_4H_8^{\cdot+}$	$C_4H_7^+$	$C_3H_7^+$	$C_3H_6^{\cdot+}$	$C_3H_5^+$
Methanol	8.44±0.21	3.90±0.78	L	3.37±0.35	3.37±0.41	4.55±0.51
1-Propanol	1.88±0.11	2.51±0.07	L	3.16±0.35	3.54±0.22	11.9 ±1.4
2-Propanol	1.84±0.05	5.67±0.57	L	6.02±0.51	1.95±0.18	3.07±0.32
1-Pentanol	2.27±0.21	4.19±0.92	L	2.9 ±1.5	L	S
2-Pentanol	6.75±0.18	8.22±0.85	L	9.55±0.61	L	28.4 ±13.1
3-Pentanol	2.36±0.24	2.93±0.70	4.1±1.5	3.87±0.14	6.36±0.27	3.51±0.58
1-Hexanol	7.92±0.99	4.11±0.82	L	2.2 ±1.1	S	S
2-Hexanol	13.35±0.83	13.0 ±1.1	L	1.65±0.42	S	S
3-Hexanol	9.95±0.78	13.53±0.97	L	17.99±0.95	L	L
2-Fluoroethanol	6.5 ±1.1	2.24±0.66	L	2.26±0.18	L	L
2-Chloroethanol	L	L	L	23.2 ±4.1	L	L

S: Computation was not carried out as experimental data was badly scattered.

L: The function log (I_n/I_n^o) varied linearly with sample pressure.

* Temperatures and isobutane pressures are listed in table (4-4).

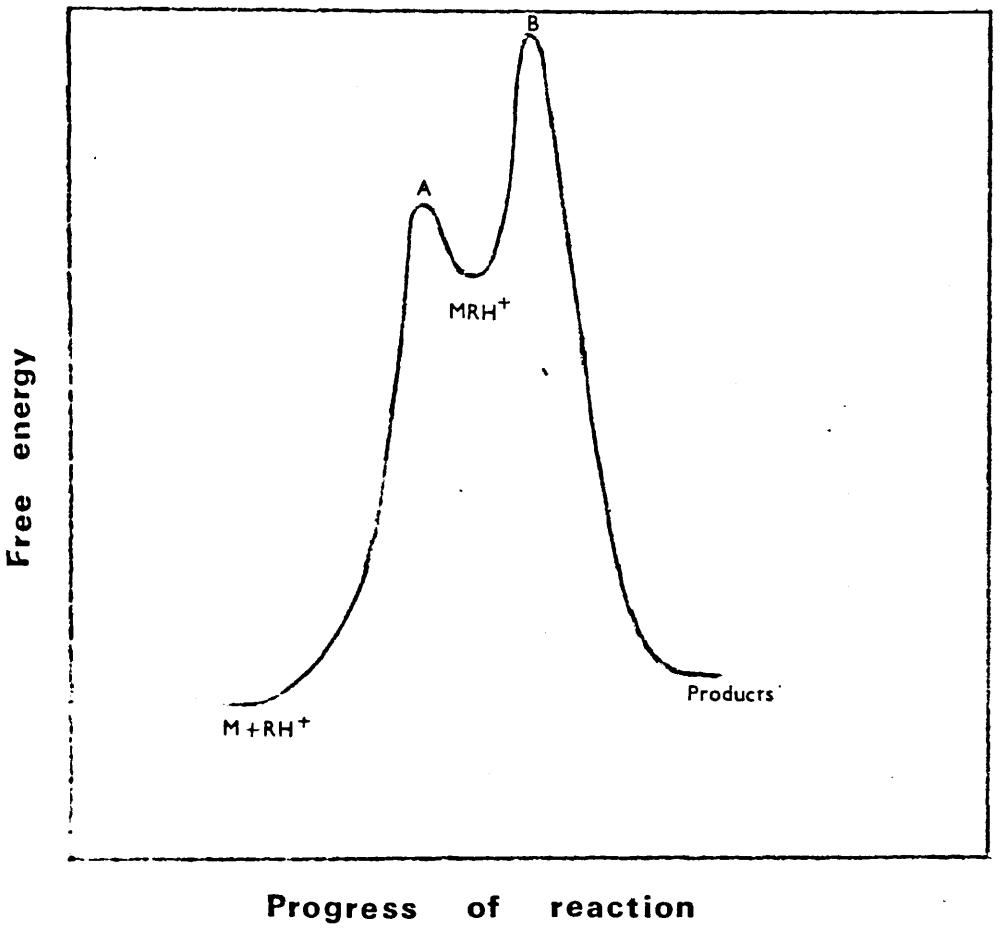

FIGURE (4-1). Energy diagram for reactions (4.2-4) to (4.2-6)

Although the collision complex is formed with excess energy, this is insufficient to cause the system to traverse the barrier B. The products are formed, then, only after the collision complex has acquired this energy from a second collision. If a second collision does not occur within a certain time (ca.1-10 μsec, see section 4.2.E) after the formation of MRH^+, then the excess energy acquired from the first collision causes the reactants to be reformed.

B. Rationalization of the effects of variation of isobutane and acetone pressures on the chemical-ionization mass spectrum of acetone.

The variation of the relative abundance of the $C_4H_9^+$ ion with variation of the pressures of isobutane and acetone (see section 3.4) may be explained by reference to equation (4.2-4) to (4.2-6). In the particular case of the reaction between the $C_4H_9^+$ ion with acetone, these equations become

$$C_4H_9^+ + CH_3.CO.CH_3 \underset{k_{-1}}{\overset{k_1}{\rightleftharpoons}} (CH_3.CO.CH_3)C_4H_9^{+*} \qquad (4.2\text{-}17)$$

$$(CH_3.CO.CH_3)C_4H_9^{+*} + CH_3.CO.CH_3 \xrightarrow{k_2} \text{Products} \qquad (4.2\text{-}18)$$

$$(CH_3.CO.CH_3)C_4H_9^{+*} + C_4H_{10} \xrightarrow{k_3} \text{Products} \qquad (4.2\text{-}19)$$

By using an equation analogous to (3.1-2), equation (4.2-13) may, after rearrangement, be written in the form

$$\log \left(\frac{I_{57}}{I_{57}^o}\right) = - k_1 N^2 \tau p_M \left(\frac{(k_2/k_{-1})p_M + (k_3/k_{-1})p}{1 + (k_2/k_{-1})Np_M + (k_3/k_{-1})Np}\right) \qquad (4.2\text{-}20)$$

where M now represents acetone, p_M is the acetone pressure, p is the isobutane pressure, and N was defined in equation (3.1-2). It was shown in section 3.2 that residence times of ions in isobutane for the conditions employed in this experiment are directly proportional to the isobutane pressure when the latter is greater than ca.0.05 torr. If it is assumed that the drift velocities of the reactant ions are not perturbed by the presence of sample molecules, then the residence times are given by

$$\tau = \beta p \qquad (4.2\text{-}21)$$

where β may be calculated from equation (3.1-8). Substitution of

equation (4.2-21) into (4.2-20) then gives

$$\log\left(\frac{I_{57}}{I_{57}^{o}}\right) = -\gamma P_M P\left(\frac{\theta p_M + \phi p}{1+\theta p_M+\phi p}\right) \qquad (4.2\text{-}22)$$

where $\gamma = k_1\beta N^2$, $\theta = k_2N/k_{-1}$, and $\phi = k_3N/K_{-1}$. The value of I_{57}^{o}, the 'initial' relative abundance of the $C_4H_9^+$ ion, changes with changes of the isobutane pressure as a result of reactions of the isobutane primary ions with isobutane. The effects of these changes may be removed from the left-hand side of equation (4.2-22) by evaluating I_{57}^{o} at each isobutane pressure employed in the experiment (see section 3.4).

The constants γ,θ, and ϕ of equation (4.2-22) were determined by fitting a three-dimensional surface of the appropriate functional form (viz., (4.2-22)) to the experimental data. Details of the computational method are given in appendix II. Graph (4-3) shows the experimental data together with cross-sections of the fitted surface taken at the isobutane pressures used in the experiment (cf.table (3-13)). It can be seen that a surface of the functional form of equation (4.2-22) gives a good fit to the experimental data, thus providing further evidence for the mechanism proposed in equations (4.2-4) to (4.2-6).

A contour map of the surface is given in graph (4-4). Each of the lines in the map represents a constant value of $\log (I_{57}/I_{57}^{o})$, the left-hand side of the equation (4.2-22). It is apparent from the map that changes in the value of $\log (I_{57}/I_{57}^{o})$, are very much greater when the acetone pressure is varied whilst the isobutane pressure is held constant, than are those when the isobutane pressure is varied whilst

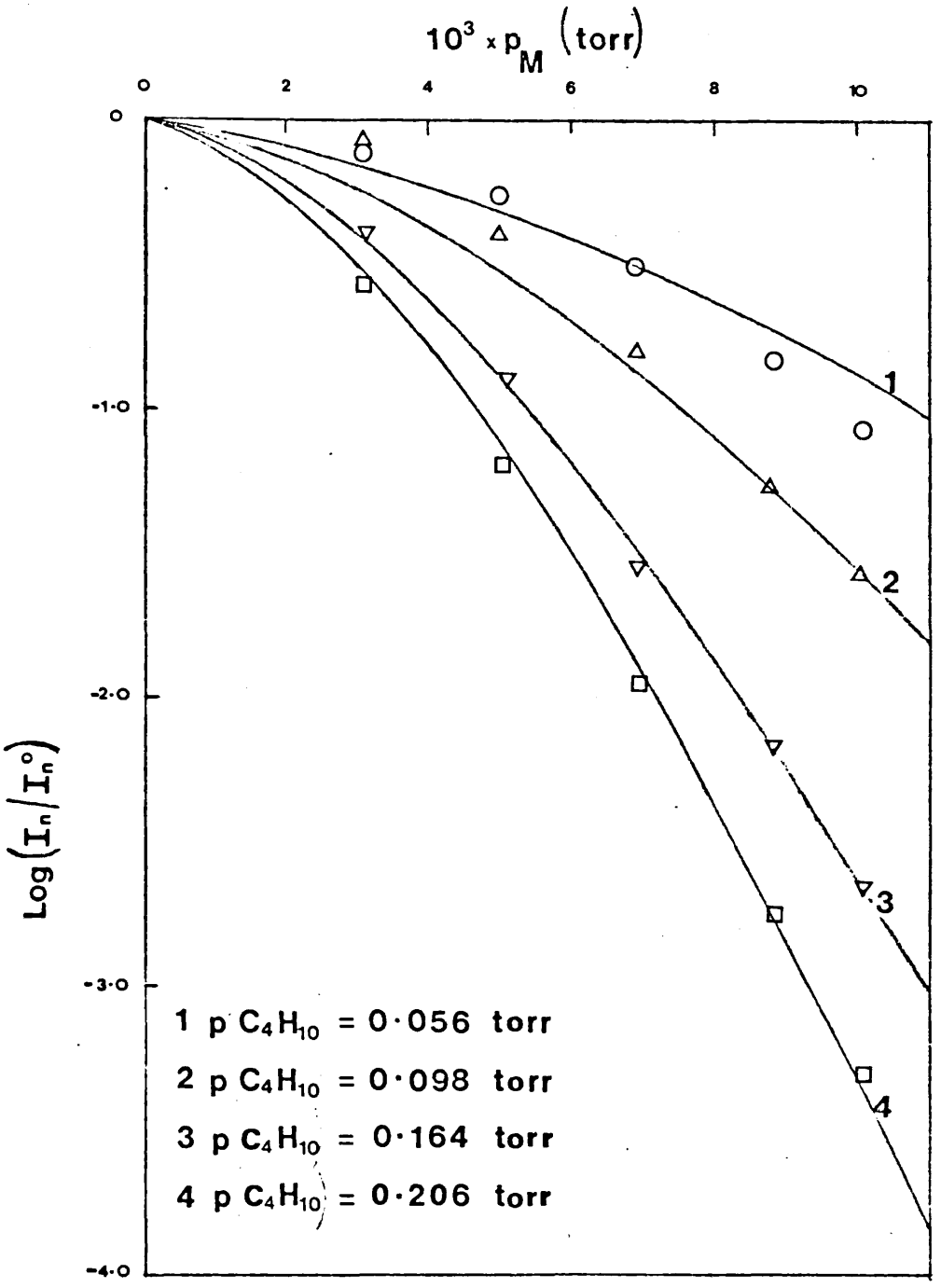

GRAPH (4-3). Kinetic plots for reaction of $C_4H_9^+$ with acetone at various isobutane pressures.

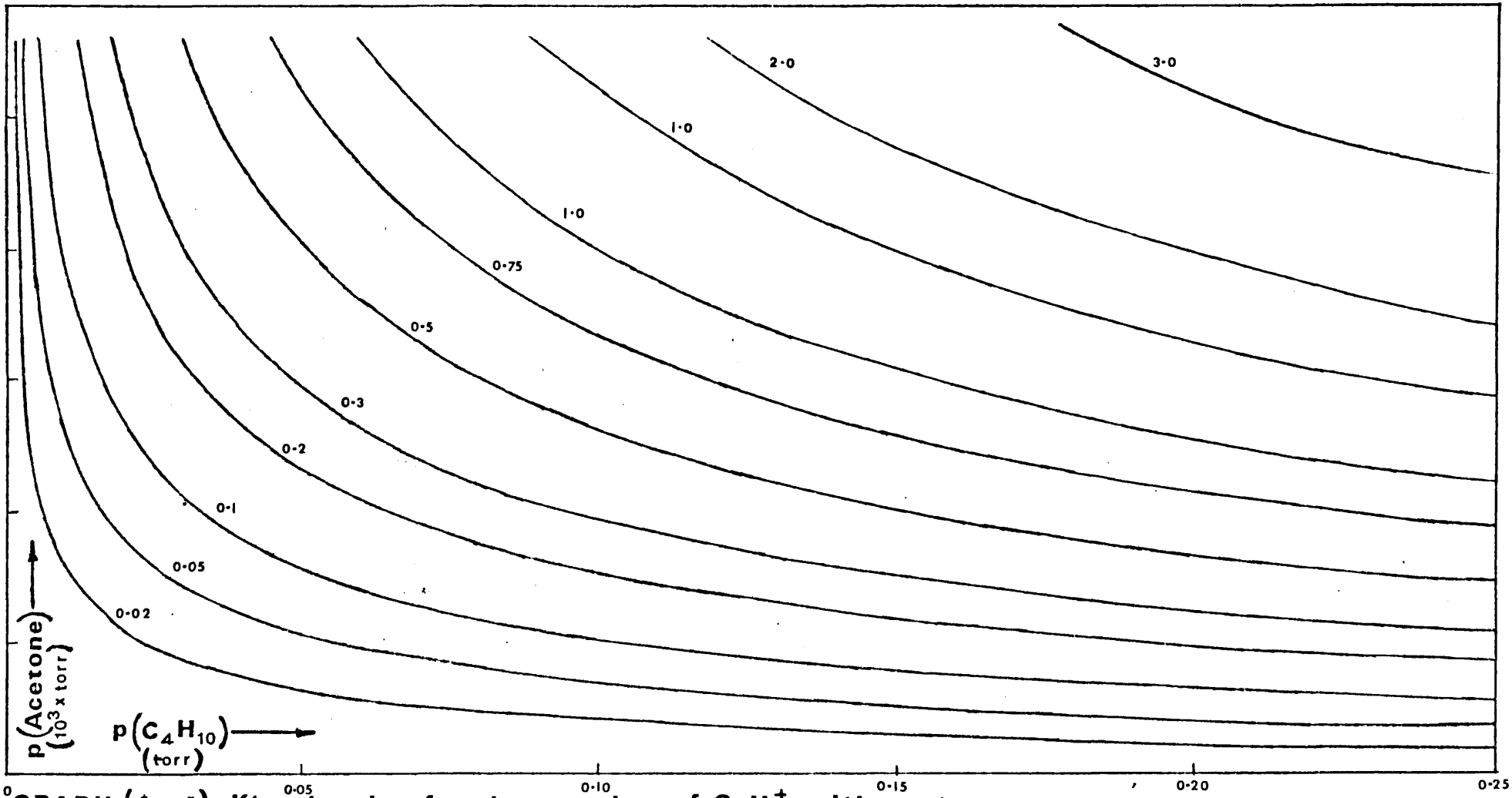

GRAPH (4 - 4). Kinetic plot for the reaction of $C_4H_9^+$ with acetone.

Lines represent constant values of $\log(I_{57}/I^{o}_{57})$

the acetone pressure is held constant. The implication of this result is that reaction (4.2-18) is very much faster than reaction (4.2-19) (see table (4-8)), i.e. that $k_2 \simeq 10^3 k_3$, and that, for the ranges of p and p_M, $k_2|CH_3.CO.CH_3| >> k_3|C_4H_{10}|$ (see equation (4.2-13)). The results of the experiment suggest, therefore, that acetone is much more efficient as a third-body than is isobutane.

The values of $k_1, k_2/k_{-1}$, and k_3/k_{-1} (see equation (4.2-22)) obtained from this experiment are given in table (4-8), which also shows that the values of k_1 and k_2/k_{-1} for the reaction between $C_4H_9^+$ and acetone obtained by the method given in section 4.2.A. Error analysis was not carried out by the computer program which computed the surface shown in graph (4-4).

Table (4-8).

Rate constants of reactions (4.2-17)-(4.2-19)

Designation	Rate Constant	Comment
k_1	21.44×10^{-10} cm^3 molecule^{-1} sec^{-1}	Equation (4.2-22)
k_1	$(23.08 \pm 0.82) \times 10^{-10}$ cm^3 molecule^{-1} sec^{-1}	Equation (4.2-16)
k_2/k_{-1}	7.03×10^{-15} cm^3 molecule^{-1}	Equation (4.2-22)
k_2/k_{-1}	$(5.88 \pm 0.95) \times 10^{-15}$ cm^3 molecule^{-1}	Equation (4.2-16)
k_3/k_{-1}	9.09×10^{-18} cm^3 molecule^{-1}	

C. Rationalization of the effects caused by varying the pressure of one component of a two-component mixture upon the chemical-ionization mass spectrum.

It was shown in section 3.5 that variation of the pressure of either water or carbon tetrachloride effected significant changes in the spectra of acetone, anisole, and 4-fluoroanisole. It was found that, in general, the relative abundances of reactant ions decreased as the pressure of water or carbon tetrachloride was increased whilst the pressure of the main component was kept constant. Furthermore, this decrease occurred such that the function $\log (I_n/I_n^{\circ})$ varied linearly with the pressure of water or carbon tetrachloride, although, in some cases, there was a comparatively large, non-linear decrease of $\log (I_n/I_n^{\circ})$ for the lowest pressures used (see section 3.5).

In section 4.2.A it was postulated that the reactions which give rise to chemical-ionization mass spectra proceed via a collision complex which may undergo either unimolecular decomposition to reactants, or collision-induced decomposition to products. Normally the only molecules available to take part in the collision-induced decomposition are those of isobutane and the sample (see equations (4.2-4) to (4.2-6)). When a two-component mixture is present in the ion-source (in addition, of course, to the isobutane), both components may take part in the collision-induced decomposition of the complex. Thus a fourth equation (equation (4.2-23)) may be added to equations (4.2-4) to (4.2-6), to take account of the effects of, for example, water or carbon

tetrachloride, ie.,

$$MRH^{+*} + T \xrightarrow{k_4} \text{Products} \qquad (4.2\text{-}23)$$

in which T (H_2O or CCl_4) represents a third-body molecule. With this reaction incorporated into the scheme, the kinetic analysis results in the equation

$$-\log\left(\frac{I_n}{I_n^{\,o}}\right) = k_1[M]\tau\left(\frac{k_2[M]+k_3[C_4H_{10}]+k_4[T]}{k_{-1}+k_2[M]+k_3[C_4H_{10}]+k_4[T]}\right) \qquad (4.2\text{-}24)$$

where $I_n^{\,o}$ is the relative abundance of ions having m/z = n in the absence of any sample. This equation is simply a modification of (4.2-13). If the efficiency of isobutane as a third-body is very much lower than that of either M or T then the $k_3|C_4H_{10}|$ terms may be omitted from equation (4.2-24), and the resulting equation may be written in the form

$$-\log\left(\frac{I_n}{I_n^{\,o}}\right) = k_1N^2\tau p_M\left(\frac{k_2p_M+k_4p_T}{k_{-1}+k_2Np_M+k_4Np_T}\right) \qquad (4.2\text{-}25)$$

where p_T is the pressure of the 'third-body' compound. If $k_{-1} >> k_4Np_T$, and $k_2p_M >> k_4p_T$, (ie. for low pressures of the third-body compound) then equation (4.2-25) becomes

$$-\log\left(\frac{I_n}{I_n^{\,o}}\right) = k_1N^2\tau p_M\left(\frac{k_2p_M+k_2p_T}{k_{-1}+k_2Np_M}\right) \qquad (4.2\text{-}26)$$

from which it is apparent that, for low pressures of the third-body compound, $\log (I_n/I_n^{\,o})$ varies linearly with p_T[†]. It was seen in section 3.5 that this linear variation was observed with the mixtures studied. In deriving equation (4.2-26) it has been

---

[†] Note that this would still be true had the $k_3[C_4H_{10}]$ terms been left in equation (4.2-25). These terms were omitted only to obtain the required form for equation (4.2-26).

assumed that the compound represented by T in equation (4.2-23) does not undergo reaction with the RH^+ ions. It has been shown, however, that both water and carbon tetrachloride react with certain of the reactant ions. As these reactions are bimolecular, allowances can easily be made for their effects upon the relative abundances of RH^+. For a given value of n, the slope of the plot of log $(I_n/I_n^{\,o})$ against p_T obtained when the sample, M, is not present is subtracted from the slope of the similar plot obtained when M is present. The number, s, so determined is given by

$$s = \frac{k_1 k_4 N^2 \tau p_M}{k_{-1}+k_2 N p_M} \qquad (4.2\text{-}27)$$

as can be seen from equation (4.2-26). Hence

$$k_4/k_{-1} = s(1+(k_2/k_{-1})Np_M)/k_1 N^2 \tau p_M \qquad (4.2\text{-}28)$$

Values of the ratio k_4/k_{-1} obtained for the various mixtures are presented in table (4-9). These results will be discussed further in section 4.4.

The ionic products of reaction (4.2-23) are presumably the same as those produced by reactions (4.2-7) to (4.2-11). Furthermore, it is possible that the M_2H^+ species observed in the spectra are formed by similar mechanisms:

$$MH^+ + M \longrightarrow M_2H^{+*} \qquad (4.2\text{-}29)$$

$$M_2H^{+*} + M \longrightarrow M_2H^+ + M^* \qquad (4.2\text{-}30)$$

$$M_2H^{+*} + C_4H_{10} \longrightarrow M_2H^+ + C_4H_{10}{}^* \qquad (4.2\text{-}31)$$

$$M_2H^{+*} + T \longrightarrow M_2H^+ + T^* \qquad (4.2\text{-}32)$$

Table (4-9)

Rate-constant ratios (k_4/k_{-1}) for decomposition reactions of collision complexes.

Mixture (M + T)	Pressure of component M (torr x 10^3)	Temp. (^{0}C)	Isobutane pressure (torr)	k_4/k_{-1} (10^{15} x cm^3 molecule^{-1})							
				$C_4H_9^+$	$C_4H_8^{\cdot+}$	$C_4H_7^+$	$C_3H_7^+$	$C_3H_6^{\cdot+}$	$C_3H_5^+$	$C_2H_5^+$	$C_2H_3^+$
Acetone + CCl_4	1.3	163	0.102	1.47±0.28	7.41±0.38	11.89±0.70(143)		19.0±1.3	21.6 ±1.1	S	9.72±0.94
	2.5	163	0.102	3.35±0.31	7.91±0.56	12.01±0.73(135)		12.03±0.91	13.2 ±1.0	S	10.4 ±1.2
	3.8	162	0.102	3.67±0.34	7.58±0.32	10.86±0.70(157)		16.2 ±1.2	13.66±0.91	S	10.1 ±1.4
	5.1	161	0.102	3.29±0.43	7.19±0.60	10.66±0.78(178)		11.43±0.92	12.55±0.83	S	S
Acetone + H_2O	3.2	174	0.105	1.89±0.09	2.93±0.07	3.87±0.17(34)		1.69±0.13	1.28±0.11	1.62±0.20	
	7.0	174	0.105	1.88±0.31	2.70±0.24	3.73±0.23(19)		1.99±0.14	1.05±0.13	1.27±0.38	1.10±0.21
Anisole + H_2O	4.7	175	0.113	26.21±0.59							
Anisole + CCl_4	4.8	174	0.089	47.6 ±5.4							
4-Fluoro-anisole + CC14	4.7	174	0.112	28.8 ±3.3							
Acetone + CCl_4	(Mean values)			3.44±0.44†	7.53±0.58	11.4±1.0	-	13.2±2.6†	13.1±1.1†	-	10.1±1.3
Acetone + H_2O	(Mean values)			1.89±0.26	2.82±0.24	3.80±0.25	-	1.84±0.23	1.17±0.19	1.43±0.44	1.31±0.39

† Average of 3 values

The lifetime of M_2H^{+*} may, however, be sufficiently long (see sections 3.3.A and 4.2.E) that the peak ascribed to M_2H^+ could correspond to a mixture of excited (M_2H^{+*}) and stabilized (M_2H^+) ions. The results of table (3-16) show that, the increase of the relative abundance of the M_2H^+ ion when water or carbon tetrachloride is added to acetone is larger than that of any of the other product ions. Equations (4.2-29) and (4.2-32) show possible ways in which this occurs. First, the relative abundance of the MH^+ ion is increased by reaction (4.2-23), hence the relative abundance of M_2H^{+*} is increased via (4.2-29). Secondly, the third-body compound is able to stabilize some M_2H^{+*} ions (reaction (4.2-32)) which would otherwise decompose before being analysed.

An alternative to the products of reaction (4.2-30) could be M_3H^{+*}. It should be noted that the $(CH_3.CO.CH_3)_3H^+$ (or $(CH_3.CO.CH_3)_3H^{+*}$) ion was not observed in the spectrum of acetone alone, but <u>was</u> observed when carbon tetrachloride was added. Hence it is possible that the M_3H^+ ion is formed via the M_3H^{+*} ion in reactions analogous to (4.2-29)-(4.2-32). Although M_3H^{+*} may have a lifetime which is rather shorter than the ion residence time, some M_3H^+ ions could be produced via stabilization of M_3H^{+*} by carbon tetrachloride. A similar argument would, of course, apply to the $M_2C_3H_5^+$ ion observed in the spectra of this mixture.

When a mixture of ethyl methyl ketone and acetone is present in the ion-source the following reactions, in which A represents acetone and B ethyl methyl ketone, may occur:

$$A + RH^+ \underset{k_1}{\overset{k_1}{\rightleftharpoons}} ARH^{+*} \qquad (4.2\text{-}33)$$

$$B + RH^+ \underset{k_{-4}}{\overset{k_4}{\rightleftharpoons}} BRH^{+*} \qquad (4.2\text{-}34)$$

$$ARH^{+*} + A \xrightarrow{k_2} \text{Products} \qquad (4.2\text{-}35)$$

$$ARH^{+*} + B \xrightarrow{k_3} \text{Products} \qquad (4.2\text{-}36)$$

$$BRH^{+*} + A \xrightarrow{k_5} \text{Products} \qquad (4.2\text{-}37)$$

$$BRH^{+*} + B \xrightarrow{k_6} \text{Products} \qquad (4.2\text{-}38)$$

By application of Bodenstein's steady-state hypothesis to both ARH^{+*} and BRH^{+*} it can be shown that

$$[ARH^{+*}] = \frac{k_1[A][RH^+]}{k_{-1}+k_2[A]+k_3[B]} \qquad (4.2\text{-}39)$$

and

$$[BRH^{+*}] = \frac{k_4[B][RH^+]}{k_{-4}+k_5[A]+k_6[B]} \qquad (4.2\text{-}40)$$

Since the rate of disappearance of RH^+ is given by

$$-\frac{d[RH^+]}{dt} = k_1[A][RH^+]\left(\frac{k_2[A]+k_3[B]}{k_{-1}+k_2[A]+k_3[B]}\right) + k_4[B][RH^+]\left(\frac{k_5[A]+k_6[B]}{k_{-4}+k_5[A]+k_6[B]}\right) \qquad (4.2\text{-}41)$$

it can easily be shown that

$$\frac{-1}{\tau}\log\left(\frac{I_n}{I_n^0}\right) = \frac{k_1k_2[A]^2}{k_{-1}+k_2[A]+k_3[B]} + \frac{k_4k_6[B]^2}{k_{-4}+k_5[A]+k_6[B]} + \left(\frac{k_1k_3}{k_{-1}+k_2[A]+k_3[B]} + \frac{k_4k_5}{k_{-4}+k_5[A]+k_6[B]}\right)[A][B] \qquad (4.2\text{-}42)$$

from which it is apparent that, for sufficiently small concentrations of ethyl methyl ketone (B) (for which $[B]^2$ can be neglected), log (I_n/I_n°) varies linearly with the pressure of this compound, in agreement with the experimental results presented in section 3.5. Although it is not possible to obtain any rate constants from this experiment, the results do support the general reaction mechanism postulated in equations (4.2-4) to (4.2-6).

It was also shown in section 3.5 that the addition of small quantities of water or carbon tetrachloride to acetone or anisole sometimes resulted in a comparatively large, non-linear decrease of log (I_n/I_n°). The results of an experiment in which small quantities of carbon tetrachloride were added to anisole suggested that log (I_n/I_n°) initially varied linearly with the square root of the pressure of carbon tetrachloride (see graph (3-16)). This behaviour suggests that from every molecule of carbon tetrachloride introduced there are produced, on average, two species which are able to act as third-bodies. It is tentatively suggested that subsequent upon the reaction of carbon tetrachloride with thermal-energy electrons present in the ion-source*,

$$CCl_4 + e^- \longrightarrow Cl_3C^{\cdot} + Cl^- \qquad (4.2\text{-}43)$$

the trichloromethyl radical dissociates (4.2-44) giving chlorine atoms and dichlorocarbene,

$$Cl_3C^{\cdot} \longrightarrow Cl^{\cdot} + Cl_2C:$$

which act as third-bodies. The problem remains, however, as to why the pressure dependence of log (I_n/I_n°) described above is

* It is known that the attachment rate for carbon tetrachloride with thermal-energy electrons is very large [58].

not observed at higher pressures of carbon tetrachloride.

Experiments in which small quantities of water are added to a sample have not been carried out. It seems unlikely, however, that the low-pressure, non-linear decrease of log (I_n/I_n°) could be explained by reactions of water with low-energy electrons since the cross-sections for such reactions are small. Clarification of the above observations can only result from further experimentation.

There is, then, substantial evidence to suggest that the ion-molecule reactions which give rise to chemical-ionization mass spectra proceed via a collision complex that may undergo either unimolecular decomposition to reactants or collision-induced decomposition to products. Furthermore, under the conditions of the experiments reported herein, it is likely that the fastest collision-induced decomposition reaction of the complex is that in which the sample molecules act as third-bodies.

Other workers have proposed similar mechanisms for this type of reaction. Porter [59] has proposed that low-temperature clustering reactions occurring in chemical-ionization mass spectrometry proceed via a collision complex (reactions (4.2-45) to (4.2-47))†.

$$I^+ + M \rightleftharpoons IM^{+*} \qquad (4.2\text{-}45)$$

$$IM^{+*} \longrightarrow J^+ + N \qquad (4.2\text{-}46)$$

$$IM^{+*} + T \longrightarrow IM^+ + T^* \qquad (4.2\text{-}47)$$

† Tiedemann and Riveros[60] have also proposed this kind of mechanism for the reactions of ketone molecular ion-radicals with their parent ketone which were observed in an ion cyclotron resonance spectrometer.

In this mechanism the third-body enters only the stabilization reaction (reaction (4.2-47)), whereas in the mechanism proposed in reactions (4.2-4) to (4.2-6) the decomposition of the collision complex to products also involves a third-body interaction. Porter's work, however, was concerned with the chemical-ionization mass spectra of BF_3 and HBF_2 using deuterium as the reagent gas. These systems are, of course, chemically very different from those discussed in section 3.3.

The mechanism proposed by Miasek and Harrison[57] for the reactions of $C_3H_5^+$ with ethylene is rather more comparable with the mechanism proposed in the present work:

$$C_3H_5^+ + C_2H_4 \rightleftharpoons C_5H_9^{+*} \qquad (4.2\text{-}48)$$

$$C_5H_9^{+*} + T \longrightarrow C_5H_9^+ + T^* \qquad (4.2\text{-}49)$$

$$C_5H_9^{+*} + T \longrightarrow C_5H_7^+ + H_2 + T^* \qquad (4.2\text{-}50)$$

$$C_5H_9^{+*} \longrightarrow C_5H_7^+ + H_2^* \qquad (4.2\text{-}51)$$

These workers found that in this case it was necessary to incorporate a unimolecular decomposition of the collision complex in addition to the collision-induced decomposition in order to explain the observed pressure dependence of the $[C_5H_9^+]/[C_5H_7^+]$ ratio.

It is interesting to note that the scheme proposed by Franklin[61] for the reaction of CH_2F^+ with methyl fluoride is somewhat similar to that proposed in reactions (4.2-4) to (4.2-6), except that he did not include the possibility of the collision complex undergoing unimolecular decomposition to

reactants.

$$CH_2F^+ + CH_2F \longrightarrow CH_2F.CH_2F^{+*} \qquad (4.2\text{-}52)$$

$$CH_3F.CH_3F^{+*} + CH_3F \longrightarrow (CH_3)_2F^+ + CH_2F_2 \qquad (4.2\text{-}53)$$

Since Franklin's experiments involved a straightforward high-pressure mass spectrometric technique the reaction conditions are closely related to the experimental conditions of the present work. Similar mechanisms to this have also been proposed for ion-molecule reactions consequent upon the electron-impact ionization of other fluorohydrocarbons [62,63].

Field [56] has proposed four alternative mechanistic schemes for the reactions which are responsible for the production of the principal ions in the chemical-ionization mass spectrum of benzyl acetate when isobutane is the reagent gas. All the schemes assume that the reactions proceed via a collision complex. Of the schemes, he favours the following as the most probable mechanism

$$C_4H_9^+ + BzOAc \longrightarrow (BzOAc).C_4H_9^{+*} \qquad (4.2\text{-}54)$$

$$(BzOAc).C_4H_9^{+*} \longrightarrow (BzOAc)H^+ + C_4H_8 \qquad (4.2\text{-}55)$$

$$(BzOAc).C_4H_9^{+*} \longrightarrow Bz^+ + C_4H_8 + AcOH \qquad (4.2\text{-}56)$$

where Bz represents $C_6H_5.CH_2$ and Ac represents $CH_3.CO$. This mechanism differs in two ways from that proposed in the present work: the collision complex is not formed by a reversible reaction and the formation of products does not involve a third-body. However, one of the other mechanistic schemes proposed for these reactions does involve reversible formation of the collision complex, and his results do not prove that this reaction cannct

be reversible.

By incorporating some of the elements of the foregoing schemes it seems plausible to suggest that the mechanism of the reactions which give rise to chemical-ionization mass spectra is actually of the form proposed by Harrison for the reactions of $C_3H_5^+$ with ethylene. Accordingly the general case of a reaction of an ion (RH^+) generated from isobutane with a sample molecule (M) is thus proposed:

$$RH^+ + M \underset{k_{-1}}{\overset{k_1}{\rightleftharpoons}} MRH^{+*} \qquad (4.2\text{-}57)$$

$$MRH^{+*} + M \xrightarrow{k_2} \text{Products} \qquad (4.2\text{-}58)$$

$$MRH^{+*} \xrightarrow{k_3} \text{Products} \qquad (4.2\text{-}59)$$

The integrated rate equation for the disappearance of RH^+ is then

$$-\log\left(\frac{I_n}{I_n^{\,o}}\right) = k_1[M]\tau\left(\frac{k_3+k_2[M]}{k_{-1}+k_3+k_2[M]}\right) \qquad (4.2\text{-}60)$$

from which it is apparent that the overall kinetic order of the reaction is dependent upon the ratio $k_2[M]/k_3$. For very small sample concentrations the kinetic behaviour is second order with an experimental rate constant corresponding to $k_1k_3/(k_{-1}+k_3)$. However, as the sample concentration increases it is possible that the kinetic behaviour becomes third order, with an experimental rate constant corresponding to k_1k_2/k_{-1}, while for very large sample concentrations the kinetic behaviour is again second order with the experimental rate constant corresponding to k_1.

Now since Field was working with higher isobutane pressures and lower sample pressures than those employed in the experiments

described in section 3.3, it is feasible that his results corresponded to the low-pressure limit of equation (4.2-60). The present results relate to the sample-pressure range for which $k_2[M] >> k_3$. It is notable that the low-pressure limit of equation (4.2-60) does not reveal the reversibility of reaction (4.2-57) since

$$\log\left(\frac{I_n}{I_n^o}\right) \sim \frac{k_1 k_3 [M]}{k_{-1} + k_3} \qquad (4.2\text{-}61)$$

D. Rate constants of the formation of the collision complexes.

The rate constants (k_1) of the formation of the collision complexes (equation (4.2-4)) are listed in tables (4-2) to (4-5). These tables also contain rate constants (k_o, see equation (4.2-3)) which may correspond to reactions of the type (4.2-1) rather than the formation of a collision complex (see section 4.2.A). It is emphasized here that all rate constants may be subject to the effects of mass discrimination by the ion-source, collector slit, and electron multiplier. Although some precautions were taken with the ion-source and collector slit (see section 2.2), it was not possible to make allowances for mass discrimination by the multiplier[4]. The relative rate constants for the reactions of a given reactant ion with the various compounds should, nevertheless, be fairly accurate since, in this case, mass-discrimination effects perturb only the total ion current computed from each spectrum. Comparisons

between the rate constants of the reactions of two different reactant ions with a given compound are likely, however, to be subject to these effects, and it can only be assumed that, since the mass range in question (m/z = 27 to m/z = 57) is comparatively small, the effects are not significantly greater than the error limits of the rate constants themselves.

The collision frequency (k_c) of reaction (4.2-4)

$$RH^+ + M \longrightarrow MRH^+ \qquad (4.2\text{-}4)$$

may be calculated from The Average-Dipole-Orientation (A.D.O.) theory of Su and Bowers [19]. The equation used for these calculations was

$$k_c = 2\pi e \left[\left(\frac{\alpha}{\mu}\right)^{\frac{1}{2}} + \frac{C\mu_D}{\mu v} \right] \qquad (4.2\text{-}62)$$

where α and μ_D are respectively the angle-averaged polarizability and dipole moment of the molecule (M), e is the electronic charge, μ is the reduced mass of the ion (RH^+) and the molecule, v is the drift velocity of the ion, and C is a parameter which depends on μ_D, α, and the temperature. Polarizabilities and dipole moments are listed in appendix I. Polarizabilities not listed in tables[80] were calculated by the Lippincott delta-function method[79]. Wherever possible dipole moments measured in the gas phase were used. If these figures were not available, the value given for a solution of the compound in benzene was employed. Values of C were obtained from the data given by Su and Bowers [19]. The drift velocity,v, was calculated from equation (3.1-5). The resulting values of k_c are listed in appendix III. The dipole moments for the 2- and

3-pentanols,2- and 3-hexanols, fluoroethanol and iodoethanol, the anisoles and the 2-halopropionitriles were not available.

The ratio of the reaction rate constant to the collision frequency (k_1/k_c) for a given reaction represents the fraction of collisions which result in formation of the complex MRH^{+*}. These are listed in the table (4-10). It is immediately apparent from this table that reactions of the $C_3H_3^+$ ion with all the compounds are exceedingly slow; in general less than 4% of collisions result in reaction, and, in the cases of 2-chloroethanol and 2-bromoethanol, less than 1%. Reactions of the $C_4H_5^+$ ion are also slow; generally less than 16% of collisions result in reaction, and again here the reactions of the halohydrins are very slow. These results suggest that the $C_3H_3^+$ and $C_4H_5^+$ ions possess greater stability than the other reactant ions. It seems likely, then, that these ions are the aromatic cyclopropenyl [64], [29], and methylcyclopropenyl, cations respectively.

Reactions of the ketones with the $C_4H_9^+$ and $C_4H_8^{+\cdot}$ ions are very fast. In fact the experimentally determined values of k_1 are greater than the collision frequency, suggesting that the experimental results are too large. Most probably the error is in the estimation of the ion residence times, or in the assumption that residence times are not altered by the presence of fairly large concentrations of the sample.

Reactions of the ketones with the $C_4H_7^+$, $C_3H_6^{+\cdot}$, $C_3H_5^+$, and $C_2H_3^+$ ions all proceed with an efficiency of 40-70%. Furthermore there is fair agreement between values of k_1/k_c for the reaction

Table 4-10)

The percentage of collisions which result in complex formation between isobutane reactant ions and various ketones, nitriles, anisoles, and alcohols.

Compound	Temp. (°C)	Isobutane pressure (torr)	100 x k_1/k_c									
			$C_4H_9^+$	$C_4H_8^+$	$C_4H_7^+$	$C_4H_5^+$	$C_3H_7^+$	$C_3H_6^+$	$C_3H_5^+$	$C_3H_3^+$	$C_2H_5^+$	$C_2H_2^+$
Acetone	176	0.108	125.2	108.2	61.6	15.1	49.0	66.9	61.1	2.1	106.6	52.4
Ethyl methyl ketone	175	0.109	117.0	133.3	54.0	15.4	81.2	73.6	65.8	2.5	31.2	42.6
Acetonitrile	174	0.100	20.9	22.1	34.3	10.9	46.7	MW	27.8	3.0	19.5	25.9
Propionitrile	174	0.100	54.8	MW	S	S	96.8	39.9	75.9	2.9	S	S
Butyronitrile	174	0.104	68.2	84.4	82.7	13.5	92.1	66.4	101.9	0	23.2	S
Anisole	175	0.240	15.3									
4-Fluoroanisole	175	0.240	5.2									
4-Methylanisole	175	0.240	52.4									
Methanol	167	0.110	8.6	16.4	4.2	4.5	41.2	28.0	23.4	1.8	13.7	15.9
1-Propanol	167	0.110	30.7	80.6	24.0	15.8	44.8	69.3	41.0	1.8	26.5	20.9
2-Propanol	166	0.111	63.5	67.9	24.4	15.8	42.0	72.4	63.7	1.8	24.7	18.8
1-Pentanol	174	0.099	68.7	73.6	0	14.4	113.4	22.5	S	3.9	0	12.2
1-Hexanol	174	0.100	45.6	49.2	0	8.5	74.6	S	S	1.9	12.8	3.0
2-Chloroethanol	175	0.115	7.2	10.0	7.3	4.0	31.4	16.2	17.8	0.6	9.3	4.8
2-Bromoethanol	175	0.115	5.4	5.3	3.9	2.2	17.1	10.9	13.0	0.2	4.0	3.1

of each of these ions with the two ketones. This observation would seem to reflect the structural similarity of the compounds. Experimentally determined rate constants of proton-transfer reactions have been found to be significantly less than k_c by other workers. For example, Solka and Harrison[65] studied reactions of the type

$$CH_3SH_2^+ + M \longrightarrow CH_3SH + MH^+ \qquad (4.2\text{-}63)$$

and found $100xk_{exp}/k_c = 34$ and 28 for M = CH_3CHO and $CH_3.CH_2.CHO$ respectively. It is interesting to note that their results were consistent with the formation of a proton-bound complex.

Agreement between the values of k_1/k_c for the reactions of $C_3H_7^+$ with the two ketones is poor. It seems likely that the experimentally determined value of k_1 for the reaction of this ion with acetone was erroneously low.

For the reactions of acetonitrile, propionitrile, and butyronitrile with the $C_4H_9^+$, $C_3H_7^+$, and $C_3H_5^+$ ions the magnitude of k_1/k_c tended to increase as the molecular weight of the sample increased. It is unfortunate that rate constants of the reactions of $C_3H_6^{+\cdot}$ with acetonitrile, and of $C_4H_8^{+\cdot}$ with propionitrile, could not be determined because of the presence of MH^+ ions having the same mass-to-charge ratio as the reactant ions. Consideration of the other two values of k_1/k_c in each case suggests, however, that the trend in these values was the same as that for the $C_4H_9^+$, $C_3H_7^+$, and $C_3H_5^+$ ions. Similar arguments apply to the reactions of $C_4H_7^+$, $C_4H_5^+$, and $C_2H_5^+$, where scatter of experimental data prevented determination of k_1.

Values of k_1 for the reactions of the 2-halopropionitriles (see tables (4-2) and (4-3)) are, in some cases, much larger than would be anticipated for compounds containing electron-withdrawing substituents. For the reactions of $C_4H_9^+$ and $C_3H_5^+$ with 2-chloropropionitrile k_1 is greater than the rate constant obtained for the reactions of these ions with acetonitrile. Also, the rate constants of the reactions of $C_4H_9^+$ and $C_3H_7^+$ with 2-bromopropionitrile are at variance with the rate constants for the reactions of the other reactant ions with this compound. No explanation has been found for this behaviour.

Values of k_1 for the reactions of the anisoles with $C_4H_9^+$ are approximately in the order expected from electronic considerations: reactions of the fluoro-substituted anisoles are slower than anisole, while reactions of the methyl-substituted anisoles are faster than anisole. The relative magnitudes of these rate constants will be discussed further in section 4.3.

Values of k_1/k_c, the fraction of effective collisions, for the formation of collision complexes between the $C_4H_9^+$, $C_4H_8^{\cdot+}$, and $C_3H_7^+$, ions and the n-alkyl alcohols (R_1OH) followed the order $R_1 = CH_3 < C_3H_7 < C_5H_{11} < C_6H_{13}$. The inversion of the relative reactivity of 1-propanol and 1-pentanol for the two sets of reactant ions suggests that the experimental rate constant is not simply k_1 and that additional processes are contributing to the value in some cases. A possible source of error in the determination of k_1 was the presence of small concentrations of water in the alcohols. The presence of water has been shown to

have a significant effect upon the rates of reaction (see section 4.2.C).

Values of k_1/k_c for the formation of collision complexes of the $C_4H_7^+$, $C_4H_5^+$, $C_3H_6^+$, $C_3H_6^+$, $C_2H_5^+$, and $C_2H_3^+$ ions with 1- and 2- propanol were of comparable magnitude for each ion, suggesting that differences in the structures of these two compounds do not affect the rate of complex formation. It seems, however, that the rates of reaction of 2-propanol with the $C_4H_9^+$ and $C_3H_5^+$ ions were faster than the corresponding reactions of 1-propanol, while the reaction between $C_4H_8^+$ and 2-propanol was slower than the reaction of this ion with 1-propanol. Explanation of these results is not, as yet, forthcoming.

Consideration of the values of k_1 for the formation of complexes between reactant ions and the various pentanols and hexanols shows that, in general, the relative reactivities are in the order 3-ROH>2-ROH>1-ROH. The $C_2H_5^+$ ion, however, does not react with any of the pentanols to a measurable extent. Furthermore, the values of k_1 obtained for reactions of $C_4H_7^+$ with the hexanols suggest that only 2-hexanol reacts with this ion.

Rate constants for complex formation between the halohydrins ($X.CH_2.CH_2.OH$) and all the reactant ions except $C_2H_5^+$ lie in the order X = F>Cl>Br>I. Presumably this order should also be followed in the case of reactions with $C_2H_5^+$. However, the experimental value of k_1 for the reaction of iodoethanol with this ion was much higher than the rate constants for the reactions of this compound with all the other reactant ions. The relative

magnitude of the rate constants for complex formation by the alcohols will be discussed in more detail in section 4.3.

It was stated in section 3.3.E that the only ion produced from carbon tetrachloride was CCl_3^+. This ion was presumably formed by chloride-transfer reactions:

$$RH^+ + CCl_4 \longrightarrow CCl_3^+ + RHCl \qquad (3.3\text{-}28)$$

The rate constants, k, of these reactions are listed in table (4-11), and the values normalized with respect to the collision frequencies, k_c, calculated from the A.D.O. theory are given in table (4-12). It is apparent from the results that carbon tetrachloride does not undergo reaction with the $C_4H_8^{+\cdot}$ and $C_3H_6^{+\cdot}$ ions - the only odd-electron ions (except $C_4H_{10}^{+\cdot}$) formed from isobutane.

The reaction between $C_4H_5^+$ and carbon tetrachloride is comparatively fast: 22% of all collisions result in reaction. This result would seem to complement the observation that the proton-transfer reactions of this ion are slow, and therefore goes to substantiate the supposition that $C_4H_5^+$ is the methylcyclopropenyl cation (vide supra). Similarly the rate of the chloride-transfer reaction undergone by $C_3H_3^+$, for which the cyclopropenyl structure has been proposed, is somewhat faster than the rates of reaction of this ion with the other compounds discussed above. The observation that the rate of reaction of $C_4H_7^+$ is also comparatively fast may be used tentatively to suggest that some of these ions possess the methylcyclopropyl structure.

Table (4-11)

Rate constants of the reactions of isobutane reactant ions with carbon tetrachloride and water.

Compound	k (10^{10} x cm^3 $molecule^{-1}$ sec^{-1})						
	$C_4H_9^+$	$C_4H_8^+$	$C_4H_7^+$	$C_4H_5^+$			
Carbon Tetrachloride	0.68±0.13	0*	1.52±0.70	2.73±0.91			
Water	0*	0.12±0.07	0.40±0.11	0.13±0.13			
	$C_3H_7^+$	$C_3H_6^+$	$C_3H_5^+$	$C_3H_3^+$	$C_2H_5^+$	$C_2H_3^+$	
Carbon Tetrachloride	0.45±0.41	0*	0.72±0.28	0.86±0.24	0.40±0.15	1.53±0.85	
Water	0.78±0.27	1.09±0.37	1.17±0.32	0.03±0.10	0.14±0.41	1.13±0.22	

* The method did not permit determination of rate constants lower than ca.10^{-12} cm^3 $molecule^{-1}$ sec^{-1}

Table (4-12)

The percentage of collisions which result in reaction of isobutane reactant ions with carbon tetrachloride and water.

Compound	100 x k/k_c									
	$C_4H_9^+$	$C_4H_8^+$	$C_4H_7^+$	$C_4H_5^+$	$C_3H_7^+$	$C_3H_6^+$	$C_3H_5^+$	$C_3H_3^+$	$C_2H_5^+$	$C_2H_3^+$
Carbon Tetrachloride	5.8	0	12.8	22.6	3.4	0	5.4	6.3	2.6	9.7
Water	0	0.7	2.2	0.7	4.2	5.8	6.2	0.2	0.7	5.8

The rates of the chloride-transfer reactions from carbon tetrachloride to the other reactant ions are generally slow; with the exception of $C_2H_3^+$, less than 6% of all collisions result in reaction.

The rate constants, k, found for the proton-transfer reactions from the reactant ions to water are listed in table (4-11), and the values normalized with respect to the A.D.O.-theory collision frequencies, k_c, are given in table (4-12). Proton transfer does not occur from the $C_4H_9^+$ ion, and the rate constants corresponding to the $C_3H_3^+$ and $C_4H_5^+$ ions are zero within experimental error. The other reactant ions undergo slow reactions with water; generally less than 7% of all collisions result in reaction.

E. Lifetimes of the collision complexes.

Experimental values for k_2/k_{-1}, the ratio of rate constants of the decomposition reactions of the collision complexes (MRH^{+*}), are listed in tables (4-6) and (4-7). The ratios may be used to estimate the lifetimes of the complexes with respect to unimolecular decomposition to reactants. The following method is similar to that employed by Anicich and Bowers [66], and by Miasek and Harrison [57], in their studies of collisional deactivation of excited ions.

The collision frequency (k_c') of reaction (4.2-5)

$$MRH^{+*} + M \longrightarrow \text{Products} \qquad (4.2\text{-}5)$$

may be calculated analogously to k_c, from equation (4.2-62).

(The products of this reaction were discussed in section 4.2.A). The calculated values of k_c' are listed in appendix III. Provided the height of the energy barrier B (see figure (4-1)) is not too large, reaction (4.2-5) may be assumed to proceed at the collision frequency. If this assumption is valid, then k_c' may be identified with k_2, and division of the measured value of k_2/k_{-1} by k_c' will result in an estimate of $1/k_{-1}$, the lifetime of the collision complex.

Values of $1/k_{-1}$ obtained by this method are listed in table (4-13) from which it is immediately apparent that the collision complexes have relaxation lifetimes that are generally in the range 1-10 μsec. These lifetimes are of the order of the residence times of ions in the ion-source: the estimated residence time of $C_4H_9^+$ ion is ∿7 μsec (equation (3.1-8)). Thus peaks in the spectra which correspond to the products of association reactions (eg.$(CH_3.CO.CH_3).C_3H_7^+$, see section 3.3.A) may be due in part to collision complexes which have survived long enough to be detected.

It was stated in section 3.3 that metastable peaks corresponding to the loss of a sample molecule from an M_2H^+ (or M_2H^{+*}) ion were frequently observed in the spectra of the compounds studied. This suggested that the lifetime of the parent ion was of the order of the ion-residence time. Values obtained above from $1/k_{-1}$, although not actually determined for M_2H^{+*} ions, tend to substantiate this suggestion.

Table (4-13).

Lifetimes of collision complexes.

Compound	$1/k_{-1}$ (μsec).							
	$C_4H_9^+$	$C_4H_8^{+\cdot}$	$C_4H_7^+$	$C_3H_7^+$	$C_3H_6^{+\cdot}$	$C_3H_5^+$	$C_2H_5^+$	$C_2H_3^+$
Acetone	3.7	7.3	7.8	(149)	6.7	4.7	1.4	3.1
Ethyl methyl ketone	8.6	7.1	10.8	9.7	6.7	5.1	15.8	3.5
Acetonitrile	4.6	4.7	1.3	11.3	M	9.4	9.6	12.4
Propionitrile	1.8	MW	S	4.6	10.1	2.0	S	S
Butyronitrile	2.4	2.2	1.9	5.5	1.8	1.1	-	S
Anisole	21.8							
4-Fluoroanisole	9.7							
4 Methylanisole	4.9							
Methanol	5.9	2.7		2.3	2.3	3.1	-	-
1-Propanol	1.5	2.0		2.5	2.8	9.2	-	-
2-Propanol	1.5	4.5		4.7	1.5	2.4	-	-
1-Hexanol	6.7	3.5		1.8	S	S	-	-
2-Chloroethanol	-	-		20.2	-	-	-	-

S: Computation was not carried out as experimental data was badly scattered.
M: Reactant ion was obscured by the MH^+ ion.

Collision complexes between many different ions and molecules have been observed mass spectrometrically under conditions where the lifetimes were at least 10^{-6} sec. Some representative examples are : $O_2^+.O_2$ [67], $CH_5^+.CH_4$ [68], $H_3O^+.CH_4$ [69], and $C_2H_5^+.C_2H_6$ [70]. The probability of observing a collision complex is related to the exothermicity of the reaction between the ion and the molecule. Complexes are not, in general, observed when highly exothermic reaction channels are available to them. In such cases the energy released in the exothermic reaction forces the products of decomposition of the complex apart, thereby shortening its lifetime [71], [72]. It is difficult to calculate meaningful energy changes for the reactions under discussion since the structures of most of the reactant ions are not known, and indeed, all the ions having a common composition and mass-to-charge ratio need not necessarily possess the same structure. Approximate calculations show, however, that most of the reactions are slightly endothermic,or thermoneutral. Hence lifetimes for the collision complexes of 1-10 μsec seem reasonable.

It was suggested in section 4.2.D that the value of k obtained for the reaction of the $C_3H_7^+$ ion with acetone was in error. The determined value of the lifetime of the corresponding complex is also much higher than that of the other $(CH_3.CO.CH_3)RH^+$ complexes. Other doubtful kinetic results were probably obtained such that the value for the lifetime of $(CH_3.CH_2.CO.CH_3)C_2H_5^+$ was at variance with other data for ethyl methyl ketone.

Apart from these two cases there is fair agreement between lifetimes of the complexes between the RH^+ ions and the two ketones.

No trends in the collision-complex lifetimes of the alcohols and nitriles are apparent and, in general, the data suggests that the lifetimes of all these complexes are very similar (1-5 μsec).

4.3 Relationships between molecular structure and the rate constants of the formation of the collision complexes.

Rate constants for the formation of the collision complexes MRH^{+*} (reaction (4.2-4)

$$RH^+ + M \xrightarrow{k_1} MRH^{+*} \qquad (4.2\text{-}4)$$

are listed in tables (4-2) to (4-5). Since this reaction appears to be comparatively simple it might be expected that, for a given reactant ion, the magnitude of the rate constants k_1 would reflect differences in the structure of compounds which form a homologous series.

A. Anisoles.

In previous sections it has been assumed that the $M^{+}_{\cdot}$ ion produced from the anisoles is formed entirely from the collision complex, MRH^+. It was shown in section 3.3.D, however, that for M = anisole, 3-fluoroanisole, and 4-fluoroanisole the ratio $I_{MH^+}/(I_{MH^+} + I_{M^{+}_{\cdot}})$ varied with sample pressure. This behaviour is inconsistent with the above assumption since if $M^{+}_{\cdot}$ were formed entirely from the collision complex this ratio would be independent of sample pressure.

It is more likely that $M^{+}_{\cdot}$ is formed by a direct reaction in competition with the complex formation[73]. Thus

$$RH^+ + M \xrightarrow{k_0} RH\cdot + M^{+}_{\cdot} \qquad (4.3\text{-}1)$$

$$RH^+ + M \underset{k_{-1}}{\overset{k_1}{\rightleftharpoons}} MRH^{+*} \qquad (4.3\text{-}2)$$

$$MRH^{+*} + M \xrightarrow{k2} MH^{+} + R + M^{*} \qquad (4.3\text{-}3)$$

It is assumed that the rate of decomposition of MRH^{+*} by collision with a molecule of isobutane is sufficiently slow that this reaction can be omitted from the above scheme.

Now, using equation (4.3-1), the rate of formation of $M^{+\cdot}$ is given by

$$\frac{d[M^{+\cdot}]}{dt} = k_o[M][RH^{+}] \qquad (4.3\text{-}4)$$

and, from equations (4.3-2) and (4.3-3), the rate of formation of MH^{+} is given by

$$\frac{d[MH^{+}]}{dt} = \frac{k_1 k_2 [M]^2 [RH^{+}]}{k_{-1}+k_2[M]} \qquad (4.3\text{-}5)$$

As described in section 4.2.A, this equation is obtained by applying the steady-state hypothesis to MRH^{+*}. It is apparent from (4.3-4) and (4.3-5) that

$$[MH^{+}]/[M] = (k_1/k_o)[M]/([M]+(k_{-1}/k_2)) \qquad (4.3\text{-}6)$$

Hence, by use of an equation analogous to (3.1-2),

$$(1-n)p_M/n = (k_o/k_1)p_M + k_o k_{-1}/k_1 k_2 N \qquad (4.3\text{-}7)$$

where n is the ratio $I_{MH^+}/(I_{MH^+} + I_{M^{+\cdot}})$ (see graph (3-9)). Equation (4.3-7) shows that, if the mechanism proposed in equations (4.3-1) to (4.3-3) is correct, then there is a linear correlation between $(1-n)p_M/n$ and the sample pressure, p_M. The appropriate plots are given in graph (4-5). For 3- and 4-methylanisole $(1-n)p_M/n$ varies linearly with sample pressure over the entire range, whereas for the other anisoles the correlation is observed only above ca. 2.5×10^{-3} torr. The

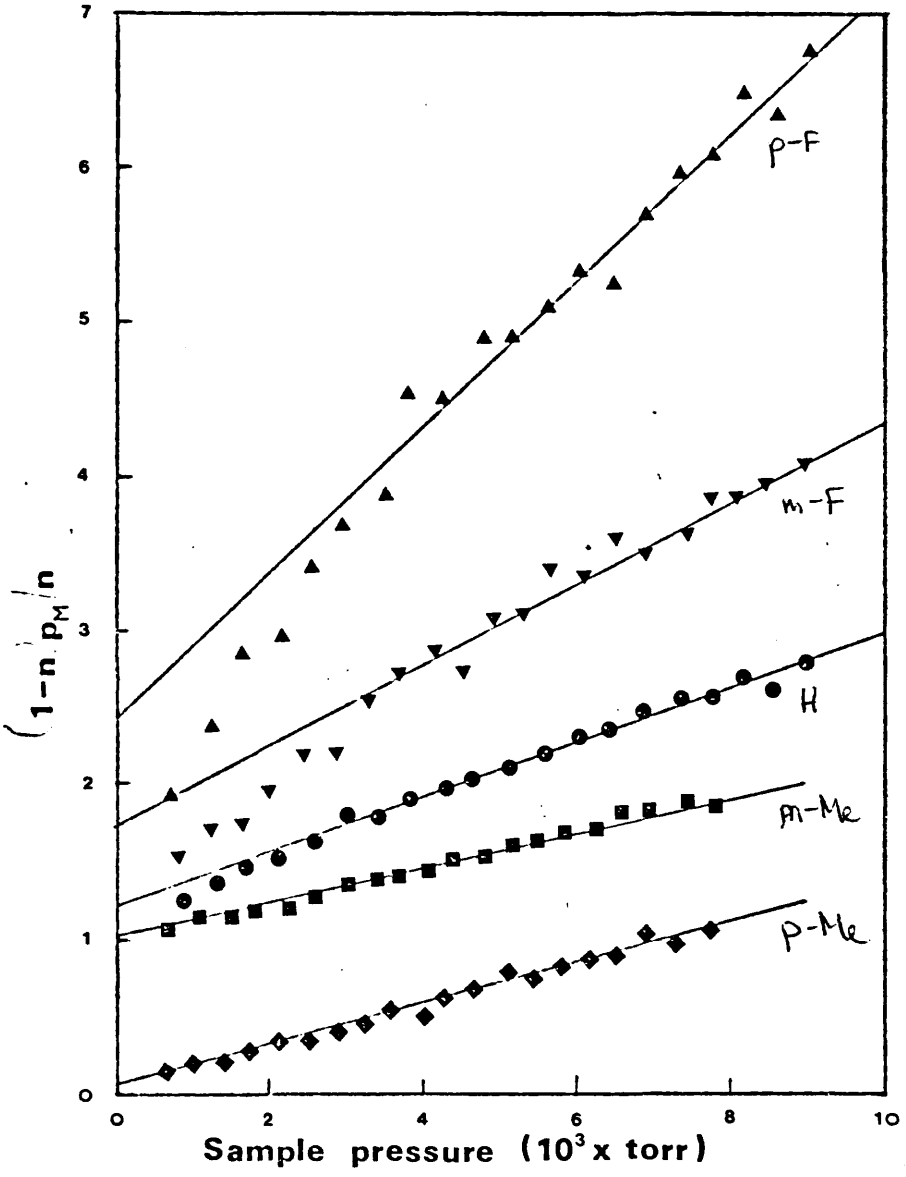

GRAPH (4-5). Variation of the ratio $(1-n)p_M/n$ with pressure of various anisoles. Origin has been shifted to (0,1) for all compounds other than p-Methylanisole.

The slopes of the lines correspond to the ratio k_o/k_1. Hence it is apparent that complex formation is preferred (low values of k_o/k_1) with molecules that are activated towards electrophilic attack. Expressions for the individual values of k_o and k_1 cannot be obtained from the above analysis. Furthermore the values of k_1 obtained in section 4.2.A cannot be employed in determinations of k_o as the assumed mechanism was in error. The equation for the disappearance of $C_4H_9^+$,

$$- \log \left(\frac{I_{57}}{I^o_{57}}\right) = k_o N \tau p_M + \frac{k_1 k_2 N^2 \tau p_M^2}{k_{-1}+k_2 N p_M} \qquad (4.3\text{-}8)$$

can, however, be obtained from equations (4.3-1) to (4.3-3) by the methods discussed in section 4.2.A. If, in this equation, $k_2 N p_M >> k_{-1}$, then

$$- \log (I_{57}/I^o_{57}) = (k_o+k_1) N \tau p_M \qquad (4.3\text{-}9)$$

Hence it would be expected that log (I_{57}/I^o_{57}) should vary linearly with sample pressure. This behaviour is observed with the anisoles for $p_M > 5 \times 10^{-3}$ torr. The slopes of the plots of log (I_{57}/I^o_{57}) against p_M are proportional to k_o+k_1 given that the condition $k_2 N p_M >> k_{-1}$ is strictly valid. Substitution of some appropriate values shows that $k_2 N p_M$ is $\sim 3k_{-1}$, so the following analysis may be subject to large errors.

Making use of the slopes of the lines given in graph (4-5) and the slopes of the linear regions of the plots of log (I_{57}/I^o_{57}) against sample pressure, gives separate values of k_o and k_1; these are listed in table (4-14).

Table (4-14)

Rate constants for the formation of $M^{+\cdot}$ and $MC_4H_9^+$* for M = anisoles.

Compound	Temp. (°C)	Isobutane pressure (torr)	Rate constants (10^{10}x $cm^3 molecule^{-1} sec^{-1}$)	
			k_o	k_1
Anisole	175	0.240	0.33	1.94
3-Fluoro-anisole	175	0.230	0.14	0.59
4-Fluoro-anisole	175	0.240	0.27	0.52
3-Methyl anisole	175	0.236	0.37	3.32
4-Methyl anisole	175	0.240	0.54	4.41

The relative magnitudes of k_o are in the order that would be predicted from electronic considerations. Hence it is of interest to investigate the extent to which the rates of these charge-transfer reactions obey the Hammett equation[76] (equation (4.3-10))

$$\log_{10}(k_X/k_H) = \sigma_x \qquad (4.3\text{-}10)$$

There are, as yet, no well-defined values of the substituent constants, σ_x, for gas-phase reactions, although evaluation of such constants is an active area of research[74]. In the following discussion, therefore, the solution-phase values of σ_x[75] will be used. The plot of $\log_{10}(k_x/k_H)$ (where $k = k_o$) against σ_x is shown in graph (4-6). It is immediately apparent from the graph that the rates of the charge-transfer reactions depend upon the effects of substituents in the anisoles. Hence it is to be expected that charge-transfer reactions will exert a

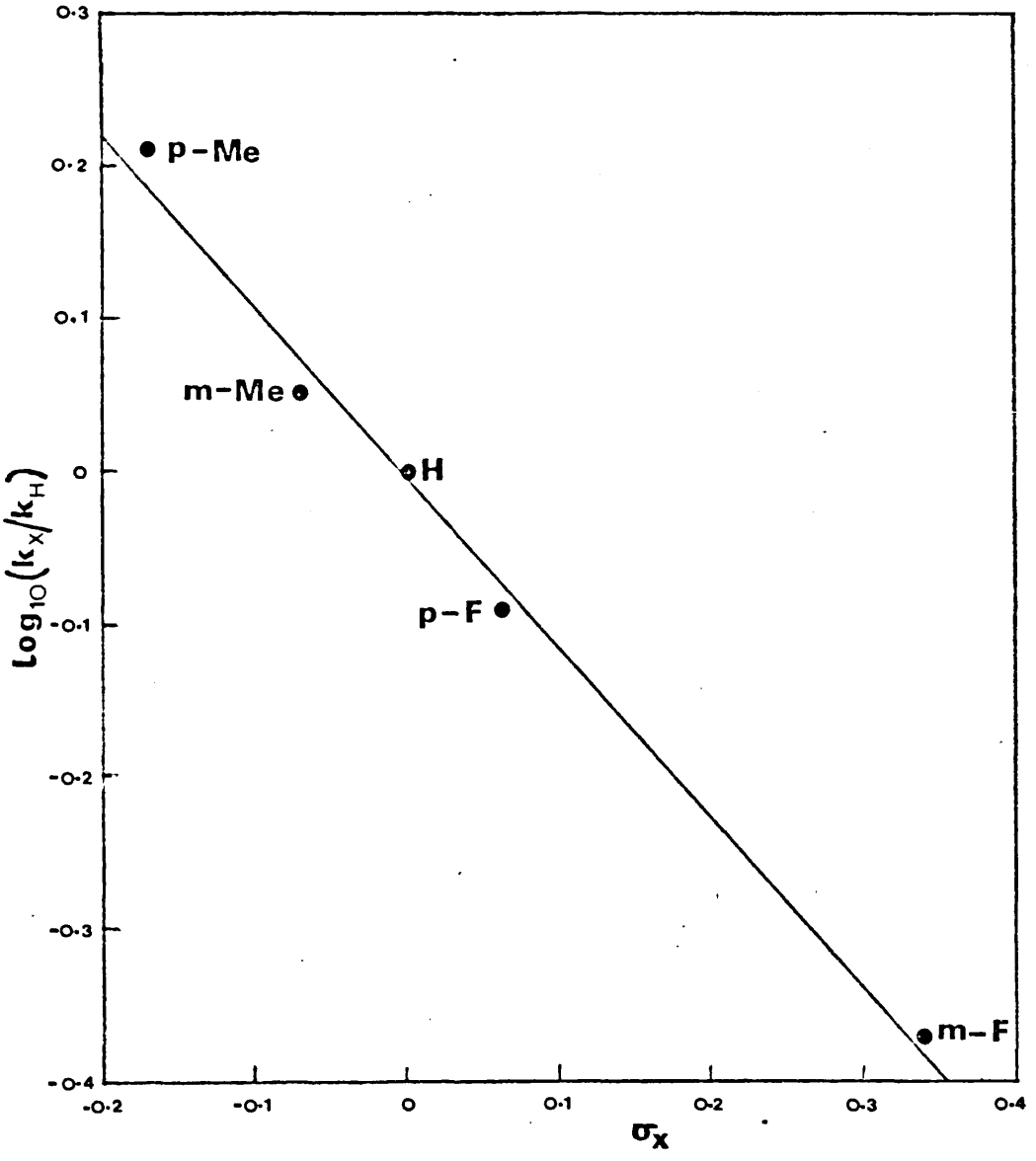

GRAPH (4-6). Hammett plot for charge-transfer reactions of $C_4H_9^+$ with various anisoles.

significant effect upon the chemical-ionization mass spectra of anisoles containing electron-donating substituents, but that the effect will be small when the anisole contains a strongly electron-withdrawing substituent, provided, of course, that no other types of charge-transfer reactions are possible.

In contrast to the charge-transfer reactions, the rates of formation of the complexes MRH^{+*} do not appear to be correlated with σ_x (see graph (4-7)). However, attack by the $C_4H_9^+$ ion upon an anisole may occur either at the oxygen atom or at one of the carbon atoms of the ring. Hence the measured rate constants, k_1, incorporate the rate constants for both these processes. In 4-fluoroanisole the four unsubstituted ring positions are all, to some extent, deactivated towards electrophilic substitution. The rate of reaction of $C_4H_9^+$ at any of these sites is, therefore, likely to be slow, and it is possible that the rate of the reaction between $C_4H_9^+$ and 4-fluoroanisole is essentially a measure of the rate of attack at the methoxy oxygen atom. If it be assumed that the electron density on the oxygen atom is similar in all the anisoles studied, then the rate constant for attack by $C_4H_9^+$ at the oxygen atom (approximated by the rate constant of reaction of $C_4H_9^+$ with 4-fluoroanisole) may be subtracted from the measured rate constants to give approximate rate constants for attack by $C_4H_9^+$ at the ring carbon atoms. These rate constants may now be divided by the number of ring carbon atoms which are available for attack. In anisole itself, and the 3-substituted

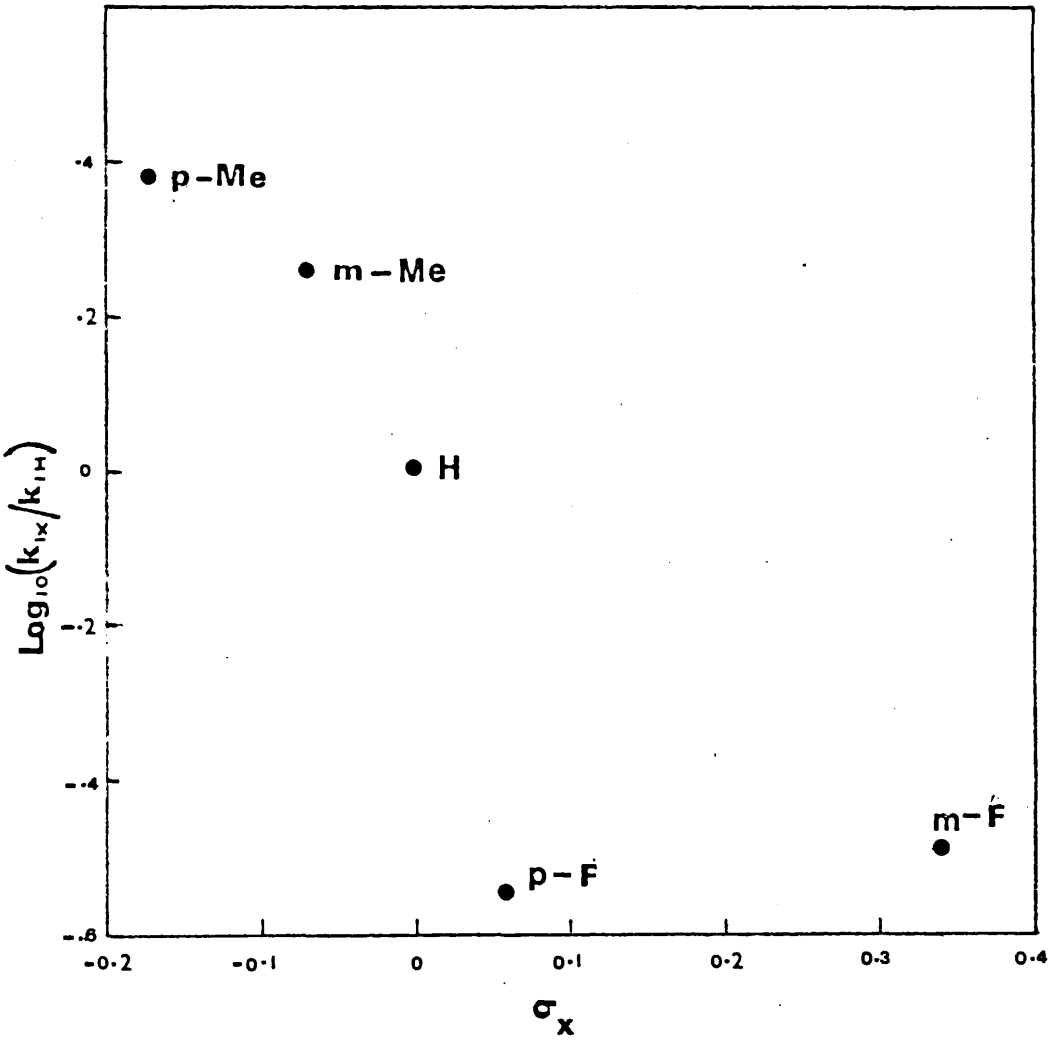

GRAPH (4-7). Hammett plot for reactions of $C_4H_9^+$ with various anisoles.

anisoles, attack is most probable at the positions ortho and para to the methoxy group, whilst in 4-methylanisole it is only the positions ortho to the methoxy group that are likely to be attacked. (It has been assumed that the rates of attack at the ipso-positions are sufficiently small that such reactions can be neglected.) Since the rates of attack are determined by the electron density at the ring atom, the rate constants (k_1') normalized with respect to the number of ring carbon atoms available for attack should be correlated with Graph (4-8), which is a plot of log (k_{1_X}'/k_{1_H}') against σ_x, shows that there is an excellent correlation.

The value of the reaction parameter, ρ, obtained from the plot is -3.85 ± 0.18. Since the magnitude of ρ is a measure of the charge developed during a reaction (a negative value corresponding to the development of a positive charge), and since reaction (4.3-2) involves a full positive charge, it would be expected that the value of ρ would be large and negative. The absolute value of ρ is, in fact, somewhat smaller than the largest (absolute) value given by Leffler and Grunwald[75] in their table of ρ-values for many different types of reaction.

By comparison, the value of ρ obtained from the Hammett plot for the charge-transfer reactions if -1.11 ± 0.05, ie., much smaller than that for the complex formation.

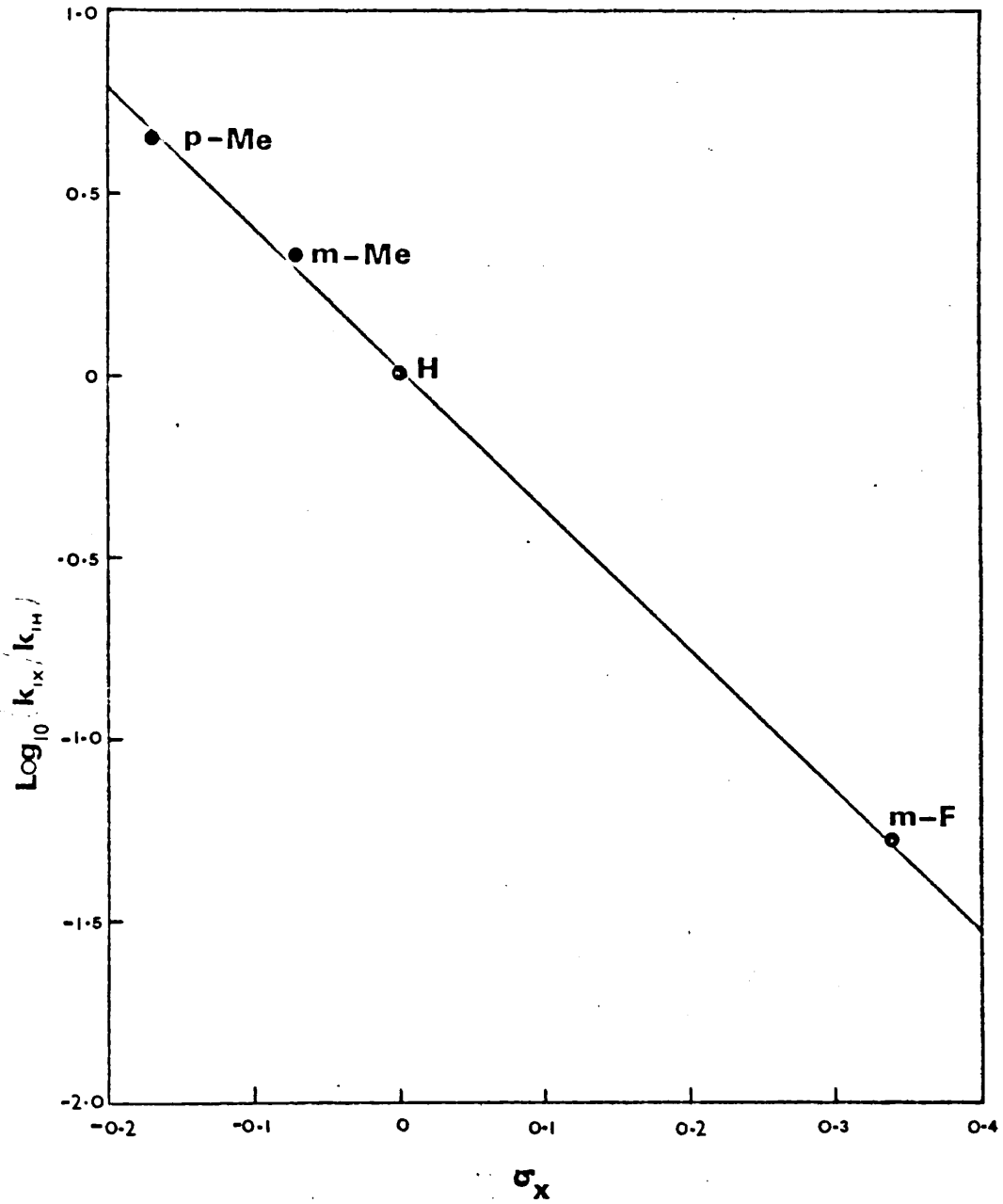

GRAPH (4-8). Hammett plot for reactions of $C_4H_9^+$ with aromatic nuclei of various anisoles

B. Nitriles.

Now since there is a relationshop between the rate constants k_1, for the formation of the $(X.C_6H_5.OMe)C_4H_9^+$ complexes and the Hammett substituent constants σ_x, it was expected that there might be a similar relationship between the rate constants for the formation of collision complexes of the RH^+ ions with the nitriles and the Taft substituent constants σ_x^*. The relationship would be defined in the equation [77]

$$\log_{10}\left(\frac{k_{1x}}{k_{1Me}}\right) = \rho^*\sigma_x^* \qquad (4.3\text{-}3)$$

in which σ^* is an empirical parameter dependent on the nature of the reaction and on the reaction conditions.

Plots of $\log_{10}(k_{1x}/k_{1Me})$ against σ_x^* for the reaction

$$RH^+ + X.CH_2.CN \longrightarrow (X.CH_2.CN).RH^{+*} \qquad (4.3\text{-}4)$$

in which $RH^+ = C_4H_9^+$, $C_3H_7^+$, or $C_3H_5^+$, and X = H, CH_3, C_2H_5, $ClCH_2$, or BrCH) are shown in graphs (4-9) to (4-11). It is apparent from graph (4-9) that there is good correlation between $\log_{10}(k_{1x}/k_{1Me})$ and σ_x^* for the formation of the $(X.CH_2.CN)C_4H_9^+$ complex when X = H, CH_3, or C_2H_5, but the data corresponding to

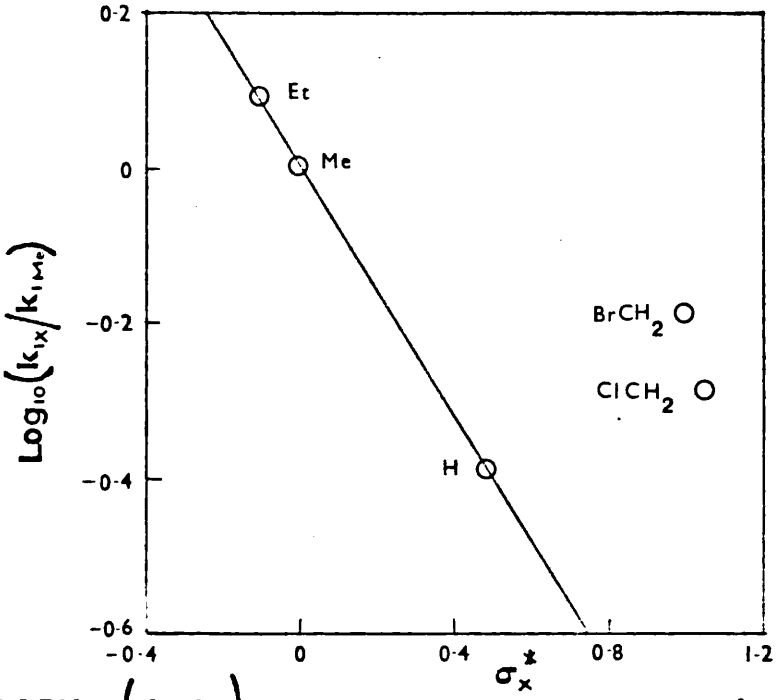

GRAPH (4-9) .....Taft plot for reactions of $C_4H_9^+$ with various nitriles.

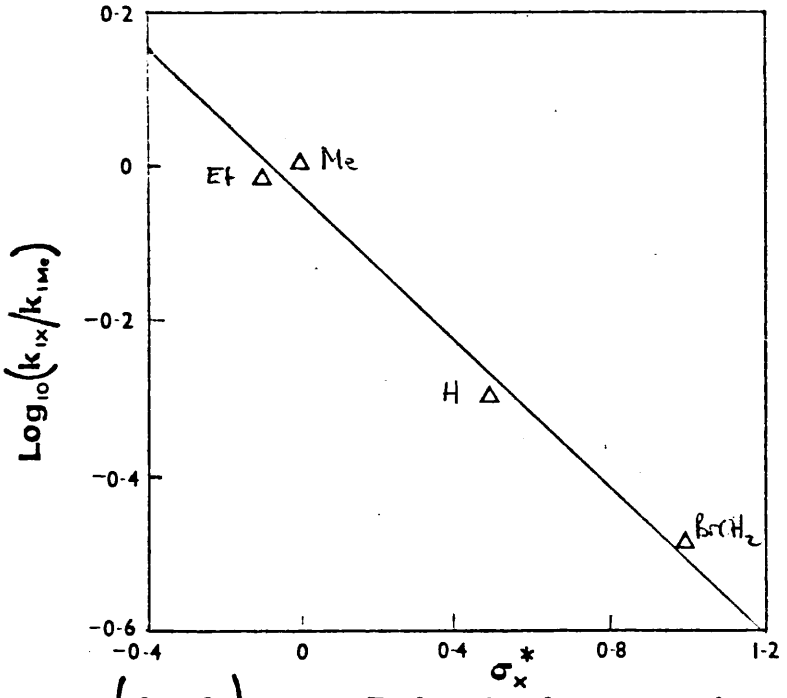

GRAPH (4-10) .....Taft plot for reactions of $C_3H_7^+$ with various nitriles.

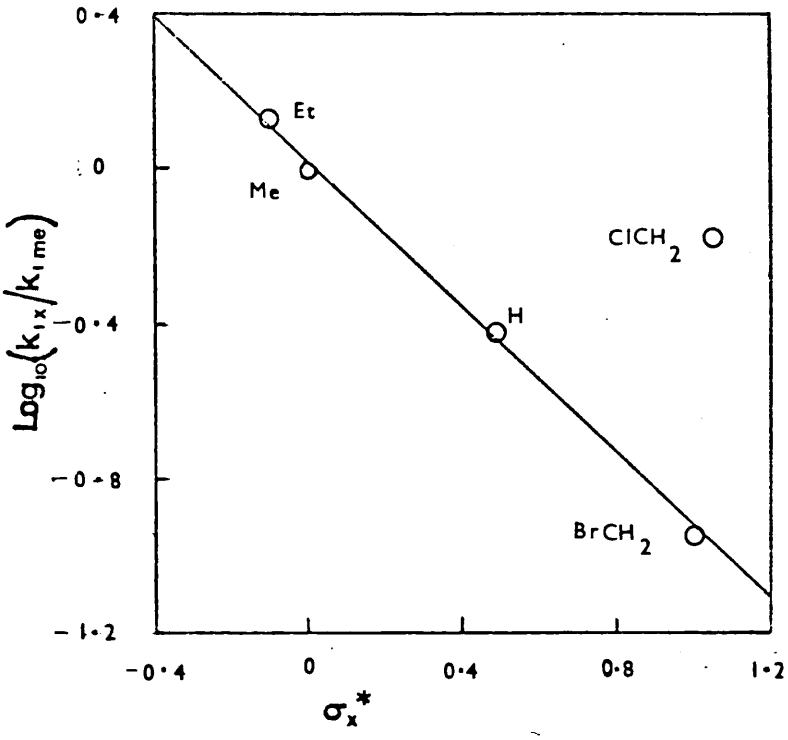

GRAPH (4-II) -- Taft plot for reactions of $C_3H_5^+$ with various nitriles.

$X=ClCH_2$ and $X=BrCH_2$ do not correlate well as the value of k_{1X} is too large. Good correlation of the data is observed (graph (4-10)) for the formation of the $(X.CH_2.CN)C_3H_7^+$ complex. In this case, however, it was not possible to obtain a value of k_{1X} for $X=ClCH_2$ (see table (4-3)). Similarly, good correlation of the data is observed (graph (4-11)) for the formation of the $(X.CH_2.CN)C_3H_5^+$ complex when X=H, CH_3, C_2H_5, or $BrCH_2$, but not when $X=ClCH_2$.

The correlations of $\log_{10}(k_{1X}/k_{1Me})$ with σ_X^* for the formation of collision complexes with reactant ions other than the three discussed above were poor. Furthermore, the values of ρ^* obtained from the lines shown in graphs (4-9) to (4-11) are much smaller than would be expected for reactions with transition states having a full positive charge (cf.anisoles, section 4.3.A).

C. Alcohols.

No correlation was found between the rate constants, k_1, for the formation of collision complexes between reactant ions, RH^+, and the alkyl alcohols.

The relative magnitudes of the rate constants for the formation of collison complexes between the RH^* ions and the halohydrins are in the reverse order to that which would be predicted from electronic considerations. This tends to suggest that the experimental rate constants are composed of rate constants for several processes. Two such processes are: attack by the RH^+ ion at (i) the hydroxyl group and (ii) the halogen atom (equations(4.3-5) and (4.3-6)).

$$RH^+ + X.CH_2.CH_2.OH \longrightarrow RH\text{-}\overset{+}{X}\text{-}CH_2.CH_2.OH \qquad (4.3\text{-}5)$$

$$RH^+ + HO.CH_2.CH_2.X \longrightarrow RH\text{-}\overset{+}{\underset{|}{O}}\underset{H}{}\text{-}CH_2.CH_2.X \qquad (4.3\text{-}6)$$

This behaviour is then similar to the situation noted above for attack by the RH^+ ion at the oxygen atoms and ring carbon atoms of the anisoles.

Despite the composite nature of the rate constants, correlations between log $(k_{1,XCH_2}/k_{1,FCH_2})$ and the substituent constant, σ_x^*, were observed for the reactant ions $C_3H_5^+$, $C_3H_6^{+\cdot}$, $C_3H_7^+$, and $C_4H_5^+$, although in these cases the signs of the reaction parameters, ρ^*, are positive (see graph (4-12)). Furthermore, similar correlations, again with positive values of ρ^*, were observed for the rate constants for the formation of $(X.XH_2.CH_2.OH)RH^+$ when X=F, Cl, and Br, and $RH^+ = C_4H_9^+$, $C_4H_8^+$, $C_4H_7^+$, $C_3H_3^+$, and $C_2H_3^+$. The rates of formation of $(I.CH_2.CH_2.OH)RH^+$ were, in all these cases, faster than that predicted by these unusual correlations.

The values of the Taft substituent constants for the X.CH - substituents were obtained from reactions which did not directly involve the halogen atoms. In reaction (4.3-5), however, the halogen atoms constitute the reactive centre of the halohydrin molecules. Hence it is to be expected that the <u>sign</u> of σ_x^* should be reversed (ie., $\sigma^*_{FCH_2} = -1.1$, etc.), so that, if reaction (4.3-5) were the only reaction occurring, then a plot of $\log(k_{1,XCH2}/k_{1,FCH2})$ against these (negative) values of σ_x^* would give a negative value of ρ^*. In view of this, the

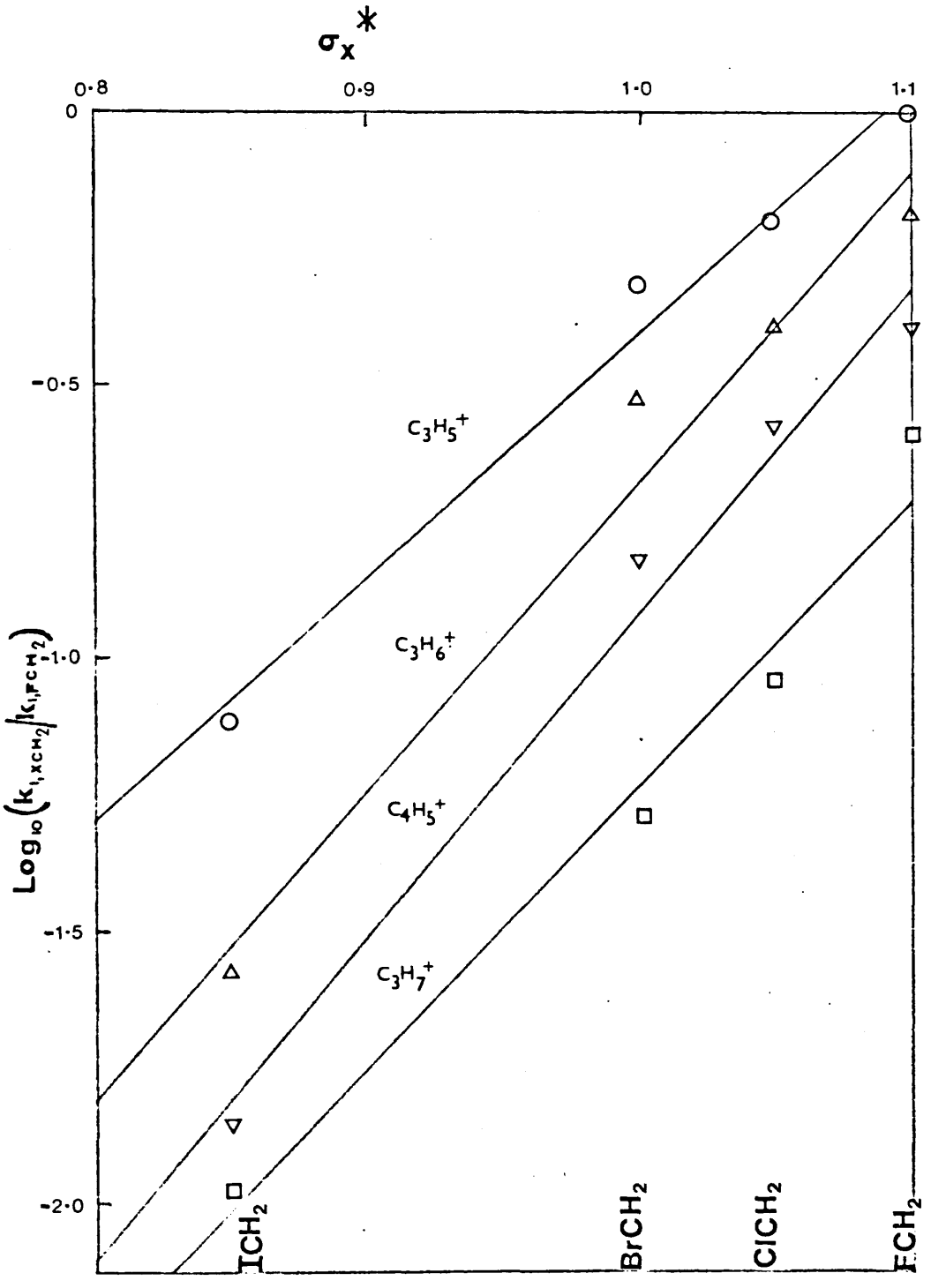

GRAPH (4-12) . ....Taft plots for reactions of various halohydrins (XCH_2CH_2OH) with the RH^+ ions.

significance of the plots given in graph (4-12) would seem to be that the slope of each line is equal to the sum of the ρ^*-values for reactions (4.3-5) and (4.3-6), the value of ρ^* for reaction (4.3-5) being positive and that for reaction (4.3-6) being negative. For example, the reaction parameter for the formation of the $(X.CH_2.CH_2.OH)C_4H_5^+$ complexes is 6.0. Hence it might be anticipated that, in this case, the value of ρ^* corresponding to attack of the hydroxyl group would be ca.-3, whilst that for attack at the halogen atoms would be ca.+9.

Data obtained by Munson [32] suggest that structural effects may influence the rates of thermoneutral, and endothermic, ion-molecule reactions, but that the rates of exothermic reactions are independent of molecular structure. Since the formation of a collision complex is certainly an endothermic process, the structural effects described in this section are to be expected.

4.4 The relative third-body efficiencies of various compounds.

Values of the rate-constant ratios k_2/k_{-1}, k_3/k_{-1} (see sections 4.2.A and 4.2.B) and k_4/k_{-1} (see section 4.2.C) represent the efficiencies with which various compounds act as third-bodies in reactions (4.2-5), (4.2-6), and (4.2-23). These values may be normalized with respect to the value of k_2/k_{-1} appropriate to the reaction in question (eg., $k_4/k_{-1} \div k_2/k_{-1}$). The values obtained (denoted by k_T) are third-body efficiencies relative to that of the compound (M), and are listed in table (4-15).

Experiments with the acetone/CCl_4 mixture were carried out using four different, but constant, pressures of acetone. The four values of k_T, obtained for each of the reactant ions, are in fair agreement with each other. The values obtained from experiments in which the lowest acetone pressure (1.3×10^{-3} torr) was used are, in some cases, at variance with the other values*. Similarly, values of k_T obtained from experiments with the acetone/H_2O mixture, for which two different acetone pressures were employed, are also, in general, in good agreement with one another.

The third-body efficiency of isobutane (measured with M = acetone) is much lower than that of either water or carbon

---

* The differences probably reflect errors involved in the determination of the quantity denoted by s (section 4.2.C).

Table (4-15)
Relative third-body efficiencies of water, carbon tetrachloride, and isobutane.

Mixture	Temp. (°C)	Isobutane pressure (torr)	Pressure of first component (torr)	k_T $C_4H_9^+$	$C_4H_8^+$	$C_4H_7^+$	$C_3H_6^+$	$C_3H_5^+$	$C_2H_5^+$	$C_2H_3^+$
(Acetone + isobutane)	175	-	-	1.6×10^{-3}						
Acetone + CCl_4	163	0.102	1.3	0.25±0.10	0.64±0.08	0.95±0.24	1.74±0.35	2.83±0.35	S*	1.88±0.37
	163	0.102	2.5	0.57±0.17	0.68±0.10	0.96±0.24	1.10±0.19	1.71±0.26	S	2.02±0.43
	162	0.102	3.8	0.62±0.19	0.65±0.08	0.87±0.22	1.48±0.26	1.77±0.25	S	1.96±0.47
	161	0.102	5.1	0.56±0.19	0.62±0.10	0.85±0.23	1.05±0.19	1.63±0.23	S	S
Acetone + H_2O	174	0.105	3.2	0.32±0.08	0.25±0.03	0.31±0.07	0.15±0.03	0.17±0.02	0.71±0.42	0.29±0.09
	174	0.105	7.0	0.32±0.44	0.23±0.04	0.30±0.07	0.18±0.03	0.14±0.02	0.56±0.46	0.18±0.10
Anisole + CCl_4	174	0.089	4.7	1.81±0.32						
Anisole + H_2O	175	0.113	4.7	1.00±0.08						
4-Fluoro-anisole + CCl_4	174	0.112	4.8	2.25±0.54						
Acetone + CCl_4		(mean values)		0.58±0.20†	0.65±0.10	0.91±0.25	1.21±0.32†	1.70±0.28		1.95±0.47
Acetone + H_2O		(" ")		0.32±0.37	0.24±0.04	0.31±0.08	0.17±0.04	0.16±0.03	0.64±0.52	0.24±0.13

* S: Computation was not carried out as data was badly scattered.

† Average of 3 values.

tetrachloride, while that for acetone (k_T= 1.0 by definition) is larger than the other values of k_T. It should be noted that reaction (4.2-5)

$$MRH^{+*} + M \longrightarrow \text{products} \qquad (4.2\text{-}5)$$

may include, in addition to the collision-induced decomposition of MRH^{+*}, a symmetric 'switching' reaction. For example, in a study of the effects of various third-bodies on the rate of reaction (4.4-1),

$$(CH_3.CO.CH_3)H^+ + CH_3.CO.CH_3 \longrightarrow (CH_3.CO.CH_3)_2H^+ \qquad (4.4\text{-}1)$$

Miasek and Harrison [78] found that acetone itself possessed a much higher efficiency than any other gas, and attributed this apparent enhanced efficiency to the presence of a switching reaction. The figures given in table (4-15) show, however, that, for the reactions between acetone and the $C_3H_6^+$, $C_3H_5^+$, and $C_3H_3^+$ ions, the value of k_T for carbon tetrachloride is larger than that for acetone itself. In these cases then, if not all, it seems that the effects of switching reactions are insignificant.

Carbon tetrachloride has a greater third-body efficiency than water in all the reactions studied. Anicich and Bowers[66] found that, for the reaction

$$CH_2.CF_2^+ + CH_2.CF_2 + T \longrightarrow C_4H_4F_4^+ + T \qquad (4.4\text{-}2)$$

there was a linear correlation of the efficiency of various third-bodies (nitrogen, carbon monoxide, and the inert gases) with the square root of the reduced mass ($\mu^{\frac{1}{2}}$) of the colliding pair. Furthermore, the third-body efficiency of 1,1-difluoroethene

itself was also well correlated with $\mu^{\frac{1}{2}}$, suggesting that, in this system also, a switching reaction did not occur. The existence of a linear correlation of third-body efficiency with $\mu^{\frac{1}{2}}$ indicates that the former is determined by the collision duration, t, which is given by (cf.,equation (3.1-8))

$$t = 273(\alpha\mu)^{\frac{1}{2}}\, dp/10546ET \qquad (4.4\text{-}3)$$

where d is the interaction distance. Plots of the values of k_T for water, acetone, and carbon tetrachloride against $\mu^{\frac{1}{2}}$, associated with reaction (4.4-4)

$$(CH_3.CO.CH_3)RH^+ + T \longrightarrow \text{products} \qquad (4.4\text{-}4)$$

are given in graph (4-13). Here RH^+ represents the $C_4H_7^+$, $C_4H_8^{\cdot+}$, and $C_4H_9^+$ ions. Although the paucity of data renders the significance of these plots questionable, there does seem to be a linear correlation of k_T with $\mu^{\frac{1}{2}}$ for T = H_2O, CCl_4, but not for T = $CH_3.CO.CH_3$ (vide supra). The value of k_T (0.002) for T = isobutane, and $RH^+ = C_4H_9^+$ is obviously not correlated with the other data. The reason for this result is, as yet, not explicable. Similarly correlations of k_T with $\mu^{\frac{1}{2}}$ were not observed with $RH^+ = C_2H_3^+$, $C_3H_5^+$, and $C_3H_6^{\cdot+}$ (see table (4-15))

In addition to the above results for reaction (4.4-4) a linear correlation of k_T (T = H_2O, CCl_4) with $\mu^{\frac{1}{2}}$ is also found for the reaction

$$MC_4H_9^+ + T \longrightarrow \text{products} \qquad (4.4\text{-}5)$$

where M = anisole (see graph (4-14)). Furthermore, the value of k_T corresponding to reaction (4.4-5) with M = 4-fluoroanisole and T = CCl_4 correlates well with the data for M = anisole.

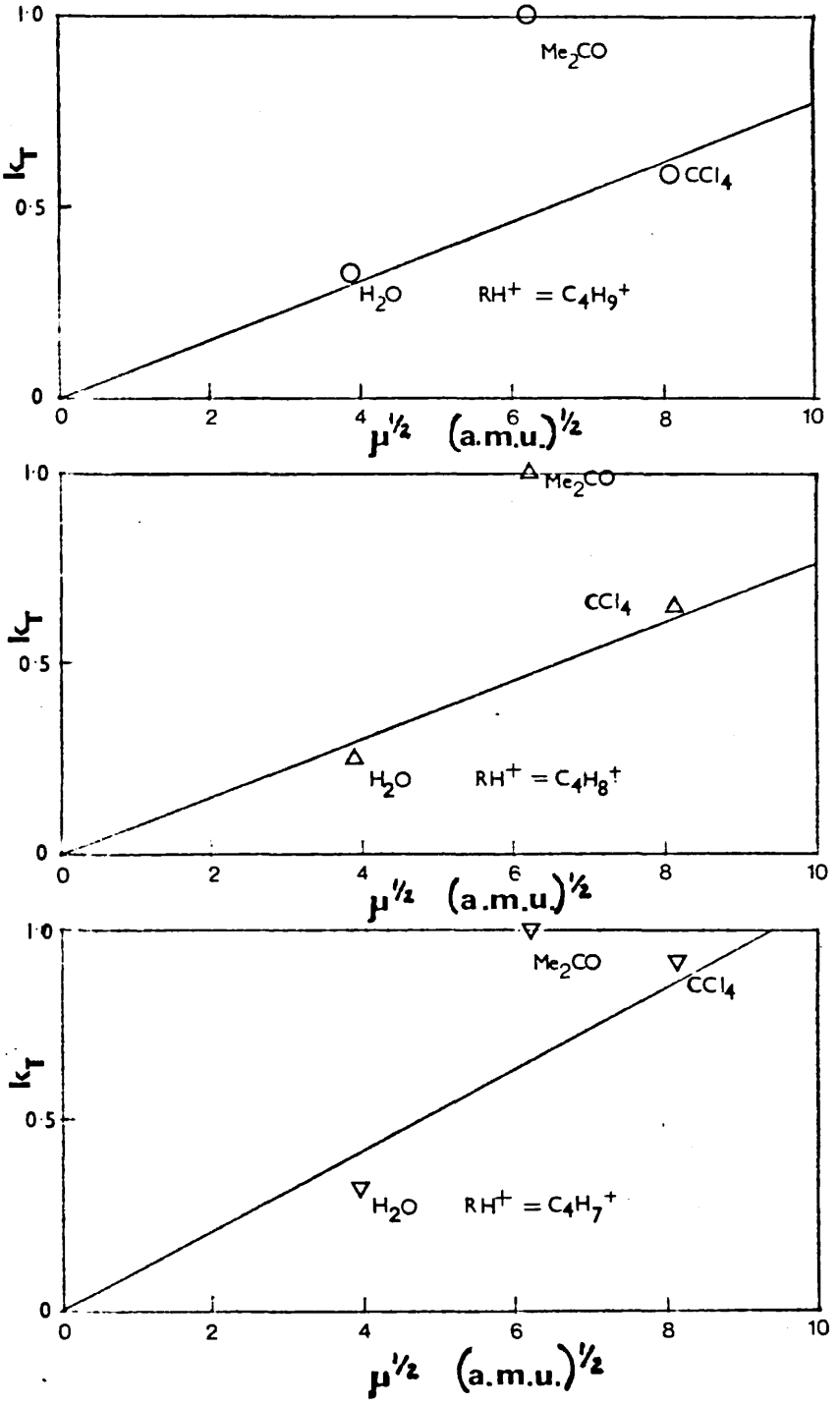

GRAPH (4-13). Plots of k_T against $\mu^{1/2}$ (M = Acetone)

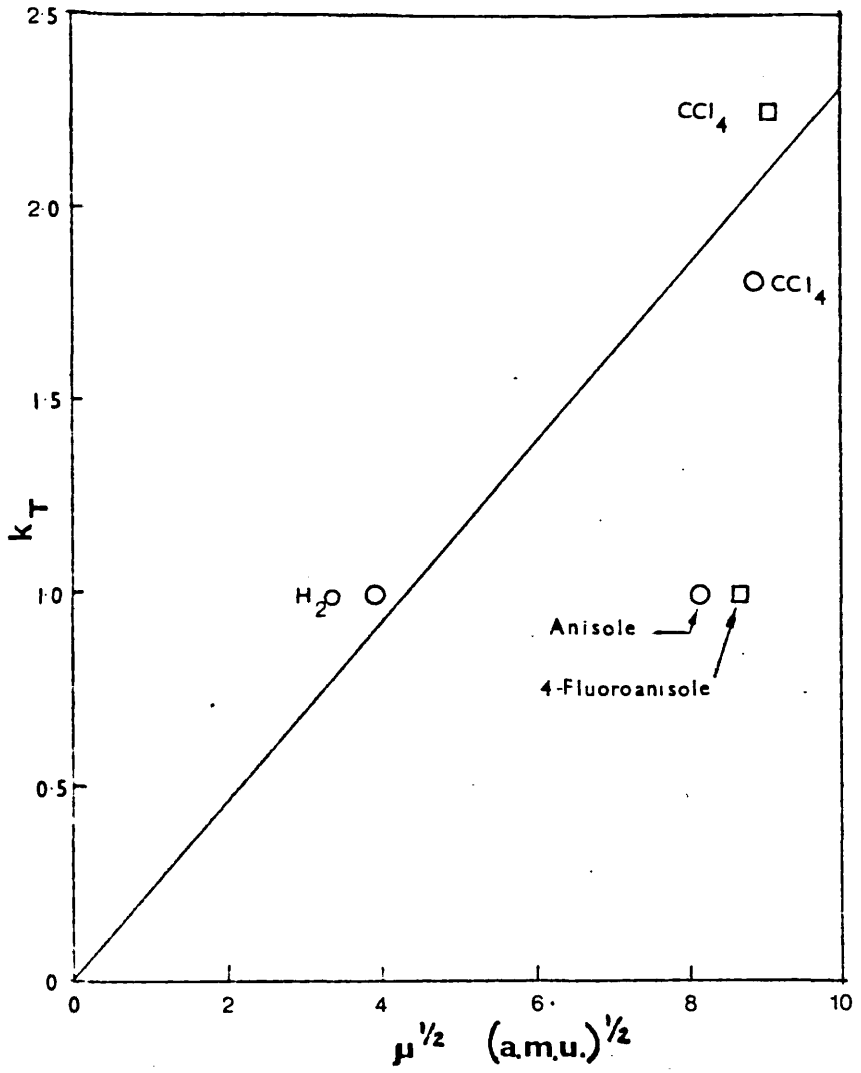

GRAPH (4-14). Plot of k_T against $\mu^{1/2}$ (M=Anisole or 4-Fluoroanisole).

In these cases, however, values of k_T corresponding to the reaction

$$MC_4H_9^+ + M \longrightarrow \text{products} \qquad (4.4\text{-}6)$$

where T = M (anisole or 4-fluoroanisole), and $k_T = 1$, were not correlated with the other data. No explanation of this behaviour can be offered.

Values of k_T for the reaction

$$(CH_3.CO.CH_3)RH^+ + CCl_4 \longrightarrow \text{products} \qquad (4.4\text{-}7)$$

decrease with increase of the mass of the RH^+ ion. It is likely that the stability of a collision complex will increase as the number of normal modes of vibration available to the complex increases since the internal energy of the ion is distributed among them. Hence the rate of reaction (4.4-7), relative to the similar reaction in which acetone is the third-body, will decrease as the number of vibrational modes of the complex increases. Graph (4-15) shows that there is an approximately linear correlation of log k_T with the number of vibrational modes available to the complex. No such correlation of the values of k_T for the reaction

$$(CH_3.CO.CO_3)RH^+ + H_2O \longrightarrow \text{products} \qquad (4.4\text{-}8)$$

is, however, observed.

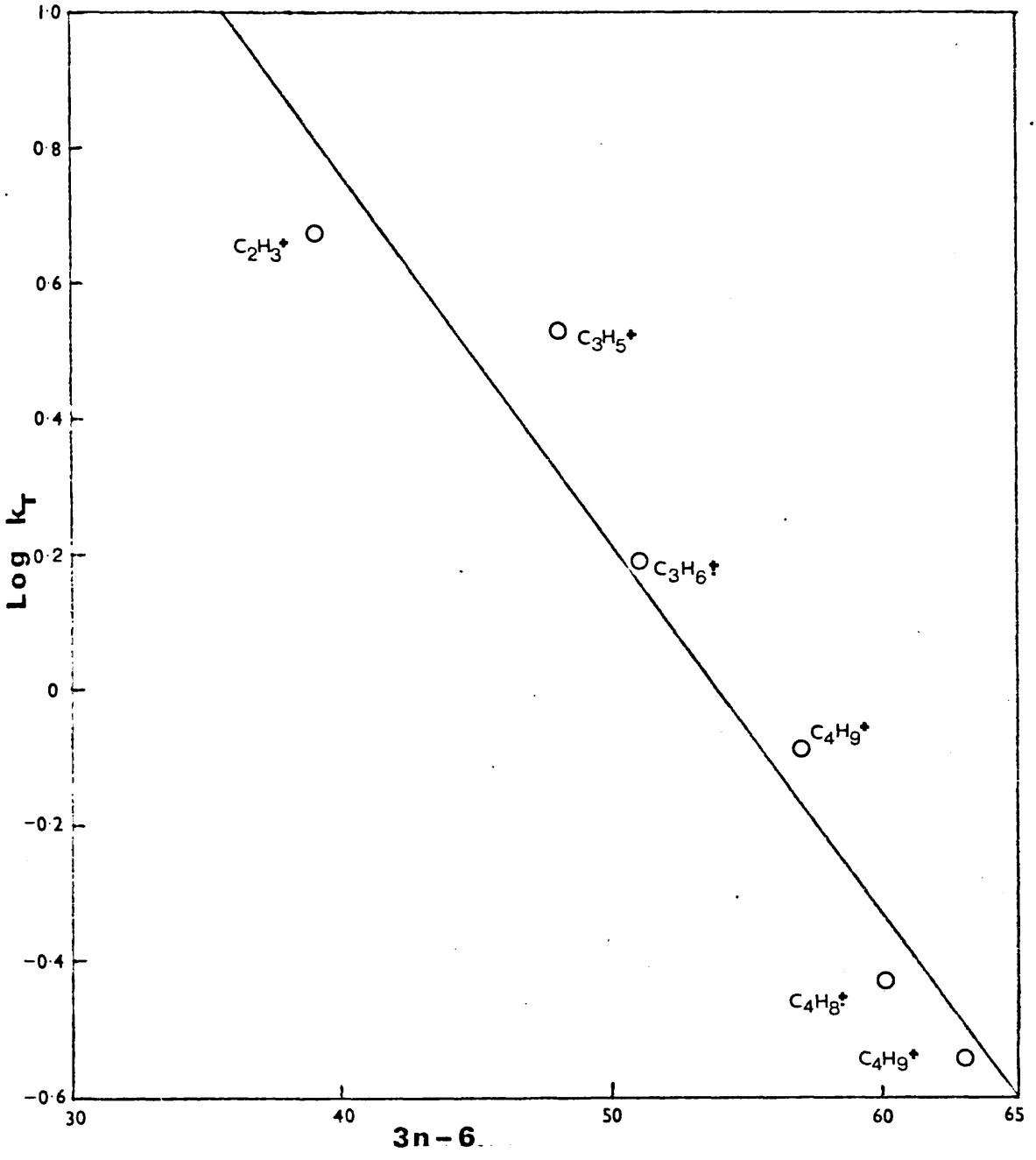

GRAPH (4-15). Plot of log k_T against number of normal modes of vibration available to complex

4.5 Conclusions.

The interpretation of chemical-ionization mass spectra of known compounds, and the determination of structures of unknown compounds from their chemical-ionization mass spectra, require good chemical intuition. The development of the appropriate intuition proceeds from the acquisition of a large body of general information about ion-molecule reactions, and of ion-molecule reactions in chemical-ionization mass spectrometry in particular. In 1976 Munson [32] pointed out that whereas most of the compounds being analyzed by chemical-ionization mass spectrometry were species possessing high molecular weights and considerable structural complexity, the compounds selected for ion-molecule-reaction studies were generally simple. This situation persists. Information is required concerning the rates and mechanisms of chemical-ionization processes, the energy transfer in these processes, and the relative reactivity of functional groups. The compilation of such a body of data logically begins with small, relatively simple molecules, and proceeds until sufficient data has been acquired to allow extrapolations to complex molecules to be made. It is hoped the the work presented in this thesis constitutes the beginning of the construction of such a body of data.

Prior to the evaluation of rate constants for chemical-ionization processes, it was necessary first to evaluate mean residence times of reactant ions in the ion-source. This was carried out by initially studying the reaction between the methane molecular ion-radical and methane, for which the rate constant is

well established. A kinetic study of the ion-molecule reactions consequent upon the electron-impact ionization of isobutane was then undertaken. Significantly it was found that whilst the residence times of ions generated from methane are independent of methane pressure, those of ions generated from isobutane showed a variation with isobutane pressure. This suggested that, for the experimental conditions employed, these ion residence times were subject to ion-mobility considerations. Both kinetic studies resulted in the development of simple methods of estimation of reagent-gas pressures.

The chemical-ionization mass spectra of various organic sample compounds were studied. It was established that the abundances of ions produced from them depended critically upon the sample pressure. Furthermore, it was observed that the abundances of ions produced from acetone were also dependent upon the isobutane pressure.

Kinetics of reactions between the isobutane reactant ions, RH^+, and various organic compounds were studied by observing the decrease of relative abundance of the reactant ions as the sample pressure was increased whilst maintaining a constant isobutane pressure. Although some of these ion-molecule reactions appeared to be simple bimolecular processes, others proceeded by a more complicated mechanism. For the latter group, the experimental data was shown to be consistent with a mechanism involving reversible formation of a collision complex followed by collision-induced decomposition to products (see reactions

(4.2-4) to (4.2-6)). The third-body essential to the collision-induced decomposition reaction of the complex could be a molecule of the sample, of isobutane, or of some compound (eg., CCl_4 or H_2O) deliberately introduced into the system to act as a third body. It was established that, for the reaction between the $C_4H_9^+$ ion and acetone, the third-body efficiency of isobutane was several hundred times lower than that of acetone itself. Furthermore, it was found that the third-body efficiency of carbon tetrachloride was generally greater than that of water, and it was tentatively suggested that the third-body efficiencies of these compounds were proportional to the collision durations.

The kinetic data was used to obtain the rate constant for formation of the collision complexes (k_1) and the ratio of rate constants for the decomposition reactions of the complexes (k_2/k_{-1}). Comparison of the values of k_1 with collision frequencies calculated from the Average-Dipole-Orientation theory showed that most of the reactions proceeded at rates considerably lower than the collision rate. By assuming that all collisions of the complex with a third body result in reaction, it was shown that the lifetimes of the collision complexes were generally in the range 1 - 10 μsec.

Kinetic data corresponding to the reactions between $C_4H_9^+$ and various substituted anisoles was found to be consistent with a mechanism in which the MH^+ species are formed via collision complexes, but the $M^{+\cdot}$ ions arise from direct charge-transfer reactions. Rate constants for the charge-transfer reactions

(k_o) were found to correlate with with the Hammett substituent constants, σ_x, showing that structural effects influence the rates of reaction of the anisoles. The rate constants for complex formation (k_1) did not correlate with σ_x. However, it was considered that the $C_4H_9^+$ ions might attack these aromatic molecules either at the methoxy oxygen atom or at one of the ring carbon atoms. By assuming that the rate of attack at the oxygen atom was the same for all the anisoles, and that attack at the aromatic nucleus did not occur in 4-fluoroanisole, it was shown that the rates of attack at ring carbon atoms in the other anisoles are correlated with σ_x.

Correlations between the rate constants for the formation of the collision complexes $(X.CH_2.CH_2.OH)RH^+$, where X=F,Cl,Br,I, and the Taft substituent constant, σ_x^*, were also found. The formation of these complexes can, however, occur in at least two ways; either by attack at the hydroxyl group or by attack at the halogen atom. In consequence, it was not possible, here, to obtain rate constants for the individual processes. Whilst the relative magnitudes of rate constants for the formation of collision complexes between RH^+ and other compounds suggested that structural effects are important, no other definitive correlations with substituent constants were found.

The mechanism proposed for the reactions which give rise to isobutane chemical-ionization mass spectra differs from the mechanism favoured by Field [56]. The two proposals were reconciled by the suggestion that the mechanism of these

reactions is critically dependent upon sample pressure. Thus a mechanism similar to that proposed by Harrison[57] for the reaction of $C_3H_5^+$ with ethylene was suggested for these reactions; the collision complex is formed reversibly and then undergoes either a unimolecular decomposition, or a collision induced decomposition, to products. For low sample pressures the unimolecular decomposition reaction of the complex is the dominant reaction, whereas, as the sample pressure is increased, the collision-induced decomposition reaction becomes more important. The implication of such a mechanism is that, as the sample pressure is increased, the overall kinetic order of the reaction changes from second to third order, and then, at comparatively high sample pressures, reverts to second order. Sample pressures employed in the present work were in the region where the transition from overall third- to overall second-order kinetics is observed.

The results presented in this study suggest that caution should be exercised when a compound is analyzed by chemical-ionization mass spectrometry. The presence of small quantities of impurities (eg., water) in the sample may have a significant effect upon the spectrum, even though the impurities do not themselves react with the isobutane reactant ions. Furthermore, exact comparison of spectra is only possible if the conditions under which spectra are recorded are known. In particular a knowledge of both sample and reagent-gas pressures, of repeller voltage and electric-field strength, and of ion-source-

block temperature, is required. However, given spectra of pure compounds, obtained under known conditions, the effects of molecular structure upon reaction rates may be of significant use in the general area of structure determination, particularly when it is required to distinguish between closely related isomers. Investigations of a similar kind have been commenced by Munson[32], who has been able to show that the isobutane chemical-ionization mass spectra of the cis- and trans-1,4-cyclohexanediols are sufficiently different for these compounds to be distinguished from one another. There is, however, a great deal of work to be done before generalizations may be made concerning relationships between spectra and molecular structure.

It is obvious from the foregoing discussion that a great deal of useful work on the ion-molecule reactions associated with chemical-ionization mass spectrometry remains to be done. Further investigation of the kinetics and mechanisms of these reactions should be undertaken with a view to studying the spectra of molecules possessing considerable degrees of complexity. A deeper understanding of the factors influencing third-body efficiencies is required, especially as it may be possible to enhance the relative abundances of product ions in spectra by adding compounds like carbon tetrachloride to samples. Furthermore, a body of data on the relationships between spectra and molecular structure will provide novel techniques for structure determination.

APPENDIX I

Polarizabilities and dipole moments.

Polarizabilities and dipole moments used in the calculation of collision frequencies (see appendix III) are listed in table (A-1). The polarizabilities of most of the compounds were computed by the Lippincott delta-function method [79]. The accuracy of this method is generally better than 5%. The polarizabilities of water, carbon tetrachloride, methanol, and the two ketones were obtained from tables [80].

Dipole moments were found from tables [81]. Where possible, values obtained from measurements made on the compound in the gas-phase were employed. In a few cases, however, gas-phase measurements had not been carried out and the dipole moments were taken from measurements made on a solution of the compound in benzene.

Table (A-1)

Polarizabilities and dipole moments of various compounds.

Compound	Polarizability (α) ($\AA^3$)	Dipole moment (μ_D) (Debye)
Acetone	6.33*	2.88
Ethyl methyl ketone	8.13*	2.77
Acetonitrile	4.14	3.92
Propionitrile	5.94	4.02
Butyronitrile	7.75	4.07
Anisole	10.95	1.38
4-Fluoroanisole	10.99	2.11†
4-Methylanisole	12.76	1.24†
Methanol	3.23*	1.70
1-Propanol	6.68	1.68
2-Propanol	6.68	1.66
1-Pentanol	10.30	1.66†
1-Hexanol	12.11	1.73†
2-Chloroethanol	6.88	1.78
2-Bromoethanol	8.46	2.18†
Carbon tetrachloride	10.5*	0
Water	1.45*	1.85

* Value found from tables [80]

† Measurement made on a benzene solution of the compound.

APPENDIX II

Curve-fitting procedure.

For the set of data points (x_i, f_i) it is required to find a set of parameters a_k $(k = 1,2,\ldots,r)$ in the function $f = f(x,a)$ (where a represents the set a_k) such that the best fit in the least-squares sense is obtained. Thus it is required to minimize the function

$$S = \sum_i (f(x_i,a) - f_i)^2 \qquad \text{(A.II-1)}$$

Since for a minimum

$$\frac{dS}{da_k} = 0 \ , \ k = 1,2,\ldots r \qquad \text{(A.II-2)}$$

therefore

$$\sum_i (f(x_i,a)-f_i)\left(\frac{\partial f(x_i,a)}{\partial a_k}\right) = 0 \ , \ k = 1,2,\ldots,r. \qquad \text{(A.II-3)}$$

This set of r equations is the set of <u>normal</u> equations.

The function $f(x,a)$ may be expanded as a Taylor series about $\bar{a}$, a set of approximate parameters. If $a = \bar{a} + \Delta a$, then

$$f(x,a) \simeq f(x,a) + \sum_k \left(\frac{\partial f(x,\bar{a})}{\partial a_k}\right) \Delta a_k \qquad \text{(A.II-4)}$$

where terms higher than first-order have been neglected. The approximate residuals, and hence the normal equations, are linear in the Δa_k. Substituting equations (A.II-4) into equations (A.II-3) and rearranging gives

$$\sum_{k'} \left[\sum_i \frac{\partial f(x_i,\bar{a})}{\partial a_{k'}} \frac{\partial f(x_i,\bar{a})}{\partial a_{k'}}\right] \Delta a_{k'} = \sum_i \left[f_i - f(x_i,\bar{a})\right] \frac{\partial f(x_i,\bar{a})}{\partial a_k}, \ k=1,2,\ldots,r \qquad \text{(A.II-5)}$$

The solution of this set of equations for each of the Δa_k leads to an improved set of parameters, $\bar{a} + \Delta a$. This process is then iterated in order to minimize S.

Now, equation (4.2-22) may be written

$$L(p_M,p,\gamma,\theta,\phi) = \gamma p_M p\left[\frac{\theta p_M + \phi p}{1 + \theta p_M + \phi p}\right] \qquad \text{(A.II-6)}$$

where $L = -\log (I_{57}/I^{o}_{57})$, and the other symbols are as defined in section 4.2.B. The function $\bar{L}\ (p_M,p,\bar{\gamma}\ \bar{\theta}\ \bar{\phi})$ may be defined by

$$\bar{L} = \gamma p_M p\left[\frac{\bar{\theta} p_M + \bar{\phi} p}{1 + \bar{\theta} p_M + \bar{\theta} p}\right] \qquad \text{(A.II-7)}$$

where $\bar{\gamma},\bar{\theta}$, and $\bar{\phi}$ are approximate values of γ,θ, and ϕ respectively. The normal equations are corresponding to the above function are

$$\sum_i \left[\left(\frac{\partial \bar{L}}{\partial \gamma}\right)^2 \Delta\gamma + \frac{\partial \bar{L}}{\partial \gamma}\frac{\partial \bar{L}}{\partial \theta}\Delta\theta + \frac{\partial \bar{L}}{\partial \gamma}\frac{\partial \bar{L}}{\partial \phi}\right]\Delta\phi = \sum_i (L_i - \bar{L})\frac{\partial \bar{L}}{\partial \gamma} \qquad \text{(A.II-8)}$$

$$\sum_i \left[\frac{\partial \bar{L}}{\partial \theta}\frac{\partial \bar{L}}{\partial \gamma}\Delta\gamma + \left(\frac{\partial \bar{L}}{\partial \theta}\right)^2 \Delta\theta + \frac{\partial \bar{L}}{\partial \theta}\frac{\partial \bar{L}}{\partial \phi}\right]\Delta\phi = \sum_i (L_i - \bar{L})\frac{\partial \bar{L}}{\partial \theta} \qquad \text{(A.II-9)}$$

$$\sum_i \left[\frac{\partial \bar{L}}{\partial \phi}\frac{\partial \bar{L}}{\partial \gamma}\Delta\gamma + \frac{\partial \bar{L}}{\partial \phi}\frac{\partial \bar{L}}{\partial \theta}\Delta\theta + \left(\frac{\partial \bar{L}}{\partial \phi}\right)^2\right]\Delta\phi = \sum_i (L_i - \bar{L})\frac{\partial \bar{L}}{\partial \phi} \qquad \text{(A.II-10)}$$

in which i = 1 to n, where n is the number of data points. Equations (A.II-8) to (A.II-10) can be solved for $\Delta\gamma,\Delta\theta$, and $\Delta\phi$ after initial values of γ,θ, and ϕ ($\bar{\gamma},\bar{\theta}$, and $\bar{\phi}$) have been chosen. The sums $\bar{\gamma} + \Delta\bar{\gamma}$, $\bar{\theta} + \Delta\theta$, and $\bar{\phi} + \Delta\phi$ are then formed and these sums are substituted back into the equations (as $\bar{\gamma}$, $\bar{\theta}$, $\bar{\phi}$). The process is repeated until self-consistency is attained. The values of γ, θ, and ϕ so obtained can, of course, be used to give calculated values of L as p_M and p are varied. In this way a surface may be fitted to the appropriate experimental data (see section 4.2.B).

Equation (4.2-22) is a generalization of equation (4.2-16). The latter equation was obtained from kinetic analysis of the mechanism proposed in reactions (4.2-4) and (4.2-5), and applies

to observed curved decreases of log (I_n/I_n°) discussed in section 3.3. Curve fitting to the experimental data corresponding to the reactions of the isobutane reactant ions with various compounds was carried out using the method described above. In these cases the normal equations are (A.II-8) and (A.II-9) with $\Delta\phi=0$, and with $\bar{L}$ replaced by

$$\bar{L} = \frac{\bar{\gamma}\bar{\theta}p_M^2}{1+\bar{\theta}p_M} \qquad \text{(A.II-11)}$$

APPENDIX III

Collision frequencies.

Collision frequencies were calculated using the average-dipole-orientation theory of Su and Bowers . Since the energies of the reactant ions, RH^+, are considerably larger than thermal, the appropriate equation is

$$k_c = 2\pi e \left[\left(\frac{\alpha}{\mu}\right)^{\frac{1}{2}} + \frac{C\mu_D}{\mu v}\right] \qquad (4.2\text{-}62)$$

where μ and μ_D are respectively the angle-averaged polarizability and dipole moment of the molecule, e is the electronic charge, μ is the reduced mass of the ion and the molecule, and v is the mean drift velocity of the ion. The latter quantity was calculated from the ion-mobility (estimated from the expression given by Ridge and Beauchamp) using the equation (see section 3.1).

$$v = kE \qquad (3.1\text{-}5)$$

where E is the electric-field strength. Values of k_c obtained from equation (4.2-62) are listed in the following tables.

Table (A-2)

Collision frequencies for the reaction $RH^+ + M \longrightarrow$ Products, where RH^+ represents an isobutane reactant ion.

Compound* (M)	A.D.O. rate constant (10^{10}x cm^3 $molecule^{-1}$ sec^{-1})									
	$C_4H_9^+$	$C_4H_8^+$	$C_4H_7^+$	$C_4H_5^+$	$C_3H_7^+$	$C_3H_6^+$	$C_3H_5^+$	$C_3H_3^+$	$C_2H_5^+$	$C_2H_3^+$
Acetone	18.44	18.53	18.61	18.79	19.90	20.04	20.18	20.48	22.49	23.04
Ethyl Methyl ketone	17.97	18.06	18.16	18.35	19.58	19.73	19.89	20.22	22.42	23.02
Acetonitrile	22.99	23.06	23.14	23.30	24.33	24.46	24.59	24.87	26.79	27.32
Propionitrile	21.93	22.03	22.12	22.33	23.60	23.75	23.91	24.26	26.57	27.20
Butyronitrile	21.84	21.95	22.06	22.47	23.77	23.95	24.14	24.54	27.18	27.89
Anisole	16.16									
4-Fluoroanisole	19.18									
4-Methylanisole	15.73									

* Isobutane pressures and ion-source-block temperatures are given in tables (4-2) and (4-3).

Table (A-3)

Collision frequencies for the reaction $RH^+ + M \longrightarrow$ products, where RH^+ represents an isobutane reactant ion.

Compound* (M)	A.D.O. rate constant (10^{10}x cm^3 $molecule^{-1}$ sec^{-1})									
	$C_4H_9^+$	$C_4H_8^+$	$C_4H_7^+$	$C_4H_5^+$	$C_3H_7^+$	$C_3H_6^+$	$C_3H_5^+$	$C_3H_3^+$	$C_2H_5^+$	$C_2H_3^+$
Methanol	15.27	15.31	15.35	15.44	16.01	16.08	16.15	16.31	17.39	17.69
1-Propanol	14.63	14.70	14.76	14.91	15.81	15.92	16.03	16.27	17.90	18.34
2-Propanol	14.61	14.67	14.74	14.89	15.78	15.89	16.00	16.25	17.87	18.31
1-Oentanol	14.97	15.05	15.14	15.32	16.42	16.55	16.69	16.98	18.94	19.47
1-Hexanol	15.64	15.73	15.82	16.02	17.24	17.39	17.54	17.87	20.02	20.60
2-Chloroethanol	13.98	14.06	14.13	14.30	15.30	15.42	15.55	15.81	17.60	18.08
2-Bromoethanol	14.57	14.66	14.76	14.97	16.22	16.37	16.53	16.86	19.06	19.65
Carbon tetrachloride	11.77	11.84	11.92	12.09	13.09	13.21	13.34	13.60	15.36	15.83
Water	18.42	18.43	18.44	18.48	18.70	18.73	18.76	18.83	19.36	19.52

* Isobutane pressures and ion-source-block temperatures for experiments with the alcohols are given in tables (4-4) and (4-5). For carbon tetrachloride and water these conditions are given in section 3.3.E.

Table (A-4)

Collision frequencies for the reaction MRH^{+*} + M ⟶ Products, where RH^{+} represents an isobutane reactant ion.

Compound (M)	A.D.O. rate constant (10^{10}x cm^3 $molecule^{-1}$ sec^{-1})								
	$C_4H_9^+$	$C_4H_8^+$	$C_4H_7^+$	$C_4H_5^+$	$C_3H_7^+$	$C_3H_6^+$	$C_3H_5^+$	$C_2H_5^+$	$C_2H_3^+$
Acetone	15.93	15.95	15.98	16.01	16.29	16.32	16.35	16.81	16.84
Ethyl methyl ketone	14.80	14.80	14.84	14.86	15.13	15.16	15.19	15.59	15.62
Acetonitrile	21.15	21.18	21.21	21.24	21.59	21.63	21.66	22.19	22.30
Propionitrile	19.15	19.18	19.22	19.26	19.59	19.62	19.66	20.15	20.26
Butyronitrile	18.14	18.16	18.19	18.22	18.55	18.59	18.62	19.08	19.18
Methanol	14.42	14.44	14.46	14.48	14.71	14.73	14.75	15.11	15.19
1-Propanol	12.55	12.57	12.59	12.63	12.84	12.86	12.88	13.21	13.27
2-Propanol	12.53	12.55	12.57	12.61	12.82	12.84	12.86	13.18	13.25
1-Pentanol	11.80	11.82	11.84	11.87	12.05	12.07	12.09	12.32	12.39
1-Hexanol	11.89	11.90	11.93	11.95	12.12	12.14	12.16	12.38	12.45
2-Chloroethanol					11.49				
Anisole	12.02								
4-Fluoroanisole	13.25								
4-Methylanisole	11.33								

REFERENCES

1. Beynon, J.H., Mass Spectrometry and Its Applications to Organic Chemistry, Elsevier, Amsterdam (1960).

2. Kiser, R.W., Introduction to Mass Spectrometry and Its Applications, Prentice-Hall, Englewood Cliffs, New Jersey (1965).

3. McFadden, W.H.,Techniques of Combined Gas Chromatography/ Mass Spectrometry, Wiley-Interscience, New York (1972)

4. La Lau, C., in Topics in Organic Mass Spectrometry, Burlingame,A.L.,Ed., Wiley-Interscience, New York (1969), p.93.

5. Thomson, J.J., Phil.Mag., 24, 209 (1912).

6. Dempster, A.J., Phil-Mag., 31, 438 (1916)

7. Hogness, T.R., and Lunn, E.G., Phys. Rev., 26, 44 (1925)

8. Smyth, H.D., Phys. Rev., 25, 452 (1925).

9. Smyth, H.D., Rev. Mod.Phys., 3, 347 (1931)

10. Hogness, T.E., and Harkness, R.W., Phys.Rev., 32, 784 (1928)

11. Eyring,H., Hirshfelder, J.O., and Taylor, H.S., J. Chem.Phys., 4, 479 (1936)

12. Stevenson, D.P., and Schissler, D.O., J.Chem.Phys., 29, 282 (1958).

13. Stevenson, D.P., and Schissler, D.O., J.Chem.Phys., 23, 1353 (1955).

14. Field, F.H., Franklin, J.L., and Lampe, F.W., J.Amer.Chem.Soc., 79, 2419 (1957)

15. Tal'roze, V.L., and Lyubimova, A.K., Dokl.Akad.Nauk, SSSR, 86, 909 (1952).

16. Field, F.H., and Lampe, F.W., J.Amer.Chem.Soc., 80, 5587 (1958).

17. Kebarle, P., NATO Adv. Study Inst. Ser., Ser.B., B.6. (Interact. Ions.Mol.), Ausloos, P., Ed., Plenum Press, New York (1975), p.459.

18. Borkowski, R.P., and Ausloos, P., J.Chem.Phys, 39, 818 (1963).

19. Su,T., and Bowers, M.T., J.Chem.Phys., 58, 3027 (1973). see also Su,T., and Bowers, M.T., Int.J.Mass Spectrom. Ion Phys., 12, 347 (1973), ibid. 17,211 (1975).

20. Hayhurst, A.N., Telford, N.R., Combust. Flame. 28,67 (1977)

21. Lias, S.G., and Ausloos, P., Ion-Molecule Reactions, American Chemical Society, Washington, D.C. (1975).

22. Ferguson, E.E., NATO Adv. Study Inst. Ser., Ser.B., B.6. (Interact. Ions.Mol.), Ausloos, P., Ed., Plenum Press, New York (1975), p.313.

23. J. Taylor, personal communication.

24. Grimsrud, E.P., and Kebarle, P., J. Amer.Chem.Soc., 95, 7939 (1973).

25. E.R. Wooding, personal communication.

26. Munson, B., Anal.Chem., 49, 772A (1977).

27. Munson, M.S.B., and Field, F.H., J. Amer.Chem.Soc., 88, 2621 (1966).

28. Hunt, D.F., Prog.Anal.Chem., 6, 359 (1973).

29. Field, F.H., in Ion-Molecule Reactions, Vol.I, Franklin, J.L., Ed., Plenum Press, New York (1972).

30. Wilson, J.M., in Mass Spectrometry, Johnstone,R.W.A., Ed., (Specialist Periodical Reports) The Chemical Society, London (1975) Vol.3, p.96.

31. Wilson, J.M., in Mass Spectrometry, Johnstone, R.W.A., Ed., (Specialist Periodical Reports) The Chemical Society, London (1977) Vol.4, p.11.

32. Munson, B., NATO.Adv.Study Inst. Ser., Ser.B., B.6. (Interact.Ions.Mol.), Ausloos, P., Ed., Plenum Press, New York (1975), p.313.

33. Jennings, K.R., in Mass Spectrometry, Johnstone, R.A.W., Ed., (Specialist Periodical Reports) The Chemical Society, London (1977) Vol.4, p.203.

34. Dzidic, I., and McCloskey, J.A., Org.Mass.Spectrom. 6, 939 (1972).

35. Milne, G.W.A., and Lacey, M.J., Crit.Rev.Analyt.Chem., 4, 45 (1974).

36. Milne, G.W.A., Fales, H.M., and Axenrod, T., Anal.Chem., 43, 1815 (1971)

37. Franklin, J.L., NATO Adv.Study.Inst.Ser.,Ser.B.,B.6 (Interact.Ions.Mol.), Ausloss, P., Ed., Plenum Press, New York (1975), p.1.

38. Henchman, M., in Ion-Molecule Reactions, Vol.I., Franklin, J.L., Ed., Plenum Press, New York (1972).

39. Tal'roze, V.L., and Frankevich, E.L., Zh.Fiz.Khim., 34, 2709 (1960)

40. Baker, F.A., and Hasted, J.B., Phil.Trans.Roy. Soc. London, A261, 33 (1966).

41. Herod, A.A., and Harrison, A.G., Int.J.Mass Spectrom. Ion Phys., 4, 415 (1970).

42. McDaniel, E.W., Martin, D.W., and Barnes, W.S., Rev.Sci.Instr. 33, 2 (1962)

43. McDaniel, E.W., J.Chem.Phys., 52, 3931 (1970).

44. Heimerl, J., Johnsen, R., and Biondi, M., J.Chem.Phys. 51, 5041 (1969).

45. Anders, L.R., Beauchamp, J.L., Dunbar, R.C., and Balderschwieler,J.D., J.Chem.Phys., 45, 1062 (1966)

46. Fehsenfeld, F.C., Ferguson, E.E., and Schmeltekopf, A.L., J.Chem.Phys., 45, 1844 (1966).

47. Solomon, J.J., Meot-Ner, M., and Field, F.H., J.Amer.Chem.Soc., 96, 3727 (1974). See also ref. 57.

48. V.G. Micromass Ltd., Altrincham, Cheshire, England.

49. Comark Electronics Ltd., Rustington, Sussex, England.

50. S.E. Laboratories Ltd., Feltham, Middlesex, England.

51. Texas Instruments Ltd., Bedford, England.

52. C.R.C. Handbook of Chemistry and Physics, 54th Ed., p.D162.

53. Ridge, D.P., and Beauchamp, J.L., J.Chem.Phys., 64, 2735 (1976).

54. Field, F.H., J. Amer.Chem.Soc., 91, 2827 (1969).

55. Weeks, D.P., and Field, F.H., J.Amer.Chem.Soc., 92, 1600 (1970).

56. Meot-Ner,M., Hunter,E.P., and Field, F.H., J.Amer.Chem.Soc., 99, 5576 (1977).

57. Miasek, P.G., and Harrison, A.G., J.Amer.Chem.Soc., 97, 714 (1975).

58. Christophorou, L.G., Atomic and Molecular Radiation Physics, Wiley-Interscience, New York, (1971), p.483.

59. Porter, R.F., NATO Adv. Study Inst. Ser., Ser.B.,B.6 (Interact.Ions.Mol.), Ausloos, P., Ed., Plenum Press, New York (1975), p.231.

60. Tiedemann, P.W., and Riveros, J.M., J.Amer.Chem.Soc. 95, 3140 (1973).

61. Pabst, M.J.K., Tan, H.S., and Franklin, J.L., Int. J.Mass Spectrom.Ion Phys., 20, 191 (1976).

62. Tan, H.S., Pabst, M.J.K., and Franklin, J.L., Int. J.Mass Spectrom.Ion Phys., 19, 163 (1976).

63. Tan. H.S., Pabst, M.J.K., and Franklin, J.L., Int.J.Mass Spectrom.Ion.Phys., 20, 247 (1976)

64. Shen, J., (Case West.Reserve Univ., Cleveland, Ohio) Ion-Molecular Reactions (Ph.D.Thesis), Diss.Abstr.Internat., B 33, 4221 (1973).

65. Solka, B.H., and Harrison, A.G., Int.J.Mass. Spectrom. Ion Phys., 17, 379 (1975).

66. Anicich, V.G., and Bowers, M.T., J.Amer.Chem.Soc., 95, 1279 (1974).

67. Payzant, J.D., Cunningham, A.J., and Kebarle, P., J.Chem.Phys., 59, 5615 (1973).

68. Field, F.H., and Beggs, D.P., J. Amer.Chem.Soc., 93, 1585 (1971).

69. Bennett, S.L., and Field, F.H., J.Amer.Chem.Soc., 94, 5188 (1972).

70. Bennett, S.L., Lias, S.G., and Field, F.H., J. Amer.Chem.Soc., 76, 3919 (1972).

71. Sieck, L.W., and Searles, S.K., J.Chem.Phys. 53, 2601 (1970)

72. Beauchamp, J.L., Holtz, D., Woodgate, S.D., and Patt, S.L., J. Amer.Chem.Soc., 94, 2798 (1972).

73. Gauglhofer,J.,and Kevan, L., Chem.Phys.Lett. 16, 492 (1972).

74. Summerhays, K.D., Pollack, S.K., Taft, R.W., and Hehre, W.J., J. Amer.Chem.Soc., 99, 4585 (1977).

75. Leffler, J.E., and Grunwald,E., Rates and Equilibria of Organic Reaction, Wiley, New York (1963).

76. Hammett, L.P., Physical Organic Chemistry, McGraw-Hill, New York (1940).

77. Taft, R.W., in Steric Effects in Organic Chemistry, Newman, M.S., Ed., Wiley, New York (1956).
see also Taft, R.W., Jr., J.Amer.Chem. Soc., 74,2729 (1952)

78. Harrison, A.G., NATO Adv. Study Inst. Ser., Ser.B., B.6 (Interact.Ions.Mol.). Ansloos, P., Ed., Plenum Press, New York (1975), p.263.

79. Lippincott, E.R., and Stutman, J.M., J.Phys.Chem., 68,2926 (1964).

80. Landolt, H.H., and Börnstein, R.,Zahlenwerte und Functionen, Vol.I, Pt.3, Springer-Verlag, Berlin (1951),p.509

81. Vaughan, W.E., Dig. Lit. Dielec. 33, 21 (1971)